UNIVERSITY OF CALIFORNIA

SANTA CRUZ

IMAGING STRUCTURAL PLASTICITY OF SYNAPSES IN THE BRAIN

A dissertation submitted in partial satisfaction
of the requirements for the degree of

DOCTOR OF PHILOSOPHY

in

MOLECULAR, CELL AND DEVELOPMENTAL BIOLOGY

by

Xinzhu Yu

September 2012

The Dissertation of Xinzhu Yu
is approved:

_____
Professor Yi Zuo, Chair

_____
Professor Bin Chen

_____
Professor David A. Feldheim

_____
Professor Theresa Jones

_____
Tyrus Miller

Vice Provost and Dean of Graduate Studies

Table of Contents

List of Figures

Abstract

Synapses are the sites where neurons contact each other and exchange information in the brain. Experience-dependent changes in synaptic connections are fundamental for numerous neurological processes, ranging from the development of neuronal circuitry to learning and memory. Dendritic spines are the postsynaptic sites of the majority of excitatory synapses in the mammalian central nervous system. The morphology and dynamics of dendritic spines change throughout the lifespan of animals, especially during early postnatal development and in response to novel experiences. Furthermore, abnormal spine morphology is a hallmark of various types of neuropathology. For instance, Fragile X syndrome (FXS) is characterized by an abnormal increase in immature spines. However, how learning behaviors affect neuronal connectivity and how the memory is structurally encoded in the intact brain, what molecular mechanisms regulate experience-dependent synaptic pruning during postnatal development, and how synaptic connections are altered during the progression of neuropathology remain unknown.

To investigate how long-lasting motor memory is structurally encoded in the intact brain, we train mice with novel motor skills and apply two-photon *in vivo* imaging to follow the dynamisms of dendritic spines in the corresponding motor cortex. We find that learning a new motor skill task leads to a rapid formation of postsynaptic dendritic spines on the output pyramidal neurons in the motor cortex. Although

selective elimination of spines that existed before training gradually returns the overall spine density back to the original level, the new spines induced during learning are preferentially stabilized during subsequent training and endure long after training stops. Furthermore, we show that different motor skills are encoded by different sets of synapses. Practice of novel, but not previously learned, tasks further promotes spinogenesis in adulthood. Our findings, therefore, reveal rapid, but long-lasting, synaptic reorganization is closely associated with motor learning. The data also suggest that stabilized neuronal connections are the foundation of durable motor memory.

To explore molecular mechanisms underlying experience-dependent synaptic pruning during postnatal development, we investigate the elimination of dendritic spines in mice deficient of different cell adhesion molecules ephrin-As *in vivo*, and also examine the expression patterns of those molecules using array tomography. We find that elimination of postsynaptic dendritic spines in various cortical regions is accelerated in *ephrin-A2* knockout (KO) mice during adolescent development, resulting in fewer adolescent spines integrated into adult circuits. Sensory deprivation reduces spine elimination in the barrel cortex, and deprived wild-type and deprived KO mice exhibit comparable spine elimination. We also show that ephrin-A2 in the cortex colocalizes with glial glutamate transporters (GLAST and GLT-1), which are significantly down-regulated in *ephrin-A2* KOs. Finally, we find that increased spine loss in *ephrin-A2* KOs depends on activation of glutamate receptors, as blockade of

the NMDA (*N*-methyl-D-aspartate) receptor by its antagonist MK801 eliminates the difference in spine loss between wild-type and *ephrin-A2* KO mice. Together, our results suggest that ephrin-A2 signaling underlies experience-dependent, NMDA receptor-mediated synapse elimination during maturation of the mouse cortex.

Fragile X Syndrome (FXS) is the most frequent form of inherited mental retardation. This mental disorder is caused by transcriptional silence of a gene called fragile X mental retardation gene 1 (*FMR1*). It has been hypothesized that absence of the Fragile X Mental Retardation Protein (FMRP, the protein product of *FMR1*) causes a defect in spine maturation and pruning, and such altered synaptic connectivity results in learning defects. To test this hypothesis, we train both wild-type and *FMR1* KO mice with motor learning tasks and follow the dynamics of dendritic spines at different age stages *in vivo*. We find that adult *FMR1* KO mice fail to improve skilled motor performance, suggesting a defect in learning behaviors. We also show that layer V neurons do not prune dendritic spines during postnatal development in *FMR1* KO mice, therefore, causing significantly higher spine density in adulthood. Moreover, while adult *FMR1* KO mice have normal spine turnover, adolescent *FMR1* KO mice exhibit elevated spine formation and stabilization, but normal spine removal. Additionally, abnormal spine dynamics in adolescent *FMR1* KO mice are layer-specific, as dendritic spines on apical dendrites of layer II/III neurons display normal spine turnover. Finally, administration of mGluR antagonist MPEP rescues

the defects of spine dynamics in adolescent *FMR1* KO mice, providing a potential therapeutic target for FXS.

To my family, for their love and support;

To my friends, for their inspiration and encouragement.

Acknowledgments

Many great people have contributed greatly to the work described in this dissertation. I owe my deepest gratitude to them, as without them none of this would have been possible.

First and foremost, I would like to acknowledge my advisor, Dr. Yi Zuo, for providing me great opportunities and freedom to explore the fantastic world of neuroscience. Her enthusiasm, insistence and knowledge led me overcome many crisis situations and guided me develop as an independent scientific researcher. I hope that one day I would become a great scientist and mentor as what Yi has been to me. I am also indebted to my committee members, Bin Chen, David Feldheim and Theresa Jones, as well as David States, for their insightful advice, constructive criticisms and continuous encouragement throughout my doctoral study. I am deeply grateful to them for setting high standards for me and teaching me how to become a real scientist.

I am also very thankful to my amazing collaborators, Gordon Wang, Kelly Tennant, Weiling Yin and Shinya Ito, for putting tremendous efforts into the projects and enforcing strict validations for every experimental result. The collaborations with them have dramatically broadened my vision and knowledge. I would also like to acknowledge the former and current Zuo lab members, Adam Aaron, Aerie Lin,

Andrew Perlik, Anthony Gilmore, Becka Roberts, Denise Garcia, Jonathan Zweig, Min Fu, Tonghui Xu, Victoria Chew and Willie Tobin, for their insights and help. I am so fortunate to work with them during different stages of my research.

Finally, I am indebted to my beloved family and friends, for having belief in me, for giving me love, care, support and strength throughout my life. I hope that I make them proud of me.

Chapter I Synapse Plasticity In The Living Cortex

1.1 Introduction

The mammalian cortex is composed of columnar aggregates of neurons that share similar functional properties, such as orientation selectivity in the visual cortex or muscle movement control in the motor cortex. Functional maps in different cortical regions are capable of rapid and long-lasting reorganization throughout the animal's life, which is associated with novel experiences and pathologies. In the motor cortex, learning a new motor task is accompanied by expansion of the functional representation of task-related muscle movements in rats, primates and humans (Kleim et al., 2004; Nudo et al., 1996; Rosenkranz et al., 2007). During the recovery following stroke or injury, surviving cortical regions adopt the function of damaged tissues (Ghosh et al., 2010; Murphy and Corbett, 2009; Nudo, 2006). In the visual cortex, the retinotopic map remodels following retinal lesions, associated with a massive rewiring of synaptic structures (Keck et al., 2008). It has been proposed that intrinsic horizontal connections (*i.e.*, intercolumnar and intracolumnar connections) of the cerebral cortex serve as a structural substrate for map plasticity. Pyramidal neurons establish these connections by extending long, horizontal axon collaterals that form excitatory synapses with their postsynaptic partners.

The synapse is the site of information exchange in the central nervous system. In the mammalian brain, the vast majority of excitatory glutamatergic synapses are formed between presynaptic axonal en passant boutons and postsynaptic dendritic spines. Dendritic spines are small protrusions emanating from dendritic shafts. Not only are spines heterogeneous in shape, their density also varies among different types of neurons and in different developmental stages (Nimchinsky et al., 2002). Spines contain all the essential components required for postsynaptic signaling and plasticity and, thus, serve as good indicators of modifications in synaptic connectivity (Harms and Dunaevsky, 2007; Segal, 2005; Tada and Sheng, 2006). Recent studies have revealed dynamics of individual, fluorescently labeled dendritic spines over time in various cortical regions of living mice using two-photon imaging, and demonstrated that sensory experience dramatically affects spine stability (Alvarez and Sabatini, 2007; Bhatt et al., 2009; Holtmaat and Svoboda, 2009). However, relatively little is known about spine dynamics in the motor cortex, how motor learning affects the connectivity of the neural circuitry, or how memory is structurally encoded in the intact brain.

1.2 Functional and structural plasticity of synapses in the motor cortex

1.2.1 Functional plasticity of synapses

Integration of synaptic signals is critical to the functional organization of neural circuitry. Long-term potentiation (LTP) and long-term depression (LTD) lead to changes in synaptic efficacy and have been proposed to be candidate mechanisms for learning-induced plasticity in the motor cortex. Evidence supporting this hypothesis comes from studies on both animals and humans. Training rats with a skilled reaching task has been shown to strengthen horizontal connections in both layer I and layer II/III motor cortex contralateral to the trained limb, resulting in elevated amplitudes of field potentials (Harms et al., 2008; Rioult-Pedotti et al., 2000). Moreover, after the animal acquires the new motor skill, LTP is reduced, while LTD is enhanced (Rioult-Pedotti et al., 2000) (Figure 1). In humans, learning of novel hand movements has also been found to prevent the subsequent induction of LTP-like plasticity, while enhancing LTD-like plasticity (Ziemann et al., 2004). The occlusion of further LTP induction in the post-learning brain suggests that LTP or LTP-like plasticity happens during motor learning.

In addition, while elevated field potentials persist long after initial learning acquisition, both LTP and LTD thresholds shift upward. As a consequence, the elevated baseline of synaptic efficacy is placed back to the middle of the LTP/LTD operating range, ensuring the possibility of further synaptic strengthening (Rioult-Pedotti et al., 2007) (Figure 1B). Furthermore, electrical induction of LTP/LTD or LTP/LTD-like plasticity in the motor cortex *in vivo* before or during motor learning

interferes with the learning process (Hodgson et al., 2005; Iezzi et al., 2010; Jung and Ziemann, 2009), providing further evidence to support LTP/LTD as a mechanism for learning acquisition of motor skills.

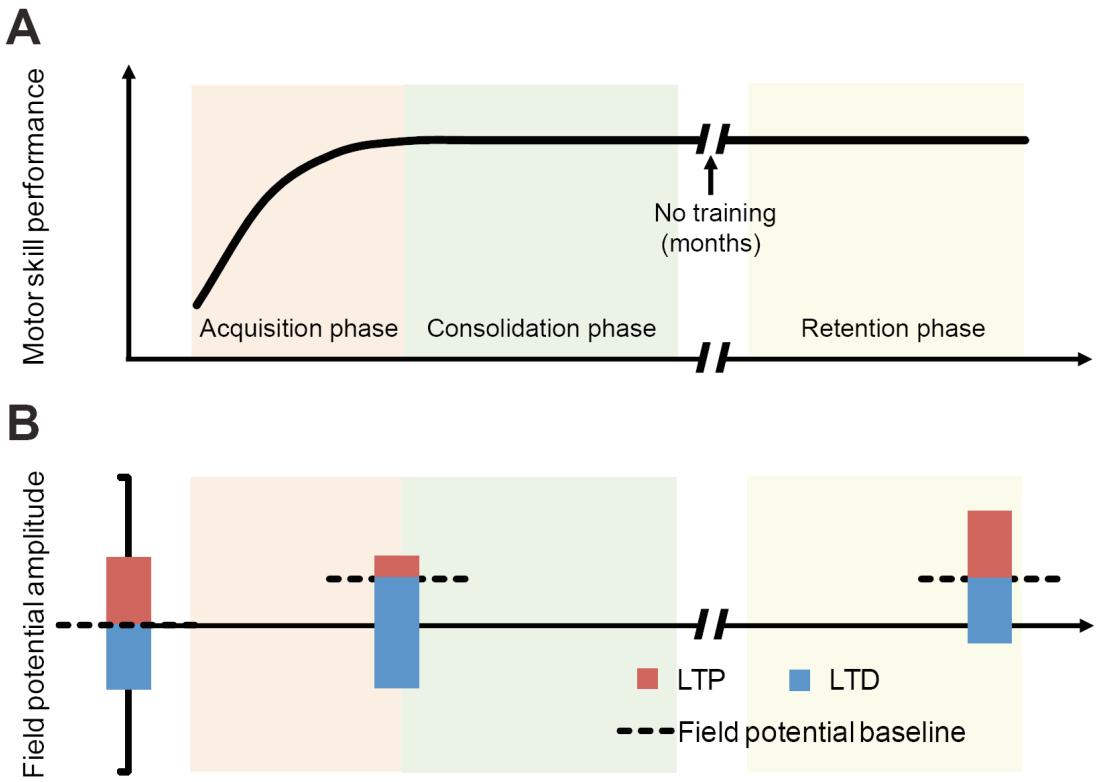

Figure 1. Changes in synapse strengths in the motor cortex during and after motor learning.

(A) Three phases of motor learning: significant improvement of performance is observed in acquisition phase, and high performance is maintained during consolidation and retention phases. (B) Synaptic efficacy baseline and LTP/LTD modification range. Elevated baseline field potentials have been observed in layer I, II/III neurons in the motor cortex after learning acquisition. This leads to reduced LTP and enhanced LTD. In the retention phase, the synaptic modification range shifts upward with time, placing the elevated baseline back to the middle of the LTP/LTD operating range.

1.2.2 Structural changes of synapses

Many lines of evidence have also shown that synaptic structural changes are associated with functional changes of neural circuitry. In the rat motor cortex, induction of LTP in the forelimb region increases spine density of layer III and layer V pyramidal neurons, and expands the forelimb representation (Monfils et al., 2004). In contrast, induction of LTD decreases spine density (Monfils and Teskey, 2004), and shrinks the forelimb representation (Teskey et al., 2007). Learning-induced LTP occlusion, as discussed above, has also been shown to be associated with enlargement of spine heads in layer I of the motor cortex (Harms et al., 2008).

For decades, both electron microscopy (EM) and the Golgi staining method have been used to examine synapse/spine numbers in the motor cortex following motor skill learning. Despite the general belief that learning promotes synaptogenesis, data from different experimental paradigms and methods have resulted in diverse and somewhat conflicting conclusions. For example, EM analysis has indicated that motor learning has no effect on synapse density, but increases the synapse/neuron ratio in both layer II/III and layer V motor cortex contralateral to the trained forelimb (Kleim et al., 2004; Kleim et al., 1996). In contrast, spine counting reveals that there is a decrease in spine density of layer III neurons, yet no effect on spine density in layer V pyramidal neurons in the motor cortex following motor skill training (Kolb et al., 2008). The layer-dependent changes in spine density imply that a sub-population, rather than all, of the neurons in the motor cortex responds to learning.

1.3 Spine dynamics in the living brain

The advent of high-resolution time-lapse imaging in conjunction with fluorescent molecular tools enables the visualization of synaptic structures in living animals. Using two-photon microscopy and transgenic animals in which a small population of neurons is fluorescently labeled, turnover and morphological changes of postsynaptic dendritic spines have been examined in various cortical regions, both during development and in association with experience and learning. While long-term *in vivo* imaging has revealed a global stability of dendritic arborization of cortical layer V neurons (Trachtenberg et al., 2002; Xu et al., 2009), spine dynamism and morphological changes have been reported throughout the cerebral cortex during development and in adulthood.

1.3.1 Spine dynamics in developing and adult brains

Despite the debate on the exact degree of spine dynamics, it is generally believed that dendritic spines change their morphology and turn over rapidly in developing animals but become much more stable in adults. During early postnatal stages, spines of cortical neurons are highly plastic, changing length and appearing/disappearing within tens of minutes (Cruz-Martin et al., 2010; Lendvai et al., 2000). Both spine motility and turnover decrease with increasing age. In adolescence, while spine

turnover rates are comparable (Majewska et al., 2006; Zuo et al., 2005a); spine motility is intrinsically different in various cortical regions, high in somatosensory and auditory cortices while low in visual cortex (Majewska et al., 2006). Rewiring visual input into the auditory cortex at birth does not alter spine motility (Majewska et al., 2006). At this stage, spine elimination is significantly higher than spine formation throughout the cerebral cortex, leading to a gradual reduction in total spine number during postnatal development (Grutzendler et al., 2002; Holtmaat et al., 2005; Xu et al., 2009; Zuo et al., 2005a; Zuo et al., 2005b). In contrast to adolescence, total spine numbers in all examined regions remain unchanged over time in adulthood, due to comparable rates of spine formation and elimination (Grutzendler et al., 2002; Hofer et al., 2009; Holtmaat et al., 2005; Xu et al., 2009; Zuo et al., 2005a; Zuo et al., 2005b). While the majority of spines stay stable, a subset of them constantly turns over (Holtmaat et al., 2005; Zuo et al., 2005a). Regardless of the divergence in spine classifications and calculation methods used in different studies, the consensus in the field is that the proportion of stable spines increases gradually from adolescence to adulthood (Cruz-Martin et al., 2010; Grutzendler et al., 2002; Holtmaat et al., 2005; Trachtenberg et al., 2002; Yang et al., 2009; Zuo et al., 2005a). For example, over 30% of spines are lost in mouse visual cortex from one to two months old of age, whereas ~96% spines in adults (>4 months old) have a half-life more than 13 months (Grutzendler et al., 2002). While the high stability of spines provides a potential structural basis for long-term information storage in the brain, the plasticity of spines offers the brain a capability to rewire in response to novel experiences.

1.3.2 Spine remodeling during motor skill learning

Two recent studies further investigate spine dynamics during and after motor learning. Xu and colleagues train mice with a forelimb reaching task. They find that new spines are formed within one hour after initiation of motor skill learning in apical dendrites of layer V pyramidal neurons residing in the contralateral motor cortex (Xu et al., 2009) (Figure 2). A similar observation is made by Yang *et al*., using an accelerated rotarod running task, in which spine formation increases within two days of training (Yang et al., 2009). The degree of spine formation is closely associated with the degree of learning acquisition (Xu et al., 2009), as well as maintenance of the skill (Yang et al., 2009). These *de novo* spines could provide a route to enlarge the memory storage capacity of the brain by creating new synaptic connections (Stepanyants and Chklovskii, 2005). Moreover, this rapid spinogenesis during initial learning is followed by enhanced spine elimination, making total spine number return to the control level after prolonged training (Figure 2). This elimination is selective for the spines that have existed before training, while the new spines induced during learning are preferentially stabilized during subsequent training, enduring long after training stops (Xu et al., 2009).

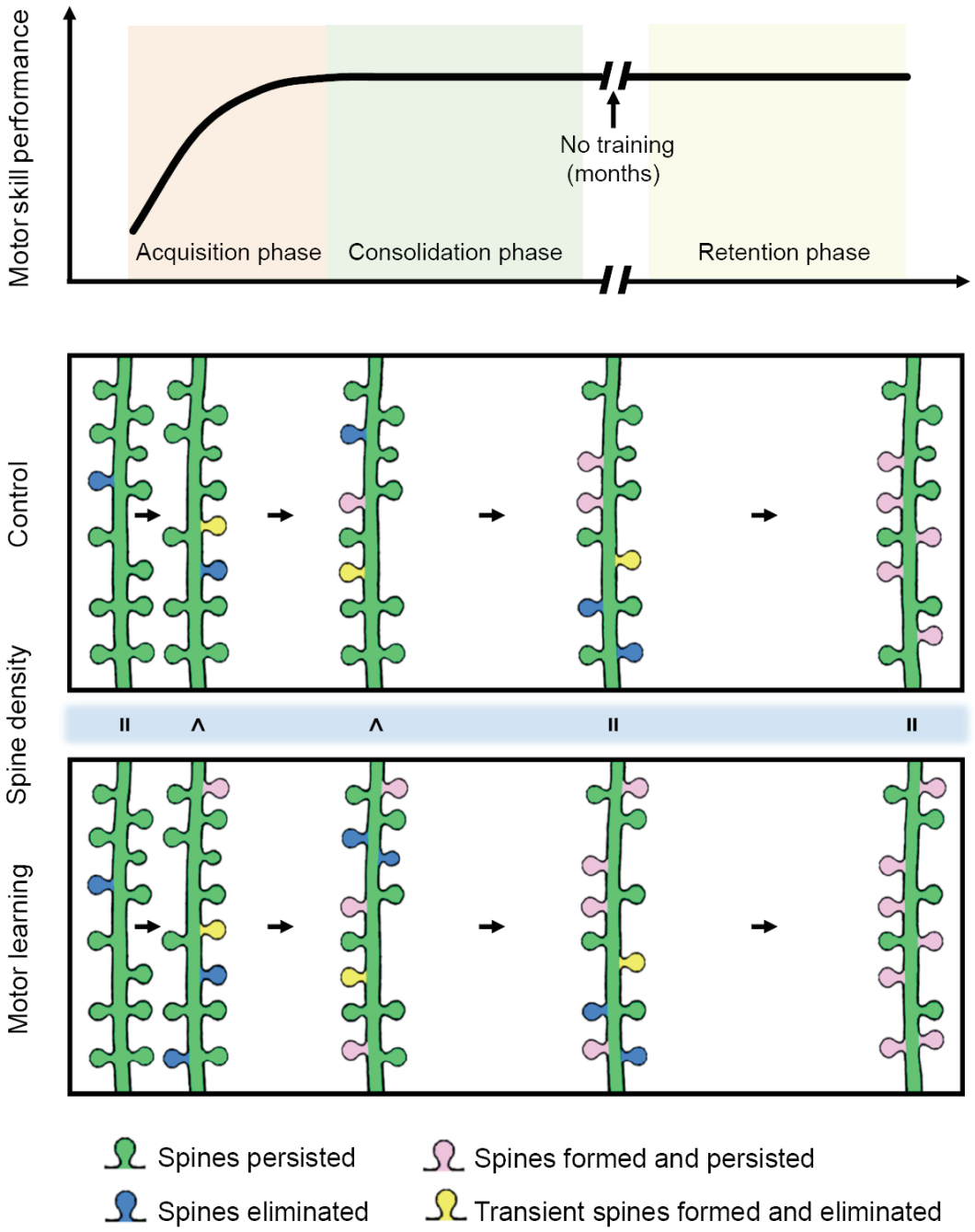

Figure 2. Changes in spine dynamics in the motor cortex during and after motor learning.

A schematic illustrating immediate and protracted spine dynamics in both control and trained animals. Learning-induced new spines are preferentially stabilized, while pre-

existing spines are selectively removed, leading to the rewiring of the neural circuitry. Motor learning temporally increases spine density, which gradually returns back to the control level.

One of the most unique characteristics of motor learning is the fact that, once a motor behavior is learned, further maintenance of the motor skill does not require constant practice (Figure 1A). Xu *et al.* have shown that retraining of the same motor skill months later does not enhance spine dynamics (Figure 3), suggesting that the circuitry needed for performing such motor tasks is made during initial training and maintained afterwards. However, training these pretrained animals with a novel motor skill continues to induce a robust spinogenesis in the primary motor cortex, suggesting that different motor memories are stored at different synaptic locations (Xu et al., 2009).

Together, these two studies suggest a critical role of long-lasting synaptic reorganization in formation of durable motor memories. However, despite the nice correlation of spine dynamics and learning behaviors illustrated in these studies, their causal relationship remains unclear. Genetic approaches to target and manipulate learning-related spines will be required to further address this question.

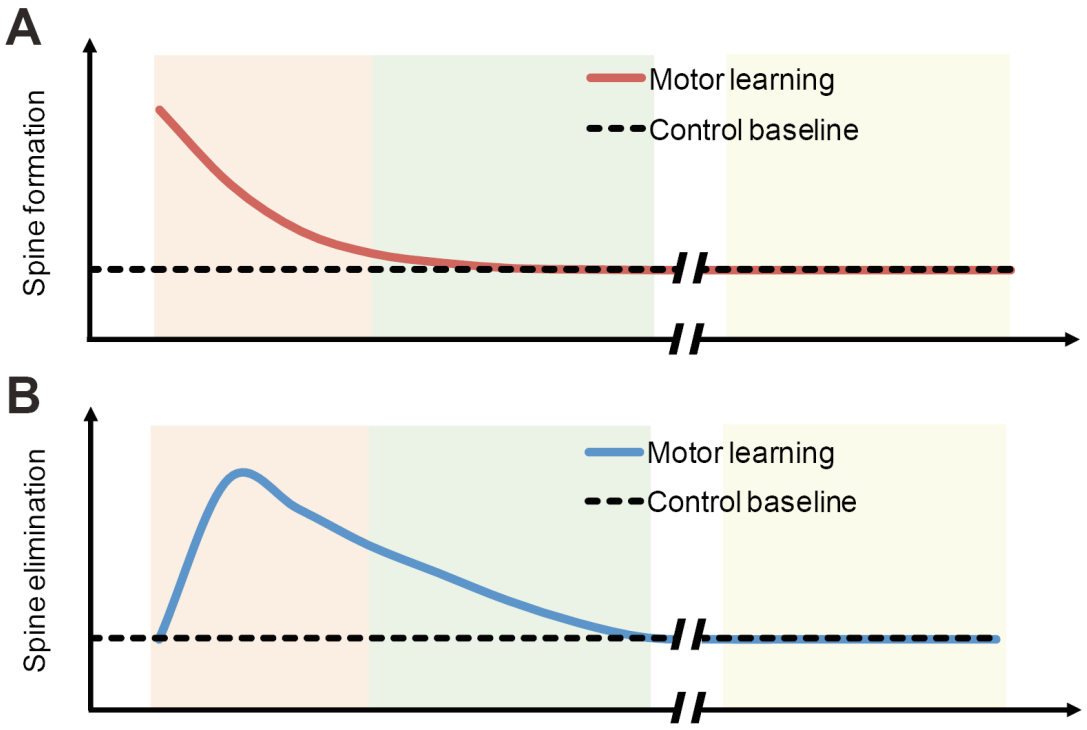

Figure 3. Time course of changes in spine formation and elimination.

Motor learning leads to a rapid increase in spine formation (A), which is followed by delayed but prolonged spine elimination (B).

1.3.3 Experience-dependent spine plasticity outside the motor cortex

Experience-dependent spine plasticity has been found in many other systems in both developing and mature animals. In the barrel cortex, while enriched environment and learning paradigms promote spine formation (Holtmaat et al., 2006; Yang et al., 2009), experience is also essential for the profound synapse pruning during adolescent development (Zuo et al., 2005b). In the visual system, monocular deprivation (MD) doubles the rate of spine formation and increases the spine density in the apical dendrites of layer V neurons in the binocular cortex of adult mice.

Restoring the binocular vision returns spine dynamics to the baseline. However, many MD-induced spines persist during binocular deprivation, providing a structural basis for the rapid functional shift during subsequent MD (Hofer et al., 2006, 2009).

Recently, another elegant study investigates spine dynamics in the forebrain nucleus HVC, a site where auditory information and motor representation merge in songbirds. Using lentivirus/GFP constructs to label neurons in HVC, the authors follow the spine dynamics in HVC during song learning in birds. Their data show that a higher level of spine turnover before tutoring correlates with greater capacity for subsequent song imitation. Furthermore, song learning experience triggers rapid stabilization of dendritic spines, and enhances spontaneous synaptic activity of these neurons (Roberts et al., 2010).

1.4 Altered spine morphology and dynamics under pathologies

While experience-dependent modification of spine plasticity provides a cellular mechanism underlying learning and memory, abnormal spine morphology and dynamics are hallmarks of injuries and neurological diseases. In Alzheimer's disease (AD), a dramatic spine loss has been observed in the vicinity of β-amyloid plaques in the living cortex of transgenic AD mice (Spires et al., 2005; Tsai et al., 2004). Fragile X Syndrome (FXS) is characterized by an abundance of immature postsynaptic dendritic spines. A recent study has revealed a delayed downregulation of spine

turnover and an increase of immature spines in layer II/III neurons during early postnatal stage in FXS mice (Cruz-Martin et al., 2010). In the motor cortex, spinal cord injury leads to spine remodeling: spine density of cortical pyramidal neurons decreases initially and partially recovers later on, together with enlarged spine heads and increased spine lengths (Kim et al., 2006). Enriched environment and transplant/neurotrophin-3 treatments abolish such injury-induced spine morphological changes, providing potential candidates for further therapies (Kim et al., 2008). Using live imaging, recent studies examine the dendritic and spine remodeling in the sensorimotor cortex following photothrombotic-induced stroke. These studies show that peri-infarct dendrites are exceptionally plastic, with elevated spine formation extending up to 6 weeks after stroke (Brown et al., 2010; Brown et al., 2007). Furthermore, such synapse rewiring is closely associated with the functional remodeling that occurs during the recovery period (Brown et al., 2009). These studies provide a better understanding of the relationship between spine alterations and brain dysfunctions, and offer valuable insights into pathogenesis and therapeutics of neurological diseases and injuries.

1.5 Conclusion

An important feature of the mammalian cortex is the capability of rapid and long-lasting functional reorganization. Our understanding of the morphological plasticity of spines, as well as their modifications with learning and altered brain functions in

the living mouse cortex, highlights the significance of spines in the functional reorganization. In the motor system, current *in vivo* evidence indicates that spinogenesis occurs rapidly after motor learning is initiated and that a large population of these new spines persists while animals maintain motor skill performance, suggesting *de novo* spines as the underlying mechanism of learning. So far, changes in synaptic strength (Rioult-Pedotti et al., 2000) and reorganization of the functional map (Kleim et al., 2004) have been observed at a relatively late phase of motor learning, in contrast to the immediate spinogenesis observed *in vivo* (Xu et al., 2009). Further investigation of the relationship between spine remodeling and motor functional map reorganization will provide valuable information to understanding the mechanisms underlying motor learning.

Some recent studies combine *in vivo* imaging of synaptic structures with functional imaging (e.g. intrinsic optic imaging) or electrophysiological examination to address this question (Brown et al., 2009; Keck et al., 2008; Trachtenberg et al., 2002). Two-photon calcium imaging, using Ca^{2+} sensitive dye or genetically encoded Ca^{2+} indicators, has monitored the activity of spatially defined neuronal populations in the mammalian cortex, and led to a direct observation of functional neuronal clusters in the awake mouse motor cortex. It is shown that neurons involved in different responses intermingle spatially (Komiyama et al., 2010), while the temporal correlation between neurons decreases with the distance (Dombeck et al., 2009). Moreover, when mice are trained with an odor-selective licking task, correlations of

coincident activity for neurons with the same response types increase with learning. This suggests that learning creates a local network of functionally related neurons in the motor cortex (Komiyama et al., 2010).

The mammalian cortex is a laminar structure. Neurons in different cortical layers have different local and subcortical connections (Anderson et al., 2010). To date, the majority of *in vivo,* dendritic spine imaging data has been collected from two transgenic lines – the YFP-H line and the GFP-M line. Both lines use the *thy-1* promoter to drive fluorescent protein expression selectively in a subset of cortical neurons (Feng et al., 2000; Yu et al., 2008). The studies described above mostly investigate dynamics of spines on apical dendrites of layer V neurons. Whether changes in spine dynamics triggered by motor learning are restricted to these neurons remains unclear. It has been shown that spine dynamics of layer II/III neurons do not change after MD (Hofer et al., 2009). Thus, it will be important to explore structural plasticity in other cell types.

Finally, spines are postsynaptic components of excitatory synapses. It is to be expected that modifications in presynaptic axonal boutons also participate in motor cortex plasticity. Using the same *thy-1* transgenic mice, previous studies have investigated axon terminal stability *in vivo*. These studies find that axon bouton dynamics are cell-type specific (De Paola et al., 2006), and axonal terminals are more stable than dendritic spines in general (De Paola et al., 2006; Majewska et al., 2006).

Studies examining axonal bouton changes in the motor cortex and during motor learning remain to be done.

Chapter II Rapid Formation And Selective Stabilization Of Synapses For Enduring Motor Memories

2.1 Introduction

Novel motor skills are learned through repetitive practice and, once acquired, persist long after training stops (Karni et al., 1995; Luft and Buitrago, 2005). Earlier studies have shown that such learning induces an increase in the efficacy of synapses in the primary motor cortex whose persistence is associated with retention of the task (Harms et al., 2008; Rioult-Pedotti et al., 2007; Rioult-Pedotti et al., 2000). However, how motor learning affects neuronal circuitry at the level of individual synapses and how long-lasting memory is structurally encoded in the intact brain remain unknown.

Here we show that synaptic connections in the living mouse brain rapidly respond to motor-skill learning and permanently rewire. Training in a forelimb reaching task leads to rapid (within an hour) formation of postsynaptic dendritic spines on the output pyramidal neurons in the contralateral motor cortex. Although selective elimination of spines that existed before training gradually returns the overall spine density back to the original level, the new spines induced during learning are preferentially stabilized during subsequent training and endure long after training

stops. Furthermore, we show that different motor skills are encoded by different sets of synapses. Practice of novel, but not previously learned, tasks further promotes spinogenesis in adulthood. Our findings, therefore, reveal rapid, but long-lasting, synaptic reorganization is closely associated with motor learning. The data also suggest that stabilized neuronal connections are the foundation of durable motor memory.

2.2 Methods

2.2.1 Motor skill training

Single-seed reaching task

Mice were food-restricted to maintain 90% of free feeding weight before the start of training. The training chamber was constructed as a clear Plexiglas box 20 cm tall, 15 cm deep and 8.5 cm wide into which each individual mouse was placed. Three vertical slits 0.5 cm wide and 13 cm high were located on the front wall of the box: in the center, on the left side, and on the right side. A 1.25 cm tall exterior shelf was affixed to the wall in front of the slits to hold millet seeds for food reward (Figure 4).

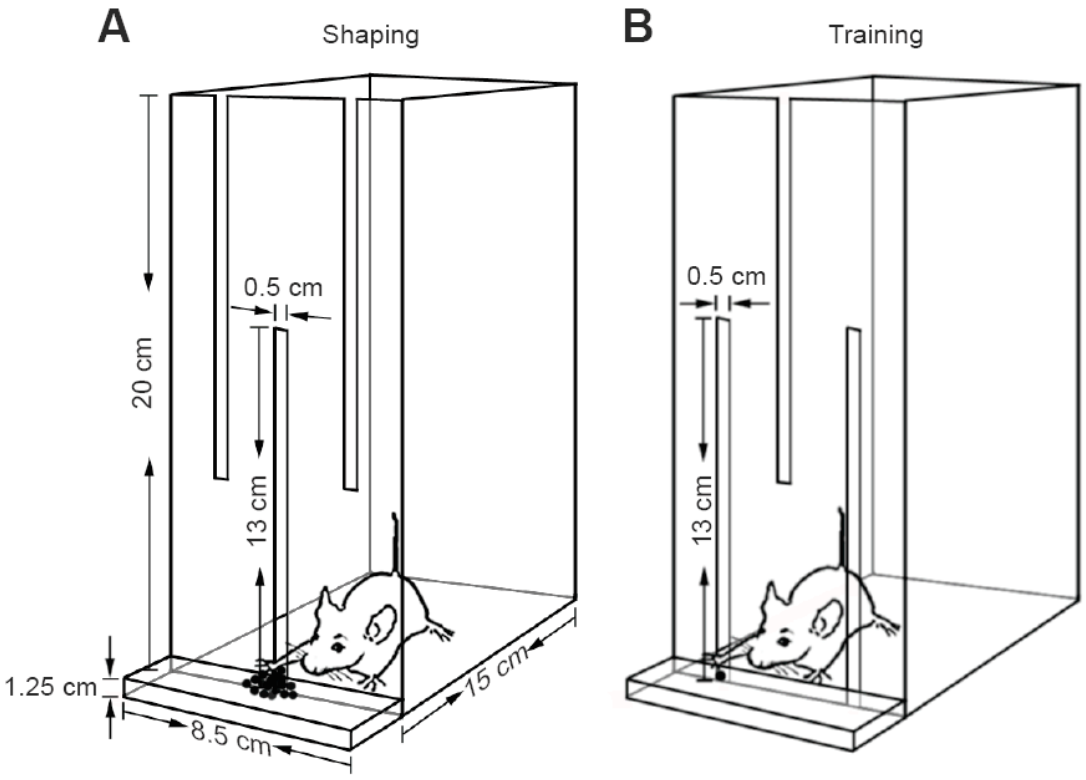

Figure 4. A cartoon drawing with dimensions of the animal chamber used during shaping and training.

(A) During 'shaping', seeds are centered in front of the middle slit and mice use both paws to reach for them. (B) The chamber is flipped upside-down during training. Seeds are placed individually only at the side slit of the preferred limb (in this example, the right limb).

The training included two phases - 'shaping' and 'training'. The shaping phase (2-5 days in duration) was used to familiarize mice with the training chamber and task requirements and also to determine their preferred limbs. During the 'shaping' phase, millet seeds were placed in front of the center slit and mice used both paws to reach for them. 'Shaping' was considered finished when 20 reach attempts were achieved within 20 minutes, and the mouse showed >70% limb preference. 'Training' started

the day after 'shaping', and each training day consisted of one session of 30 trials with preferred limb or 20 minutes (whichever occurred first). Seeds were presented individually in front of the slit on the side of preferred limb. Occasionally a mouse used the non-preferred limb. But because of the difficulties presented by reaching angle, such reaches usually were unsuccessful. Mice displayed three reach attempt types: fail, drop and success. A 'fail' was scored as a reach in which the mouse failed to touch the seed or knocked it away. A 'drop' was a reach in which the mouse retrieved the seed, but dropped it before putting into its mouth. A 'success' was a reach in which the mouse successfully retrieved the seed and put it into its mouth. Success rates were calculated as the percentage of successful reaches over total reach attempts.

About half of the mice in our experiments were right handed (55 right handed out of total 109 mice, 50.6%). All data collected from both left- and right-handed mice were pooled for analysis in this study. No significant difference was found in the reaching performance of left- and right-handed mice.

All our control mice were littermates that underwent the same food restriction. All mice were handled (i.e. removed from their cages and placed temporarily in the training chamber into which some seeds were dropped) by the same experimenters. To ensure that the increase seen in spine dynamics was learning specific, three different controls were used in our study: 1) General controls: Mice with neither

training nor shaping, but with food restriction, food reward and handling. 2) Shaping controls: Mice that received similar shaping as trained mice. During training, they were placed into the training chamber for 20 min daily, with ~15 seeds periodically dropped into the training chamber. This control group was used to determine whether the shaping period and/or experience of the training environment had any effect on spine dynamics. 3) Activity controls: Mice were given similar shaping as trained mice. During training, mice were placed into the training chamber and trained to reach for a seed placed outside the slit for 20 min daily. However, the seed was placed out of reach, so that they could never obtain it and, therefore, did not learn skillful reaching movements (as shown by testing their performance occasionally). Thus, both trained mice and activity control mice experienced similar amounts of forelimb activity, but only trained mice developed the motor skill. The activity control was used to determine whether enhanced spine dynamics were caused by increased motor activity or were specific to motor skill learning. Our results indicate that there is no difference in the spine dynamics between the activity controls and general controls.

Capellini handling task

This task was similar to the vermicelli handling tasks previously described for rats (Allred et al., 2008). Mice were food-restricted to maintain 90% of free feeding weight before training began. Daily training session consisted of 10 trials with uncooked capellini pasta pieces (2.5 cm), given one piece per trial. Mice learned to use coordinated forepaw movements to eat the pasta. The average consumption time

for one piece of capellini pasta decreased from 3.44±0.18 min on day 1 to 1.98±0.29 min on day 4 (mean ± s.e.m., $P<0.005$, 7 mice). There was no significant behavioral difference in the capellini handling task between naïve adults and adults pretrained in the reaching task in adolescence.

2.2.2 *In vivo* imaging of superficial dendrites

The procedure for transcranial two-photon imaging has been described previously (Grutzendler et al., 2002). Mice aged 1–6 months were anaesthetized with an intraperitoneal (i.p.) injection (5.0 ml per kg body weight) of 17 mg/ml ketamine and 1.7 mg/ml xylazine in 0.9% NaCl. The skull was exposed with a midline scalp incision and imaged regions were located based on stereotactic coordinates. A small region of skull (~300 μm in diameter) was manually thinned down to ~20 μm in thickness using both a high-speed drill and a microknife. To reduce respiration-induced movements, the skull was glued to a 400 μm thick stainless steel plate with a central opening for skull access. The plate was screwed to two lateral bars located on either side of the head and fixed to a metal base (Figure 5).

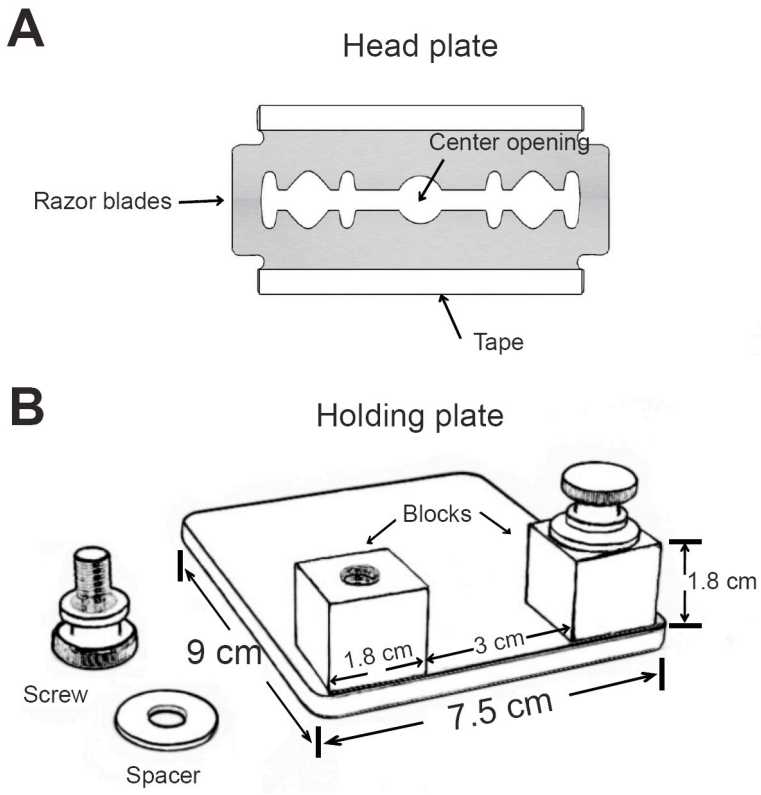

Figure 5. Schematic diagram of the designs of a custom-made head plate and a custom-made holding plate for *in vivo* imaging.

The brain of the mouse was then imaged through the thinned skull using a Prairie Ultima IV multi-photon microscope with a Ti-sapphire laser tuned to the excitation wavelength for YFP (925 nm). Stacks of image planes were acquired with a step size of 0.70 μm using a water-immersion objective (60x, NA 1.1 infrared Olympus objective) at a zoom of 3.0. For relocation of the same dendrites at subsequent imaging times, an image stack containing the dendritic structures of interest was taken without zoom with a step size of 2.0 μm and the surrounding blood vessels were imaged with a CCD camera. The patterns of blood vessels and neuronal processes in

this low-resolution image stack were used for relocating the same dendrites at each subsequent imaging session (Figure 6). After imaging, the plate was detached from the skull, the scalp sutured, and the animal was returned to its home cage until the next imaging session.

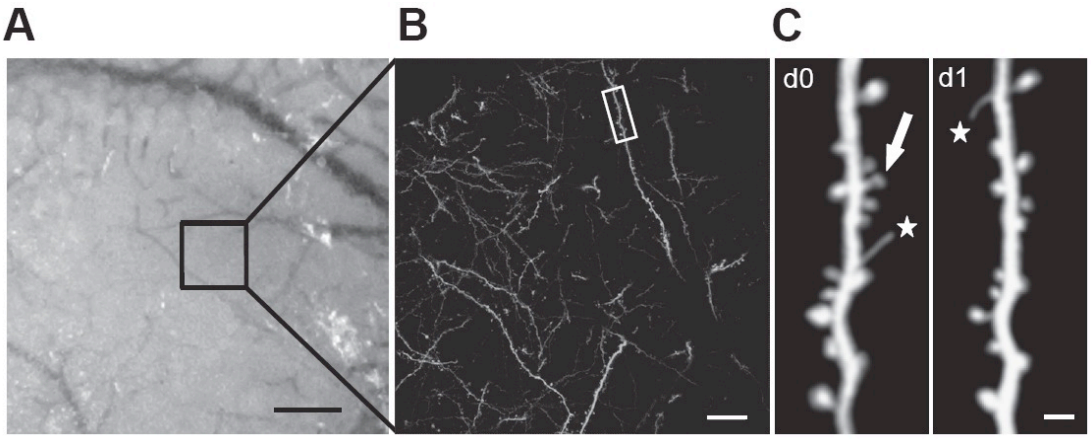

Figure 6. Transcranial two-photon imaging of the primary motor cortex from a one-month-old mouse showing dynamics of dendritic spines over one day.

(A) An image obtained from a CCD camera of the vasculature underneath the thinned skull. The black square indicates the region where subsequent two-photon images were obtained. (B) A low-magnification two-dimensional projection from a three-dimensional stack of dendritic branches and axons in the motor cortex. A higher-magnification view of a dendritic segment in the white box is shown in the left panel of (C). (C) Two images of the same dendritic branch obtained one day apart reveal spine elimination (the arrow) and filopodia (stars) in a control mouse. Scale bars: 200 μm (A), 20 μm (B) and 2 μm (C).

2.2.3 Data quantification

Spine and filopodium identification

All analysis of spine dynamics was done manually using ImageJ software, blind with regard to experimental conditions. Briefly, the same dendritic segments (~5-20μm in length) were identified from 3D image stacks selected from all views having high image quality (signal-to-background-noise ratio >4-fold). Individual dendritic protrusions were tracked manually along dendrites. 3D stacks, instead of 2D projections, were used for analysis to ensure that tissue movements and rotation between imaging intervals did not influence identification of dendritic protrusions. The number and location of dendritic protrusions (protrusion length >1/3 dendritic shaft diameter) were identified in each view. Filopodia were identified as long thin structures with head diameter/neck diameter <1.2 and length/neck diameter >3. The remaining protrusions were classified as spines.

Analysis of spine and filopodial dynamics

Notations of the formation and elimination of spines and filopodia were based on comparison of the images collected at two different time points. Spines or filopodia were considered the same between two views if they were within 0.7 μm of their expected positions, based on their spatial relationship to adjacent landmarks and/or their position relative to immediately adjacent spines. A stable spine is a spine that was present in both images. An eliminated spine is a spine that appeared in the initial image, but not the 2nd image. A newly formed spine is a spine that appeared in the 2nd image, but was absent from the initial image. Percentages of stable, eliminated and formed spines were all normalized to the initial image. Percentage changes in the

total spine number over a given interval were relative to the first view and calculated as percentage of formation minus percentage of elimination measured over that interval. Data on spine dynamics are presented as mean ± standard deviation (s. d.).

Image processing and presentation

Two-dimensional projections of 3D image stacks containing in-focus dendritic segments of interest were used for all figures. We chose very sparsely labeled regions as examples and maximum projections were made from images from 2-4 focus planes. There were normally few crossing structures in the projected images from such a shallow stack, and the presented branches could be clearly isolated. Finally, images were threshold, Gaussian filtered and contrasted for presentation.

2.2.4 Mapping of motor cortex by intracortical microstimulation

This method was adapted from those used in rat experiments (Kleim et al., 2004). Mice were anesthetized with an initial cocktail of ketamine (150 mg/kg, i.p.) and xylazine (10 mg/kg, i.p.) and supplemented with additional ketamine and isofluorane (0.5-1% in oxygen) as necessary. The mouse was placed into a mouse stereotaxic frame (Stoelting, Wood Dale, IL), lidocaine (2 mg/kg, s.c.) was injected into the scalp, and a midline incision was made. The cisterna magna was drained to prevent cortical swelling and the skull and dura overlying the motor cortex were removed. The craniotomy was then filled with warm (37°C) silicone oil to prevent drying. A picture

of the cortical surface was taken and overlaid with a 250 μm square grid in Canvas software.

Intracortical penetrations of a glass microelectrode (diameter of 20-25 μm) with a platinum wire were made at 250 μm intervals in a systematic order throughout the cortex at a depth of 790-800 μm (corresponding to deep layer V / shallow layer VI) with a hydraulic micropositioner until the entire extent of the forelimb representation was resolved. A 40 ms train of 13, 200 μs monophasic cathodal pulses were delivered at 350 Hz from an electrically isolated, constant current stimulator at a rate of 1 Hz stimulation current was increased to a maximum of 60 μA, or until a visible movement was evoked. If a movement was evoked at or below 60 μA, the threshold current was determined by gradually decreasing the stimulation until the movement stopped. The lowest current that evoked a movement was taken as the threshold current. If no movement was seen at 60 μA, the site was considered non-responsive. In cases where stimulation evoked more than one movement, the site was considered responsive to the movement that was determined to have the lowest threshold. To verify the stimulation position was located within layer V, we injected DiI in 7 mice at the end of the experiments and found that all injections left deposits extending through mid layer V-mid layer VI. In addition, penetrating electrode tracts could be observed in Nissl stained coronal sections in most mice. The majority (81.3±4.7%) of these tracts terminated in layer V at a measured depth of 782±137 μm, with the remainder terminated in upper layer VI.

2.3 Results

2.3.1 Motor skill learning induces a rapid formation of dendritic spines in the corresponding motor cortex

Fine motor movements require accurate muscle synergies, that rely on coordinated recruitment of intracortical synapses onto corticospinal neurons (Monfils et al., 2005; Sanes and Donoghue, 2000). Obtaining new motor skills has been shown to strengthen the horizontal cortical connections in the primary motor cortex (Harms et al., 2008; Rioult-Pedotti et al., 2000). In this study, we taught mice a single-seed reaching task. The majority of one-month-old mice that underwent training gradually increased their reaching success rates during the initial 4 days, and then leveled off (n=42, Figure 7). There were a few mice (n=5) that engaged in extensive reaching, but continually failed to grasp the seeds. These mice normally gave up reaching after 4-8 days (Figure 7).

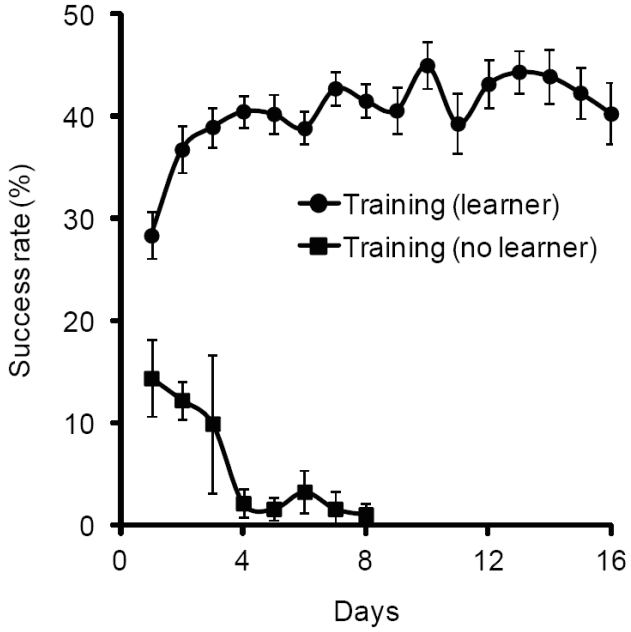

Figure 7. Average success rates during training for learning and non-learning mice.

Data are presented as mean ± s.e.m, 42 learners and 5 no learners.

To investigate the process of learning-induced synaptic remodeling in the intact motor cortex, we repeatedly imaged the same apical dendrites of layer V pyramidal neurons marked by the transgenic expression of yellow fluorescent protein (YFP-H line) in various cortical regions during and after motor learning, using transcranial two-photon microscopy (Grutzendler et al., 2002). Spines that were formed and eliminated were identified by comparing images from two time points, and then normalized to the initial images. Imaged regions were guided by stereotaxic measurements, ensuring the imaged neurons resided in the primary motor cortex. In several experiments, intracortical microstimulation was performed at the end of

repetitive imaging to confirm that images were taken from the functionally responding motor cortex (Figure 8).

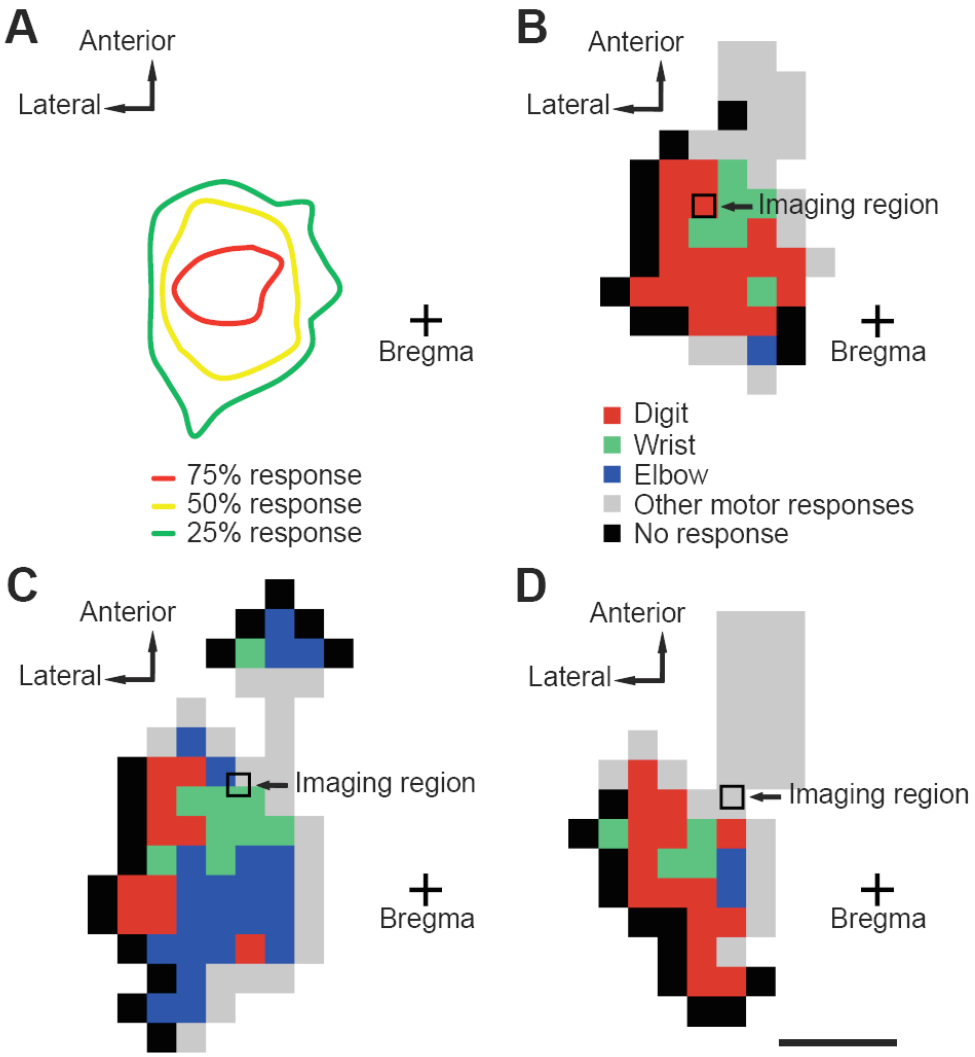

Figure 8. Locations of imaged regions in relation to the forelimb functional map.

(A) An average forelimb response map from 14 mice. Contour lines outline regions in which 75%, 50%, 25% of animals have microstimulation evoked forelimb movements. (B-D) Examples showing three typical locations of the imaging region relative to the forelimb response map. (B) The imaging region falls completely into the forelimb map. (C) The imaging region falls on the border of the forelimb map.

(D) The imaging region is located outside the forelimb map, but within 300 mm of the forelimb border. Regions with forelimb movements are shown in color. Regions in which other movements are evoked (such as hindlimb, trunk, whisker etc) are indicated in grey. Regions without any motor responses are indicated in black. The black square indicates the site of *in vivo* imaging, and the cross indicates the location of bregma. Scale bar: 1 mm.

Unexpectedly, we found that motor learning led to rapid spinogenesis, in the motor cortex contralateral to the reaching forelimb (Figures 9A and 9B). One-month-old mice that finished 30 reaches with more than 10 successes in the first day of training were imaged within one hour of the training session and showed 10.6±1.1% new spines which were not in the images acquired the day before training. This spine formation was more than double that found in age-matched controls, which were handled similarly and imaged over the same period of time, but not trained (Figure 9C, 4.7±0.6% in general controls, $P<0.001$). In contrast, spine elimination measured in the same images was not significantly altered by motor learning during single training sessions (Figure 9C, $P>0.9$). In addition, mice that went through shaping but not training (shaping controls) or mice that were trained to reach for a seed too far away to grasp (activity controls) did not show an increase in spine formation rates (Figure 9C, $P>0.1$ with general control, $P<0.001$ with trained mice; see Methods for all control conditions). This suggests that refinement of fine motor movements, rather than other training related experiences or unskilled motor activity, drives robust spine formation. Furthermore, the percentage of spines formed immediately after the first training session is linearly correlated with the number of successful reaches during the

training session, revealing a direct link between learning and spine formation (Figure 9D, R^2=0.77).

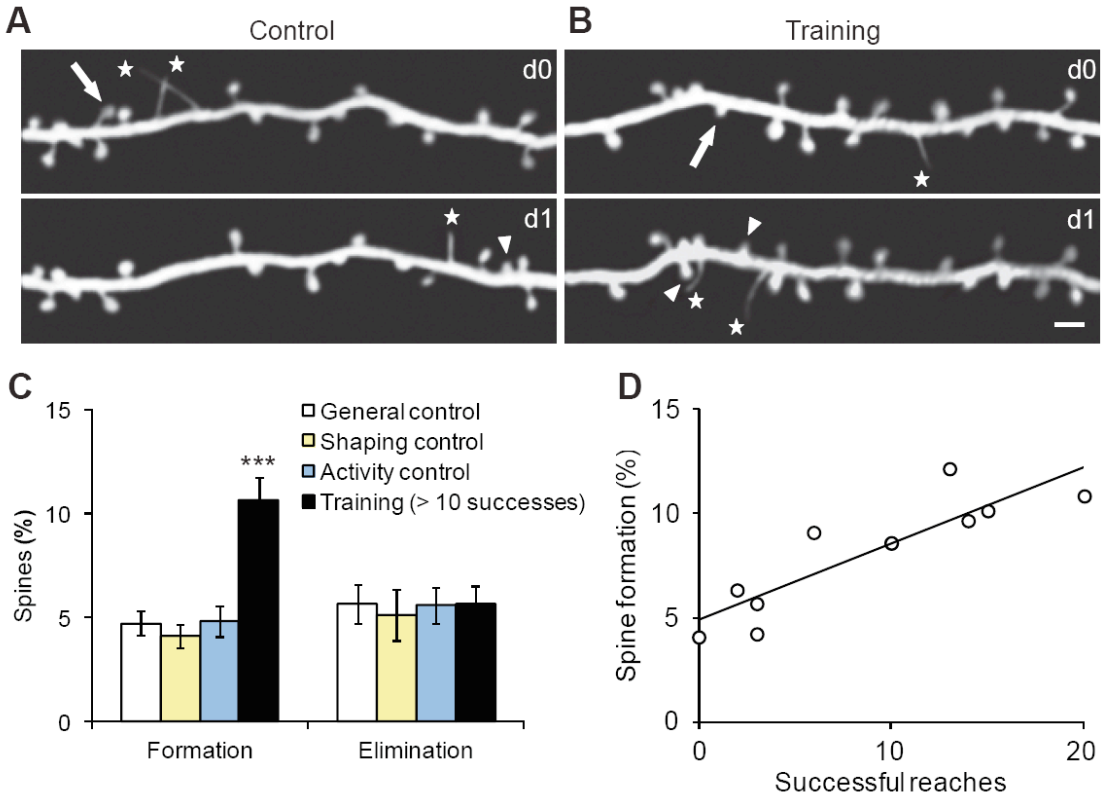

Figure 9. Motor skill learning in adolescent mice promotes immediate spine formation in the contralateral motor cortex.

(A, B) Repeated imaging of the same dendritic branches over one-day intervals reveals spine elimination (arrows) and formation (arrowheads), and filopodia (stars) in a general control (A) and a trained (B) mouse. Scale bar, 2 μm. (C) Percentage of spines formed and eliminated under various control and training conditions immediately following the first training session. (D) The degree of spine formation observed following the first training session is linearly correlated with the number of successful reaches during this session (R^2=0.77). Data are presented as mean ± s.d. (***P<0.001).

2.3.2 Prolonged motor learning promotes spine elimination in the motor cortex

Perfection of a motor skill often requires persistent practice over time. To examine how prolonged learning affects spine dynamics, we trained and imaged mice over different periods of time (i.e., from 2 to 16 days). We found training for 2 days and longer resulted in significant increases, not only in spine formation, but also in spine elimination (Figures 10A and 10B, $P<0.005$ at all time points). Although delayed, this increase in spine elimination ultimately resulted in the total spine density in the trained animals returning to control levels by day 16 (Figure 10C).

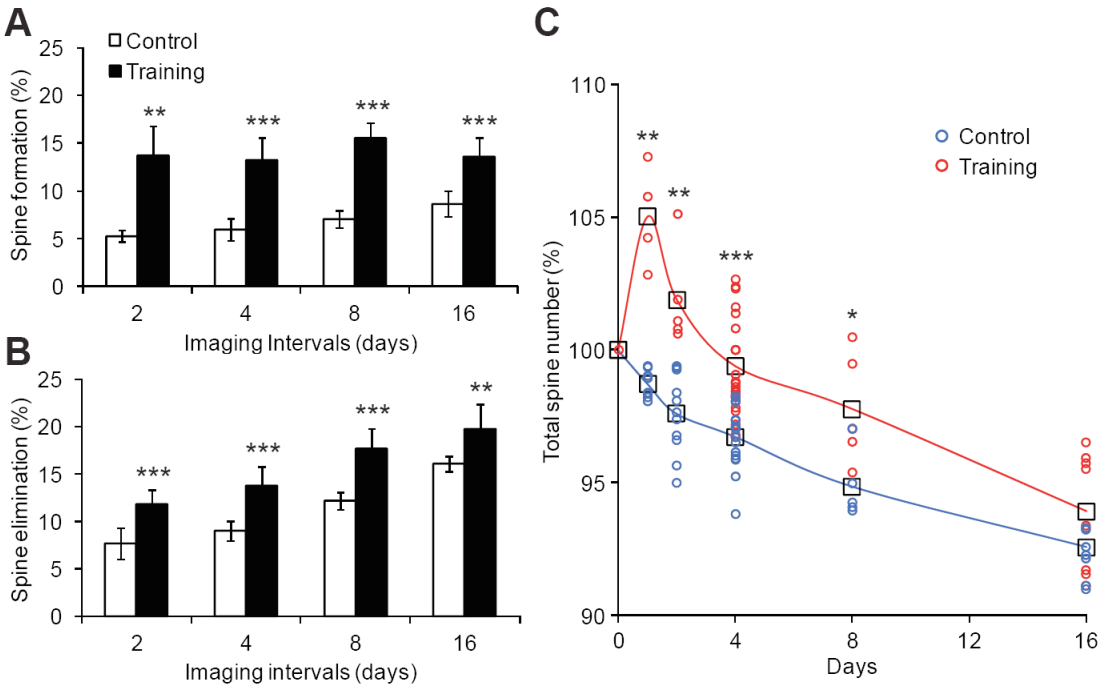

Figure 10. Prolonged motor learning promotes spine elimination.

(A, B) Percentage of spines formed (A) and eliminated (B) under control and training conditions. (C) Total spine number increases during initial learning, but returns to

normal levels with prolonged training. Data are presented as mean ± s.d. (*P<0.05, **P<0.01, ***P<0.001).

As a control, we measured spine formation and elimination over a 4-day training period in the ipsilateral (to the trained limb) primary motor cortex and the contralateral posterior sensory cortex, and found no significant increase in spine formation or elimination in either case (Figure 11, P>0.2). In addition, mice that failed to learn also failed to show an increase in either spine formation or elimination in the contralateral motor cortex (Figure 11, P>0.6). Therefore, the observed changes in spine dynamics are region- and learning-specific, indicating that motor learning causes synaptic reorganization in the corresponding motor cortex.

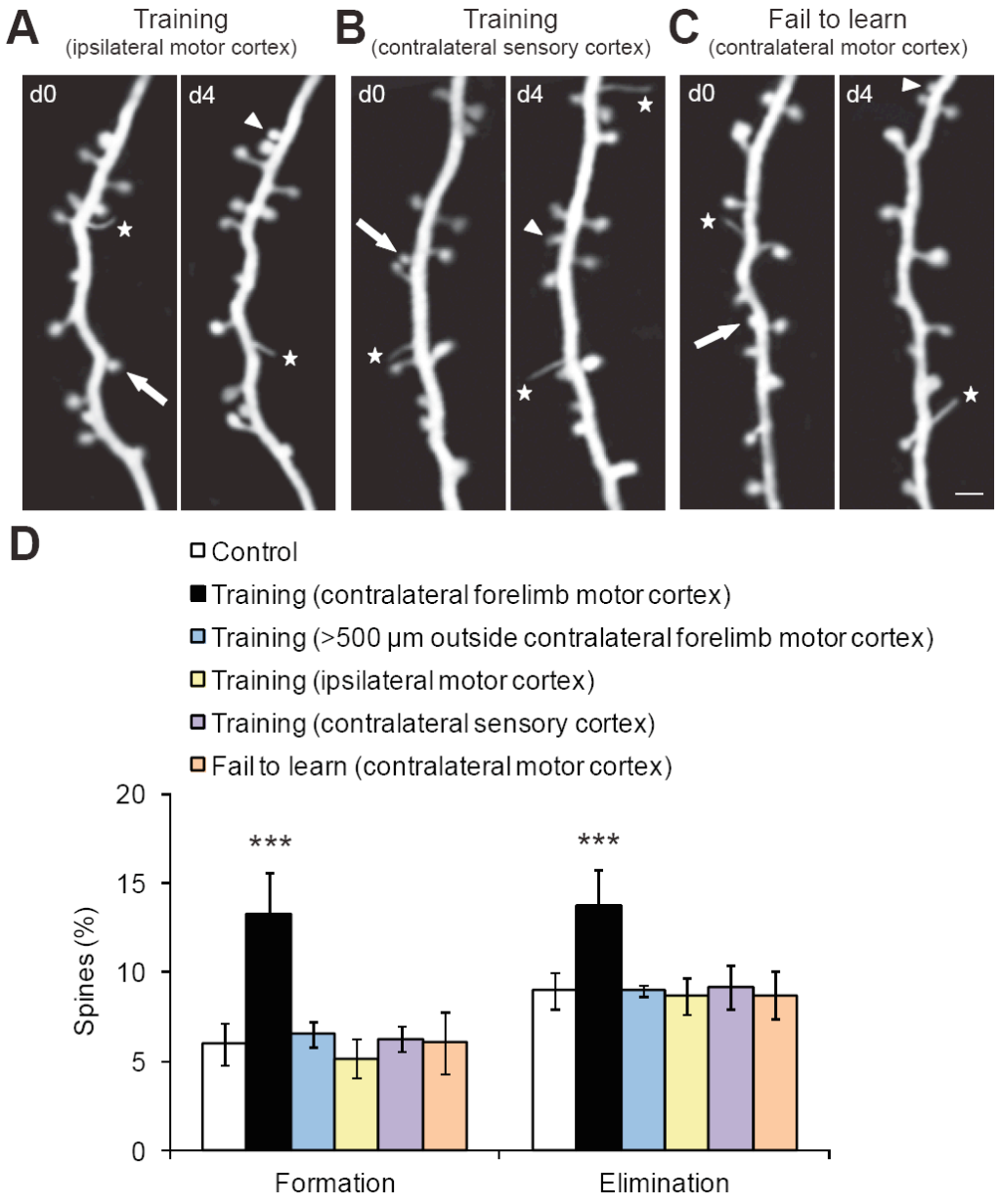

Figure 11. Enhanced spine dynamics during adolescent motor training is region- and learning-specific.

(A-C) Imaging of the same dendritic branches over 4 days in the ipsilateral primary motor cortex (A), and the contralateral sensory cortex (B) of the trained mice. (C) Imaging of the same dendritic branches over 4 days in the contralateral motor cortex of a mouse that failed to learn the task. Scale bar, 2 µm. (D) Percentage of spines

formed and eliminated under various conditions. Data are presented as mean ± s.d. (*P<0.05, **P<0.01, ***P<0.001).

2.3.3 Motor learning specifically stabilizes new spines formed during learning

The enhanced spine loss following rapid spinogenesis reflects a rewiring of the neuronal circuitry in response to learning, rather than a simple addition of new spines. To examine how learning reorganizes synaptic connections, we imaged the same mice three times, classified imaged spines into new and pre-existing spines based on their appearance in the initial two images, and then quantified their survival percentages in the third images (Figure 12).

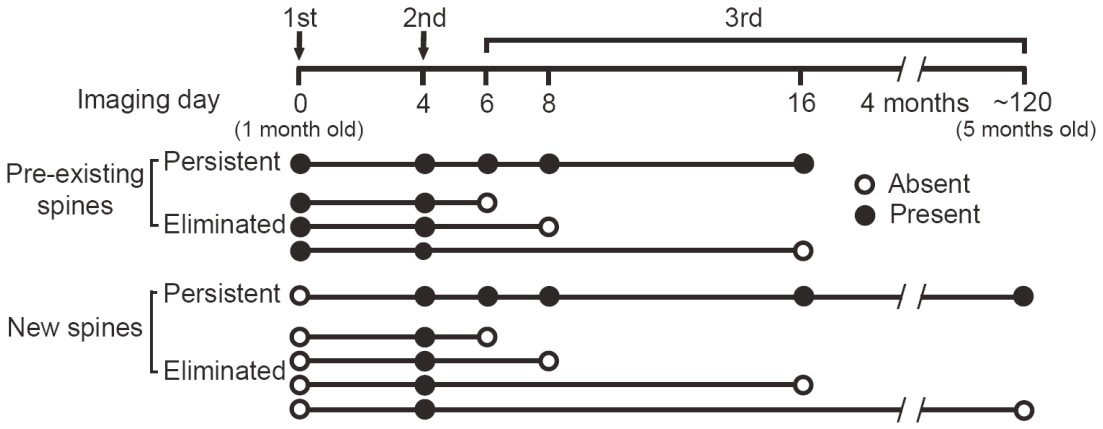

Figure 12. Timeline of experiments, showing possible outcomes.

Our data show that new spines are less stable than pre-existing spines in general (Figure 13). Specifically, in control mice, 43.8±3.1%, 25.8±5.3%, and 19.2±4.6% of the spines that formed between days 0 and 4 remained by days 6, 8 and 16,

respectively. During the same period of time, 96.7±0.5%, 94.9±1.1% and 92.8±1.9% of the pre-existing spines remained (Figure 13C, $P<0.001$ compared to new spines). These results suggest that new spines are initially unstable and undergo a prolonged selection process before being converted into stable synapses. In addition, we found that new spines were significantly more stable in trained mice, with 64.1±2.2%, 55.3±4.1% and 51.0±4.8% of the spines that formed during the initial 4-day training remaining by days 6, 8 and 16, respectively (Figure 13C, $P<0.001$ compared to new spines in control mice). In contrast, pre-existing spines in trained mice were significantly less stable than control mice over the same time periods (Figure 11C, $P<0.05$). More importantly, when the fate of the new spines formed during initial learning (day 0-4) was examined months later (day 120), we found that 42.3±2.9% of new spines persisted in the mice trained for 16 days during adolescence, while only 13.5±1.7% of new spines remained in the control mice (Figure 13C, $P<0.001$).

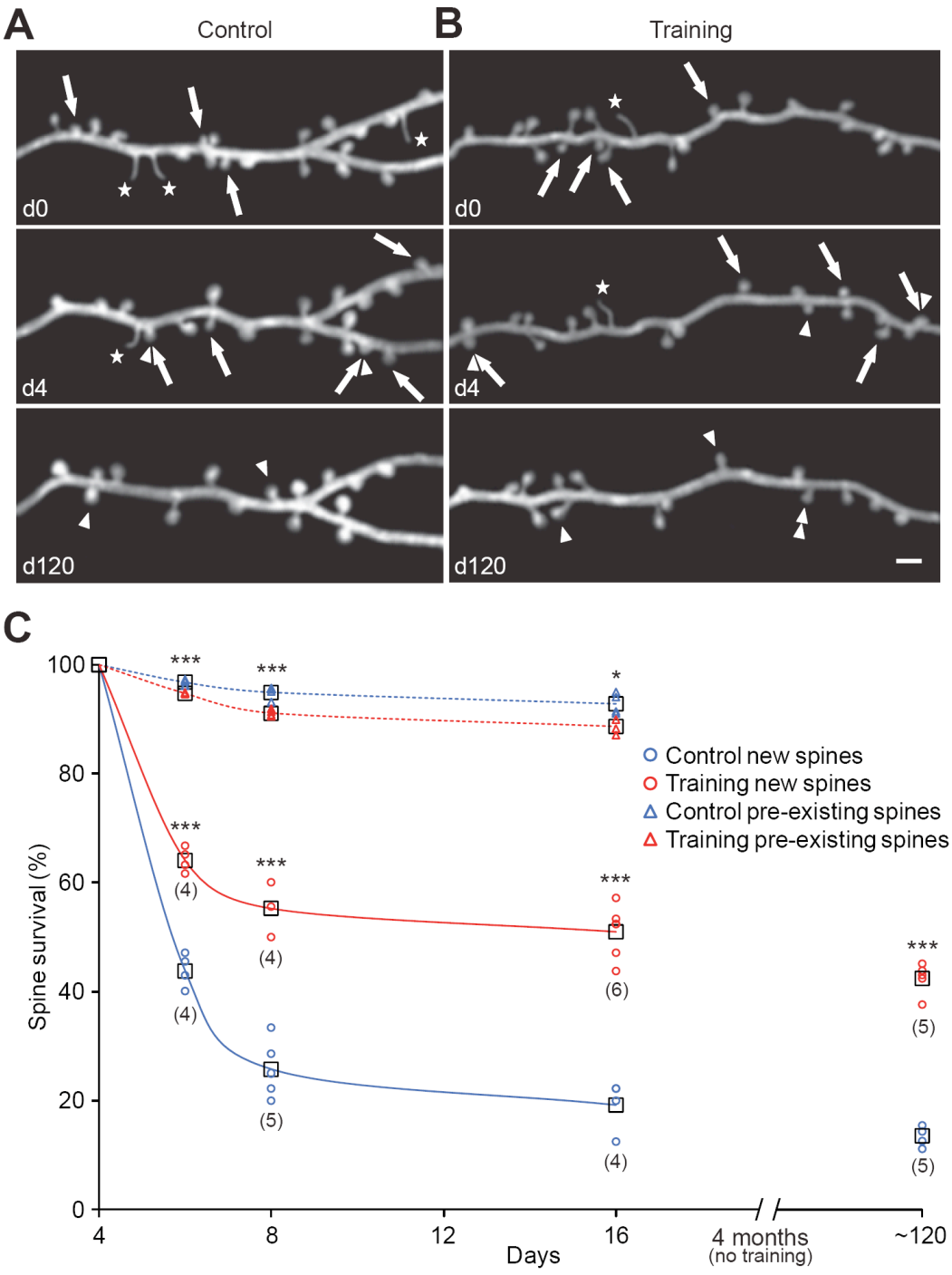

Figure 13. Motor skill learning stabilizes newly formed spines.

(A, B) Repeated imaging of dendritic branches at 0, 4 and 120 days in a control (A) and a trained mouse (B). Scale bar, 2 µm. (C) Percentages of surviving new and pre-

existing spines, as a function of time, for control and trained animals. Data are presented as mean ± s.d. (*P<0.05, ***P<0.001). Numbers of animals examined at each time point are indicated below new spine data points.

In addition, we found that spine formation and stabilization were associated with behavioral improvement. More new spines were formed daily during the learning acquisition phase (days 1-4) than during the learning maintenance phase (days 5-16); and the new spines that were formed during learning acquisition, but not during maintenance, were preferably stabilized with continuous training (Figure 14). Taken together, these data indicate that motor learning selectively stabilizes learning-induced new spines and destabilizes pre-existing spines. The prolonged persistence of learning-induced synapses provides a potential cellular mechanism for the consolidation of lasting, presumably permanent, motor memories.

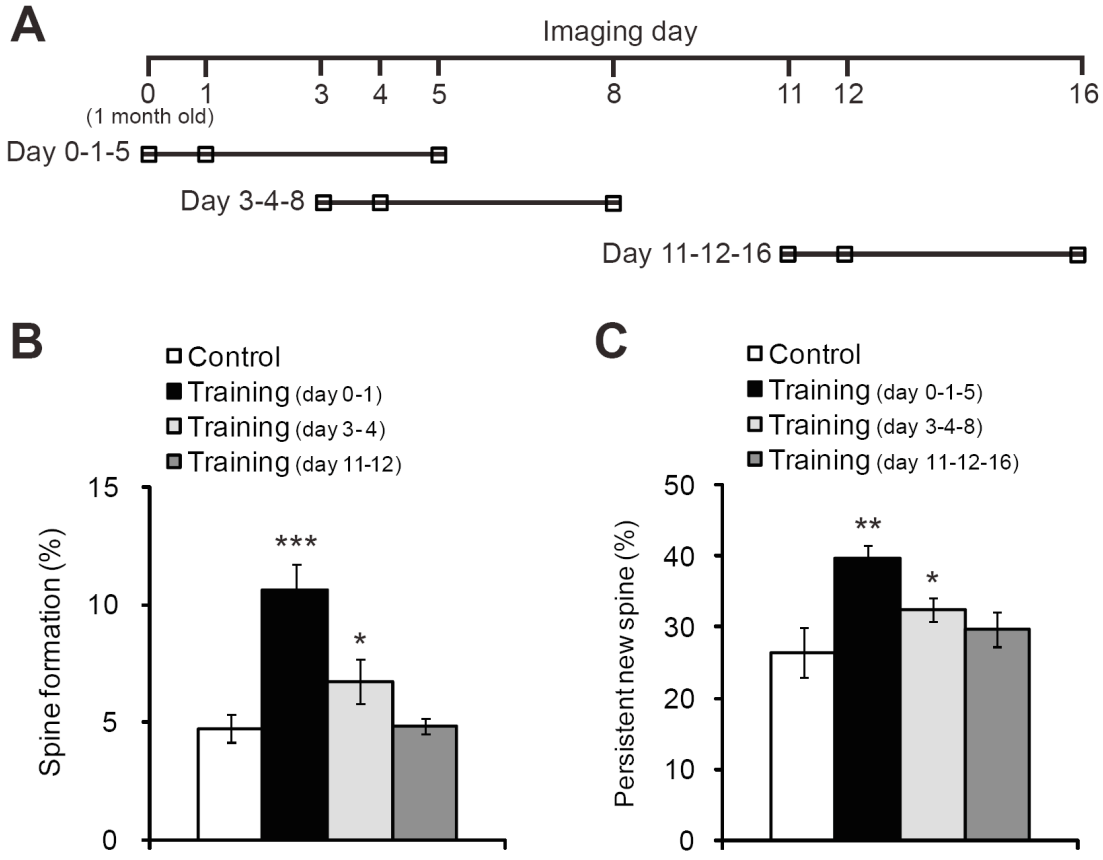

Figure 14. New spines formed during learning acquisition, but not learning maintenance, have higher survival rates than controls.

(A) Timeline of experiments, showing the imaging days. (B) Percentages of spines formed over one day in control, and on training day 1, 4 and 12. (C) Survival rates of new spines in all the categories in (B) over 4 days. Data are presented as mean ± s.d. (**P*<0.05, ***P*<0.01, ****P*<0.001).

2.3.4 Motor learning has no effect on the dynamics of dendritic filopodia

Dendrites in the mammalian brain contain not only spines, but also filopodia. Filopodia are long, thin protrusions without bulbous heads, and make up ~10% of the total dendritic protrusions in the motor cortex of one-month-old mice. Previous

studies suggest that filopodia are precursors of dendritic spines (Dailey and Smith, 1996; Ziv and Smith, 1996). We found that filopodia were very dynamic in the mouse motor cortex *in vivo* (Figure 15). Most of them turned over within one day in control mice (79.3±12.8% formation and 87.6±5.9% elimination), and motor learning had no effect on filopodial formation and elimination (91.0±15.3% formation and 86.5±8.8% elimination, $P>0.2$).

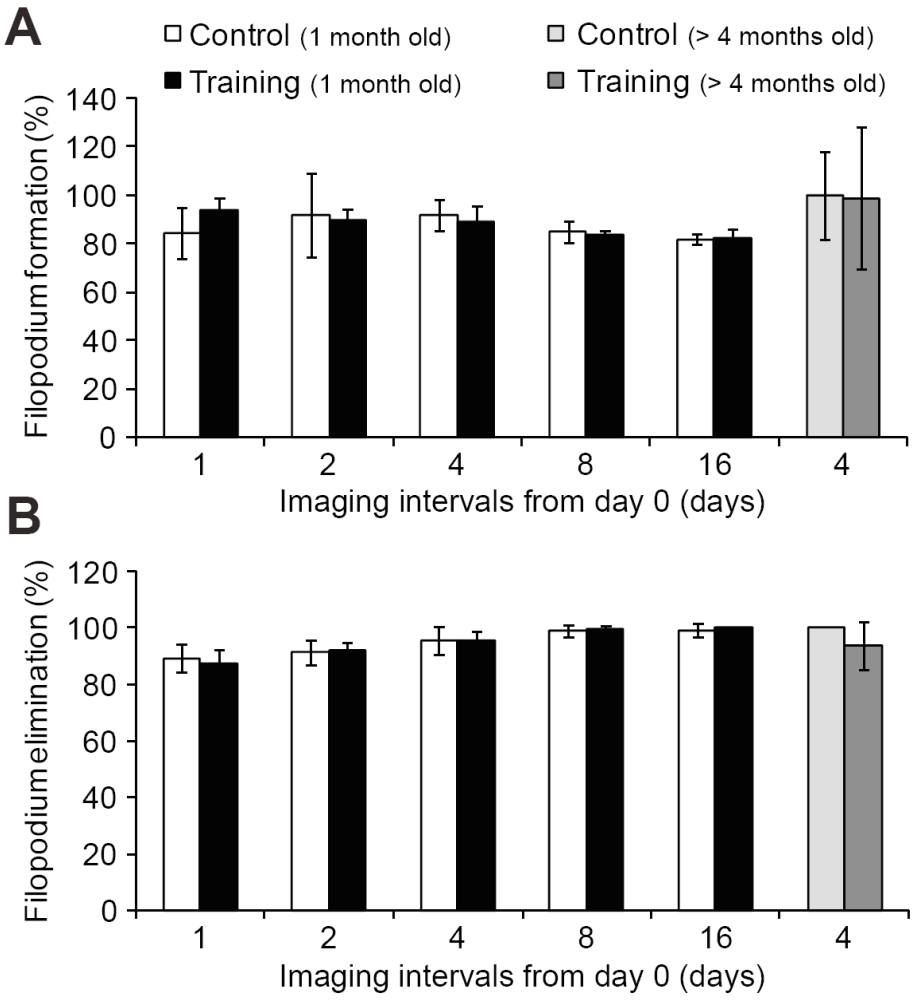

Figure 15. Dynamics of filopodia in various control and training mice.

Percentages of filopodia formed (A) and eliminated (B) under various control and training conditions. Data are presented as mean ± s.d.

Among the filopodia observed in the initial images, few of them became spines over the following day in control mice (6.3%). However, this filopodium-to-spine transition was enhanced by motor skill learning (13.1%). Furthermore, 25% of new spines formed from filopodia on training day 1 persisted after another 4 days of training, suggesting a contribution of filopodia to the rewired neuronal circuitry.

Furthermore, when filopodia and spines were pooled together for analysis, there was a ~10% increase in the dynamics of both control and training categories. Thus, the conclusion of motor learning on total protrusions was consistent with the spine analysis alone (Figure 16).

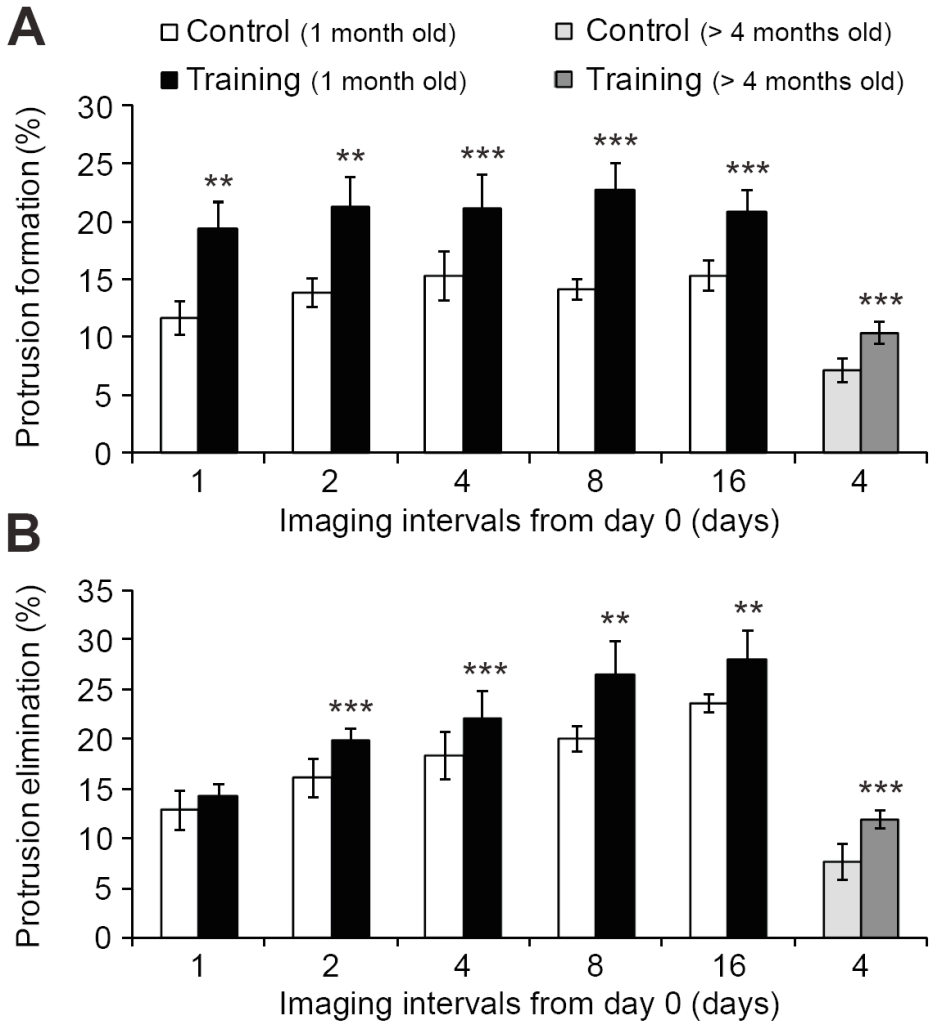

Figure 16. Dynamics of total dendritic protrusions in various control and training mice.

Percentages of total dendritic protrusions (filopodia plus spines) formed (A) and eliminated (B) under various control and training conditions. Data are presented as mean ± s.d. (**P<0.01, ***P<0.001).

2.3.5 Long-lasting motor memory is associated with the persistence of learning-induced new spines

One of the important characteristics of motor learning is that, once the skill is well learned, its further maintenance does not require constant practice. To test whether lasting motor memories might be contained within structurally stable neural circuits, we trained young mice for 8-16 days to acquire the reaching skill, housed them in control cage conditions for 4 months, and retrained them on the same task in adulthood. We found that these pretrained mice maintained skillful performance with high success rates even on the first day of reintroducing the reaching task (Figure 17).

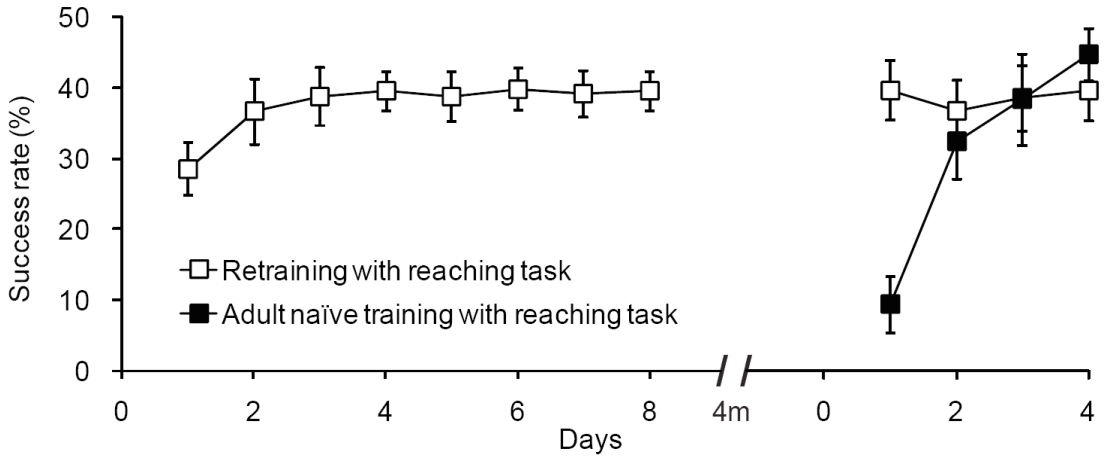

Figure 17. Pretrained mice start with high success rates during adult retraining. Data are presented as mean ± s.e.m, 10 naïve trained and 14 retrained adults.

Imaging of these pretrained adult mice showed that spine formation and elimination during retraining were similar to those of naïve adults without training (Figures 18A,

18D and 18F, $P>0.1$ for 4 and 8 days). In contrast, naïve adults learning the reaching task for the first time had a learning curve similar to adolescent mice, and showed significantly higher spine formation and elimination than control adults (Figures 17, 18A, 18B and 18F, 4 and 8 days, $P<0.01$ with control for both formation and elimination). Next, we asked if learning a novel motor skill continued to drive synaptic reorganization in the pretrained brain. To do this, we trained mice which had been pretrained on the reaching task with a new motor task – the capellini handling task, which also requires fine forelimb motor skills. We found that pretrained mice, similar to naïve adults, had enhanced spine formation and elimination during the training of this novel skill task (Figures 18C, 18E and 18F, $P<0.001$ compared to control adults). Despite high spine dynamics induced by novel skill learning, most spines, that were formed during adolescent learning of the reaching task and maintained in adults, persisted after training with the capellini handling task (95.6±7.7%), suggesting that already stabilized synapses are not perturbed by novel learning in adults.

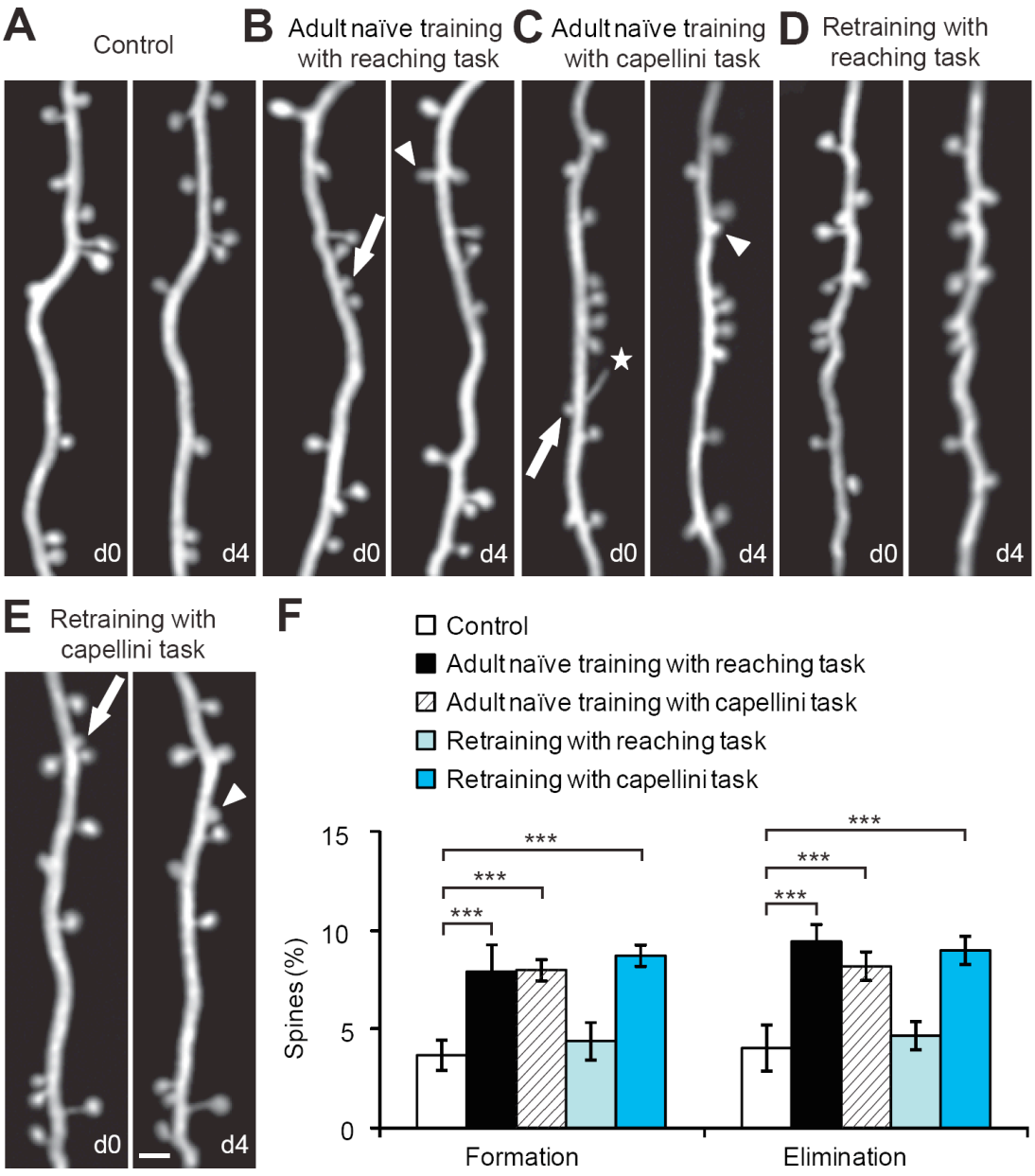

Figure 18. Novel motor skill training promotes spine formation and elimination in adult mice.

(A-E) Repetitive imaging of dendritic branches over 4 days in a control adult (A), naïve adults training with the reaching task (B) and capellini handling task (C), pretrained adults retraining with the same reaching task (D) and the new capellini handling task (E). Scale bar, 2 μm. (F) Percentages of spines formed and eliminated

over 4 days in adult mice under different conditions. Data are presented as mean ± s.d. (***P<0.001).

In summary, these results suggest that synaptic structural coding outlasts the early learning experience and persists in adulthood to support later maintenance of motor skills. The fact that novel learning experiences continue to drive synaptic reorganization without affecting the stability of synapses formed during previous learning further suggests that different motor behaviors are stored using different sets of synapses in the brain.

2.4 Discussion

Our study investigated the process of synapse reorganization in the living brain during natural learning, distinguishing it from several studies where changes were triggered by non-physiological sensory manipulation (Hofer et al., 2009; Holtmaat et al., 2006; Keck et al., 2008; Lendvai et al., 2000; Trachtenberg et al., 2002; Zuo et al., 2005b). Although rapid synapse formation has been observed during LTP *in vitro* (Engert and Bonhoeffer, 1999; Toni et al., 1999), we show, for the first time, that synapse formation in the neocortex begins immediately as animals learn a new task in the living brain (within 1 h of training initiation). Such high spine formation does not occur with motor activity alone or later practice of the established skill. The rapidity of the response contradicts the general assumption that significant synaptic structural

remodeling in motor cortex takes days to occur, following more subtle cellular activity and changes in synaptic efficacy (Adkins et al., 2006; Kleim et al., 2004; Rioult-Pedotti et al., 2000). One recent study on brain slices shows that glutamate-sensitive currents expressed in newly formed spines are indistinguishable from mature spines of comparable volumes (Zito et al., 2009), further suggesting that the new spines formed during learning are likely active. Furthermore, the persistence of new spines over months provides a long-lasting structural basis for the enhanced synaptic strength that is retained even when the task performance is discontinued.

Many previous studies have used fixed tissue preparation to investigate changes in synapse number and dendritic complexity following motor skill learning (Greenough et al., 1985; Kleim et al., 2002; Kleim et al., 1997; Kolb et al., 2008; Withers and Greenough, 1989). Our *in vivo* imaging of superficial dendrites from layer V pyramidal neurons revealed that postsynaptic dendritic spine addition was rapid, but eventually counteracted by the loss of pre-existing spines, resulting in a time-dependent spine density change during motor learning. While the synaptogenesis observed in our study is compatible with earlier results, its temporal relationship with behavioral improvement and the contribution of synapse elimination in circuitry reorganization in other brain layers and regions during motor learning require further investigation. This eventual balancing of synapse number could be a homeostatic mechanism by which the output layer V neurons integrate converging inputs into superficial cortical layers to govern precise fine motor control.

Chapter III Accelerated Experience-dependent Pruning of Cortical Synapses in *Ephrin-A2* Knockout Mice

3.1 Introduction

Postnatal experience-dependent synapse elimination is crucial for the establishment of properly connected neuronal circuits in the mature brain. Synapse elimination prunes the supernumerary imprecise connections formed during the initial overproduction of synapses, while strengthening functionally important connections (Changeux and Danchin, 1976; Hubel et al., 1977; Katz and Shatz, 1996; Lichtman and Colman, 2000). The majority of excitatory glutamatergic synapses in the mammalian brain reside at dendritic spines, which contain all necessary postsynaptic signaling machinery and serve as a good proxy for synaptic connectivity (Nimchinsky et al., 2002; Segal, 2005; Tada and Sheng, 2006; Yuste and Bonhoeffer, 2001). Recent *in vivo* two-photon imaging studies have shown that dendritic spines of cortical pyramidal neurons across various cortical regions undergo rapid elimination during adolescent development. In the adult brain, spine elimination continues at a much lower rate, and spines surviving the pruning process build the foundation of the mature circuits (Holtmaat et al., 2005; Yang et al., 2009; Zuo et al., 2005a; Zuo et al., 2005b). Although experience or activity-dependent plasticity is believed to drive the

extensive and prolonged synapse pruning, the molecular mechanisms underlying this process remain largely unknown.

The membrane-bound cell adhesion molecules, ephrins, and their Eph receptors, are attractive candidates for modulating structural plasticity of synapses, because of their synaptic expression and ability to coordinate contact-mediated bidirectional signaling in ligand- and receptor-containing cells (Aoto and Chen, 2007; Klein, 2009; Lai and Ip, 2009; Murai and Pasquale, 2004). Based on their cell membrane attachment and binding preference to Eph receptors, ephrins are classified into two groups: 1) GPI-linked ephrin-As that preferentially interact with EphA receptors and 2) transmembrane ephrin-Bs that preferentially bind to EphB receptors. While it is generally believed that ephrin-Bs and EphB receptors act through trans-synaptic interactions to modulate synapse development and plasticity (Contractor et al., 2002; Lim et al., 2008; McClelland et al., 2010; Penzes et al., 2003; Xu et al., 2011), ephrin-As and EphA receptors have been shown to mediate astrocyte-neuron interactions at mature hippocampal synapses. In particular, ephrin-A3 ligands are expressed in astrocytic processes, and EphA4 receptors are localized to postsynaptic spines of CA1 pyramidal neurons (Murai et al., 2003). In cultured hippocampal slices, while activation of EphA4 receptors by ephrin-A3 ligands induces spine retraction, disruption of this interaction leads to elongation of spine length (Murai et al., 2003). Consistent with this finding, elongated spine morphology has been described in the

hippocampi of both *ephrin-A3* KO and *EphA4* KO mice (Carmona et al., 2009; Murai et al., 2003).

Here, we show that experience-dependent elimination of dendritic spines from cortical pyramidal neurons is greatly enhanced in *ephrin-A2*, but not *ephrin-A3*, KO mice during adolescent development. The imbalance between spine formation and elimination leads to an accelerated reduction in the number of total spines in young adult mice. We also find that glial glutamate transporters (GLAST and GLT-1) are closely associated with ephrin-A2 proteins and are significantly down-regulated in *ephrin-A2* KOs. Furthermore, the elevated spine loss in *ephrin-A2* KOs requires activation of NMDA-type glutamate receptors.

3.2 Methods

3.2.1 Animals

Thy1-YFP-H line mice (Feng et al., 2000) were purchased from Jackson Laboratory. *Ephrin-A2* and *ephrin-A3* KO mice (Cutforth et al., 2003; Feldheim et al., 2000) were obtained from Dr. David A. Feldheim at UCSC. Wild-type littermates were used as controls and no difference in all analyses was observed between wild-type and heterozygous mice. Protocols for sensory manipulations and MK801 treatment have been previously described (Yang et al., 2009; Zuo et al., 2005a). MK801 (0.25 μg/g

body weight) was intraperitoneally injected twice a day. Mice were housed and bred in UCSC animal facilities according to approved animal protocol.

3.2.2 Array tomography and data quantification

Array tomography experiments were performed as previously described (Micheva and Smith, 2007). Briefly, the mouse brain was dissected, fixed, dehydrated and embedded in LR white resin. Serial 70 nm sections of the tissue were obtained and then probed consecutively with the following primary antibodies: mouse anti-bassoon (1:100; Abcam), mouse anti-GS (1:100; BD Biosciences), rabbit anti-PSD95 (1:100; Cell Signaling Technology), mouse anti-SV2 (1:100; DSHB), rabbit anti-synapsin (1:100; Cell Signaling Technology), guinea pig anti-VGluT1 (1:100; Millipore), rabbit anti-GLAST (1:100), rabbit anti-GLT-1 (1:100), rabbit anti-ephrin-A2 (1:100; Santa Cruz Biotechnology) and goat anti-ephrin-A3 (1:100; Invitrogen).

All images were obtained using a Zeiss Axio Imager.Z1 Upright Fluorescence Microscope with motorized stage and Axiocam HR Digital Camera. Image data from sequential sections were computationally aligned, registered and unwarped, as previously described (Micheva et al., 2010; Micheva and Smith, 2007). The center for each of the protein punctum was identified and the density of protein puncta was obtained by dividing the number of centers with the tissue volume (image volume subtracted by the volume of the nuclei). For distance analysis, 1 μm spheres were created for all centers of the measured proteins. Centers of other protein channels

within these spheres were identified and their relative distances to the sphere centers were measured. Puncta densities (the number of puncta/volume of each bin, which was a spherical shell) for the protein of interest were plotted as a function of the distance relative to other proteins within measured volume. *P*-values were calculated using the Student's *t*-test.

3.2.3 *In vivo* transcranial imaging and data quantification

The surgical procedure for transcranial two-photon imaging and data quantification has been described previously (Sections 2.2.2 and 2.2.3). Percentages of eliminated and formed spines were normalized to total spines counted in the initial image. Spine density was calculated by dividing the number of spines by the length of the dendritic segment. Data were presented as mean ± standard deviation (s.d.). *P*-values were calculated using the Student's *t*-test. A non-parametric Mann-Whitney test was used to confirm all conclusions. For the spine lifetime analysis, data were fitted with a two-exponential-decay equation using GraphPad Prism: percentage of survival spine = $p_1 \times (1/2)^{t/\tau 1} + p_2 \times (1/2)^{t/\tau 2}$ (p_1 and p_2: proportion of fast- and slow-decay spines, $p_1 + p_2 = 100\%$; τ_1 and τ_2: half-life of fast- and slow-decay spines).

3.2.4 Westerns blots and data quantification

Mice were sacrificed by decapitation, and cortical tissues were immediately dissected and homogenized in ice-cold RIPA buffer solution. After protein quantification,

denatured lysates were electrophoretically separated by 10% SDS-PAGE (20 μg per lane) and transferred onto nitrocellulose membrane. This was then probed at 4 °C overnight with the following primary antibodies: rabbit anti-GLAST (1:5,000), rabbit anti-GLT-1 (1:5,000), mouse anti-GS (1:90,000; BD Biosciences) and mouse anti-tubulin (1:5,000; Millipore). Horseradish peroxidase (HRP)-conjugated secondary antibodies (1:5,000; Cell Signaling Technology) were used and detection was performed with luminol. Western blots were quantified using ImageJ software. GLAST, GLT-1 and GS levels were normalized to tubulin. Data were presented as mean ± s.e.m. *P*-values were calculated using the Student's *t*-test.

3.2.5 Immunohistochemistry and data quantification

Anesthetized mice were transcardially perfused with PBS followed by 4% paraformaldehyde (PFA). Brains were dissected and postfixed in 4% PFA for 2-4 hours, then cryoprotected in 30% sucrose until sectioning. Serial 40 μm sections were collected and incubated with rabbit anti-S100β primary antibody (1:40,000; Dako) overnight at 4 °C, followed by incubation with biotinylated secondary antibody (1:400; Vector), avidin-biotin complex (ABC, Vector), and diaminobenzidine (Vector) for visualization. Bright-field images were collected on Zeiss Axio Imager.M2, using Axiovision software. Both numbers and cell body volumes of S100β-positive cells were obtained using stereological image analysis software (StereoInvestigator, Microbrightfield). Data were presented as mean ± s.e.m.

3.3 Results

3.3.1 *Ephrin-A2* KO mice have elevated spine elimination in the cortex during adolescent development

To investigate whether and how ephrin-As affect synapse development, we crossed *ephrin-A2* or *ephrin-A3* single and double KO mice with YFP-H line mice, which express cytoplasmic yellow fluorescent protein (YFP) predominantly in a subpopulation of layer V cortical neurons (Feng et al., 2000). We found normal gross cortical morphology (Figure 19) and lamination (Figure 20) of the cortex in both *ephrin-A2* and *ephrin-A3* KO mice at one month of age.

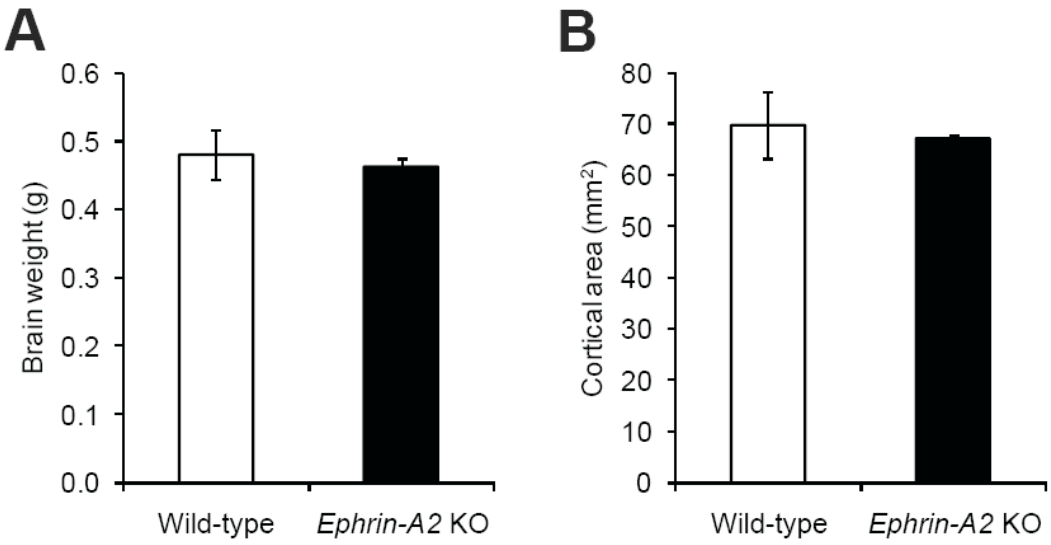

Figure 19. Gross brain morphology is normal in *ephrin-A2* KO mice at one month old of age.

Ephrin-A2 KO mice have comparable brain mass (A) and cortical surface area (B) with age-matched wild-type mice.

Figure 20. Cortical lamination is normal in *ephrin-A2* KO mice at one month old of age.

(A, B) Nuclear labeling of the coronal sections from the motor (A) and the barrel (B) cortices of wild-type and *ephrin-A2* KO mice, with endogenous YFP-labeled neurons. Scale bar, 250 μm. (C, D) Quantifications of the proportion of different layers in the motor (C) and the barrel (D) cortices reveal normal laminar distribution patterns in *ephrin-A2* KO mice. Data are presented as mean ± s.d.

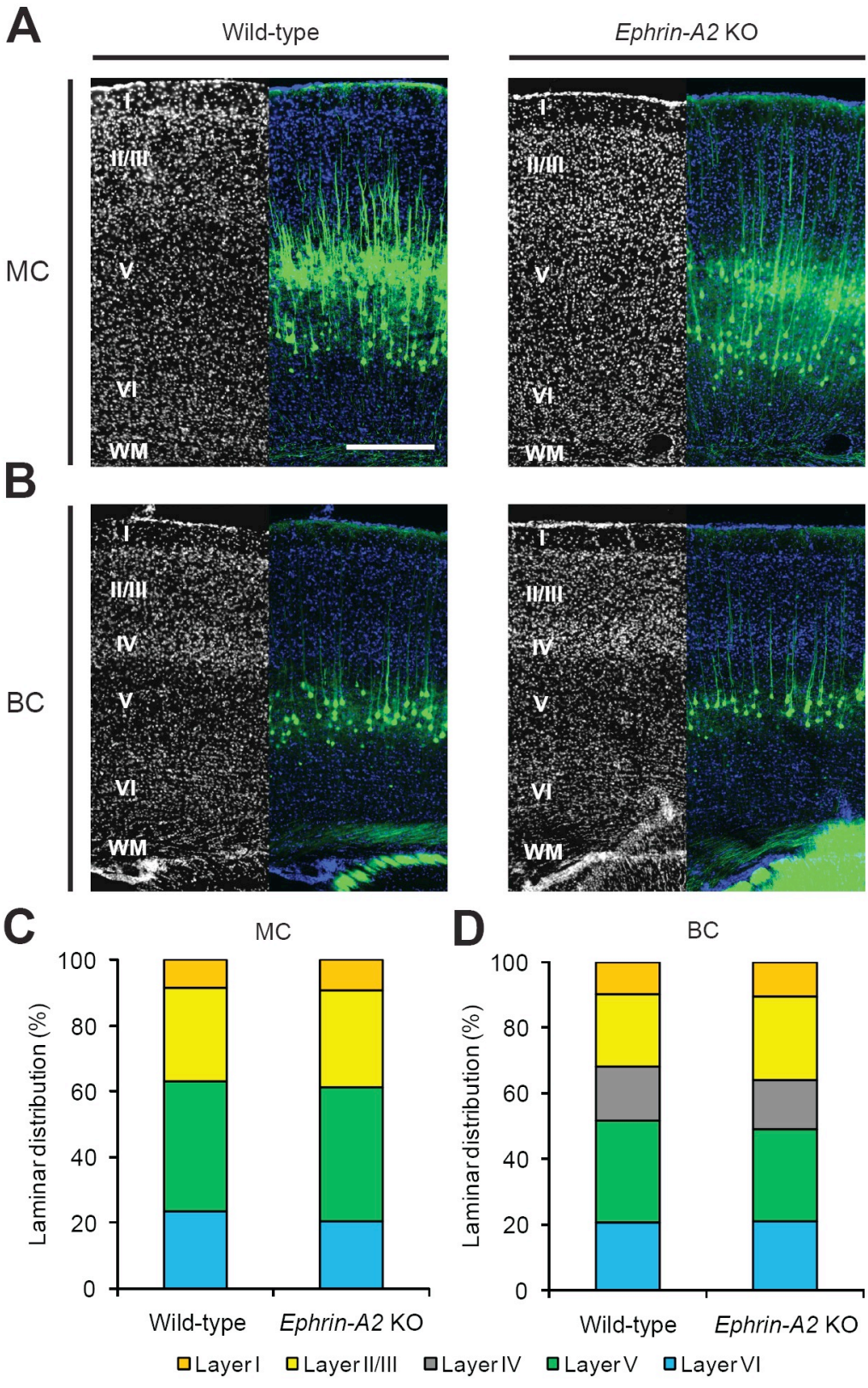
A
Wild-type
Ephrin-A2 KO
MC
I
II/III
V
VI
WM
B
BC
IV
C
MC
D
BC
Laminar distribution (%)
100
80
60
40
20
0
Wild-type
Ephrin-A2 KO
Layer I
Layer II/III
Layer IV
Layer V
Layer VI

To determine if spine dynamics were affected in *ephrin-A* KO mice, we repeatedly imaged apical dendritic branches and followed spine dynamics in the motor cortex by transcranial two-photon microscopy (Figure 21). We found that, while the amount of new spines added over 2 days was comparable between *ephrin-A2* KOs and their wild-type littermates, significantly more spines were eliminated during the same period of time in KOs (Figure 22; 11.1±1.0% vs. 7.1±1.0%, $P<0.001$). Unlike *ephrin-A2* KOs, *ephrin-A3* KOs exhibited similar spine turnover to wild-type controls (Figure 22; $P>0.1$ for both formation and elimination). In addition, spine elimination over 2 days in *ephrin-A2/A3* double KOs was comparable to that of *ephrin-A2* single KOs (Figure 22; 10.9±0.8%, $P>0.7$).

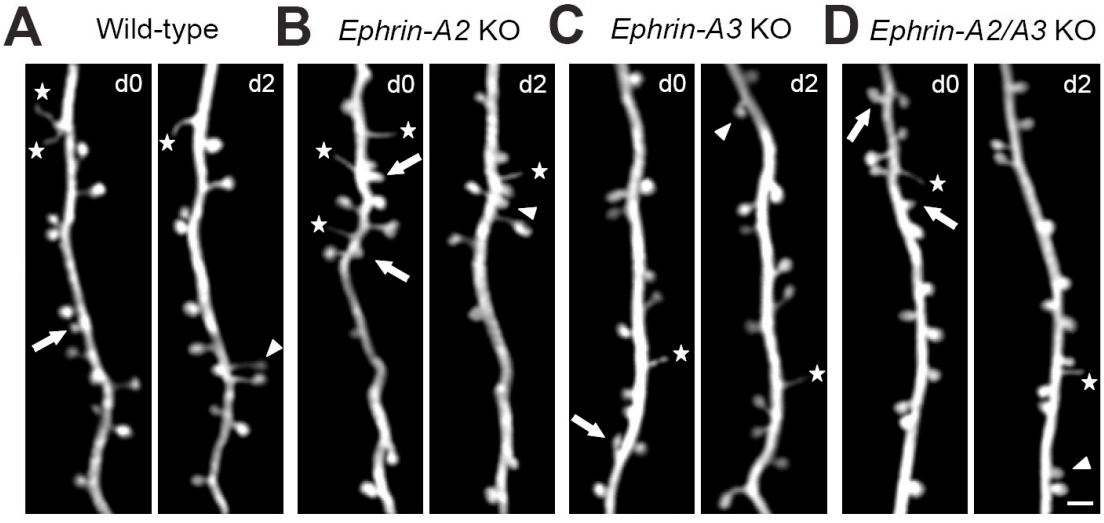

Figure 21. Examples of repeated imaging of the same dendritic branches over two-day intervals in the motor cortex.

Spine elimination (arrows) and formation (arrowheads), as well as filopodia (stars) are indicated in wild-type (A), *ephrin-A3* KO (B), *ephrin-A2* KO (C) and *ephrin-A2/A3* double KO (D) mice. Scale bar, 2 μm.

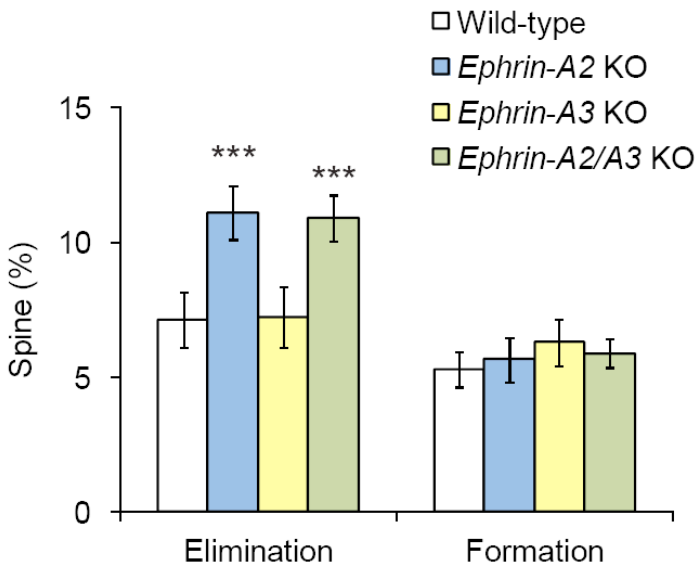

Figure 22. Dendritic spine elimination, but not formation, is significantly increased in one-month-old *ephrin-A2* KO mice.

Percentages of spines eliminated and formed over 2 days in the motor cortex of wild-type and KO mice. Data are presented as mean ± s.d. (**P*<0.05; ***P*<0.01; ****P*<0.001).

Finally, we found that the increase in spine elimination occurred in various cortical regions of *ephrin-A2* KOs (Figure 23), and persisted over prolonged imaging intervals (Figure 24A). As a consequence, despite the normal spine density at one month of age (*P*>0.2), spine density of 2-month-old *ephrin-A2* KOs was significantly lower than that of wild-type mice (Figure 24B, 0.36±0.01 vs. 0.41±0.01 spines/μm, *P*<0.005).

Thus, the developmentally-regulated reduction in total spine numbers is accelerated in *ephrin-A2* KOs.

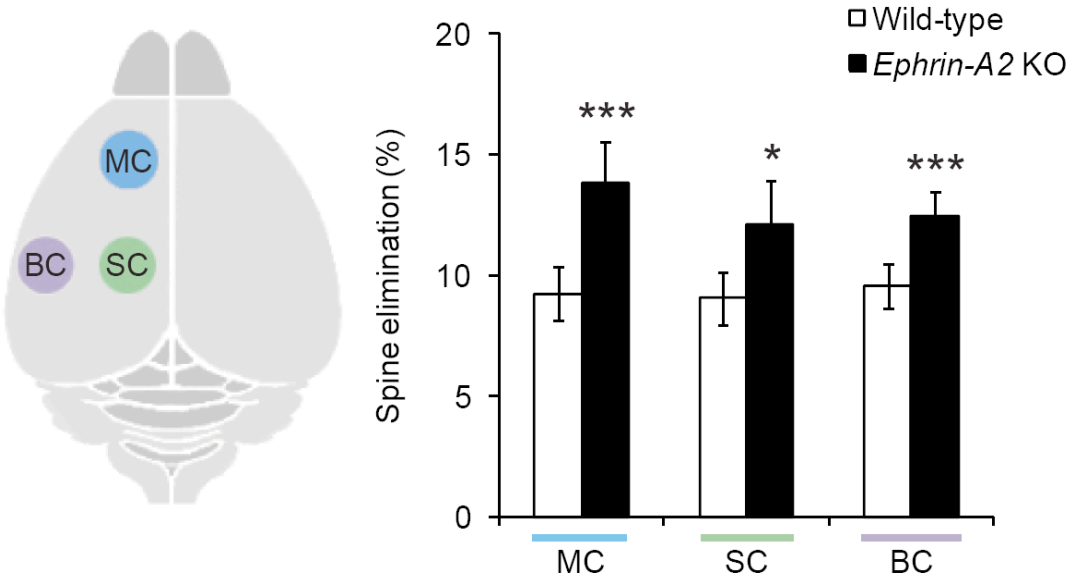

Figure 23. Spine elimination is significantly increased in various cortical regions of *ephrin-A2* KO mice.

Percentages of spines eliminated in the motor cortex (MC), the sensory cortex (SC) and the barrel cortex (BC) over 4 days in wild-type and *ephrin-A2* KO mice at one month of age. Data are presented as mean ± s.d. (*P<0.05; ***P<0.001).

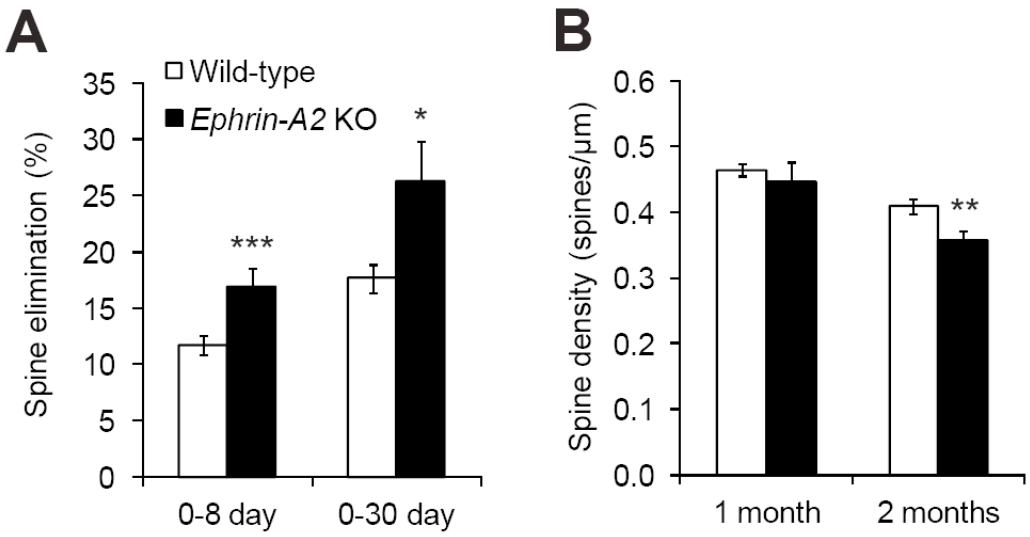

Figure 24. Accelerated pruning of dendritic spines in the cortex of adolescent *ephrin-A2* KO mice.

(A) Percentages of spines eliminated over 8 and 30 days in the motor cortex of wild-type and *ephrin-A2* KO mice. (B) Spine density of layer V neuron apical dendrites in wild-type and *ephrin-A2* KO mice at one-month and two-months of age. Data are presented as mean ± s.d. (**P*<0.05; ***P*<0.01; ****P*<0.001).

To further characterize how spine elimination was altered in *ephrin-A2* KOs during adolescent development, we calculated the lifetime of dendritic spines in both wild-type and *ephrin-A2* KO mice, based on spine elimination measured over various imaging intervals (*i.e.*, 2, 4, 8, 30 and 90 days), starting at one month of age (Figure 25). We found that the spine survival curve of wild-type mice was well fitted by a two-phase exponential decay equation (R^2=0.92, see Experimental Procedures), with a small portion of spines rapidly lost ("fast-decay spines", 15%, half-life 3.0 days) and the rest stable over months ("slow-decay spines", half-life 1112 days). Fitting the spine survival curve of *ephrin-A2* KOs with the same formula (R^2=0.90), we found

that while the half-life of the fast-decay spine population in KOs was comparable to that of wild-type mice (2.3 days, $P>0.4$), the half-life of the slow-decay spine population was significantly shorter in KOs (432 days, $P<0.01$).

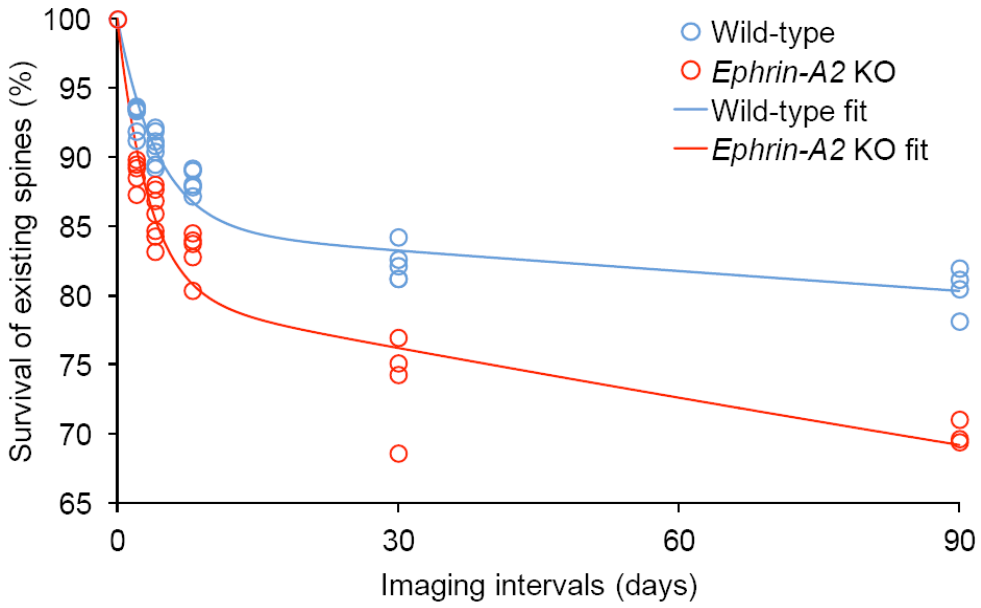

Figure 25. Percentages of spines that survived over 2, 4, 8, 30 and 90 days in wild-type and *ephrin-A2* KO mice.

Previous studies have shown that newly formed spines are much more vulnerable to elimination than pre-existing spines (Xu et al., 2009; Yang et al., 2009). Therefore, the fast- and slow-decay spines could represent new and pre-existing spines, respectively. To determine if the survival of new and pre-existing spines was, indeed, affected differently in *ephrin-A2* KOs, we imaged the same mice 3 times, identified new spines and pre-existing spines based on their appearance in the first two images,

and quantified their survival rate using the last images (Figure 26). We found that while the survival rate of new spines was comparable between *ephrin-A2* KO and wild-type mice (P>0.5), the survival rate of pre-existing spines was significantly lower in *ephrin-A2* KOs (87.0±2.1% vs. 93.4±2.1%, P<0.05). Such results agree with the lifetime analysis, suggesting a selective, but long-lasting effect of ephrin-A2 on the removal of stable spines.

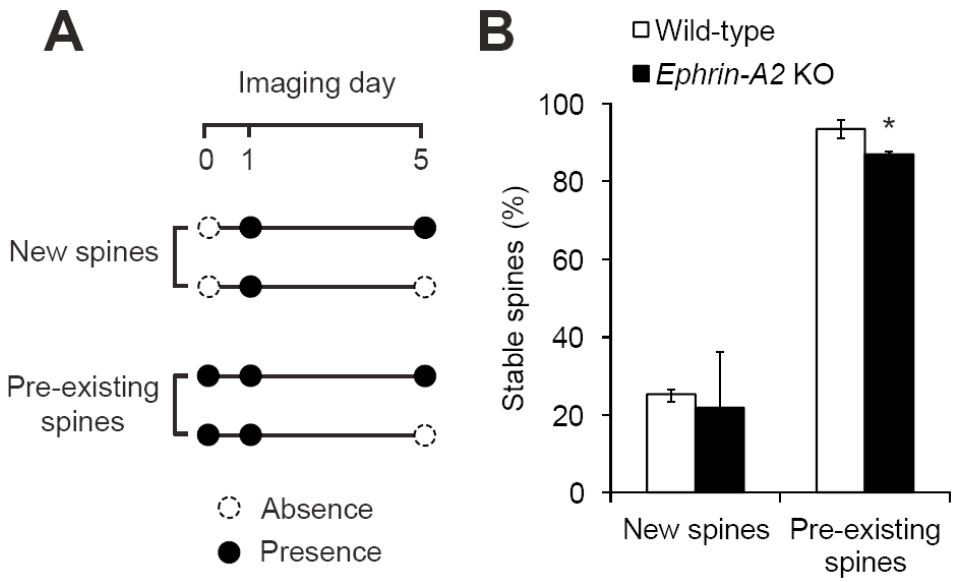

Figure 26. Decreased survival rate of pre-existing spines in *ephrin-A2* KO mice.

(A) Timeline of experiments and classifications of new and pre-existing spines. (B) Survival percentages of new and pre-existing spines over 4 days in wild-type and *ephrin-A2* KO mice. Data are presented as mean ± s.d. (*P<0.05).

3.3.2 Sensory experience is required for elevated spine elimination in the barrel cortex of adolescent *ephrin-A2* KO mice

Experience drives synapse elimination during postnatal development. To determine whether increased spine loss observed in *ephrin-A2* KOs was experience-dependent, we focused on the barrel cortex, where sensory experience could be easily manipulated. We found that sensory deprivation by unilateral whisker trimming at one month of age significantly reduced spine elimination in the contralateral barrel cortex of both wild-type and *ephrin-A2* KO mice. Spine elimination over 4 days decreased from 9.5±0.9% to 7.5±0.5% in wild-type mice (Figures 27A, 27C and 28A, $P<0.005$), and from 12.5±1.0% to 8.3±0.9% in *ephrin-A2* KOs (Figures 27B, 27D and 28A, $P<0.001$). In contrast, spine formation was unaffected by sensory deprivation in either case (Figure 28B, $P>0.07$). Furthermore, there was no difference in spine elimination between deprived wild-type and deprived *ephrin-A2* KO mice ($P>0.2$), suggesting that sensory experience is necessary for elevated spine elimination in *ephrin-A2* KO mice.

In contrast to sensory deprivation, enriched environment (EE) promotes both spine elimination and spine formation in various cortical areas of living mice (Fu et al., 2012; Yang et al., 2009). We found that EE for 4 days robustly increased spine elimination in the barrel cortex of both wild-type (12.5±0.9%, $P<0.001$) and *ephrin-A2* KO (14.7±1.0%, $P<0.01$) mice, and significantly more spines were removed under EE in *ephrin-A2* KOs compared to wild-type mice ($P<0.005$, Figures 27E, 27F and

28A). In addition, EE promoted spine formation in both wild-type (from 6.0±1.5% to 9.4±2.0%, $P<0.01$) and *ephrin-A2* KO (Figure 28B, from 5.8±0.7% to 10.5±1.2%, $P<0.001$) mice, and the spine formation is comparable between enriched wild-type and enriched *ephrin-A2* KO mice ($P>0.2$, Figure 28B). Together, these results indicate that lack of ephrin-A2 selectively affects experience-dependent spine loss, but not experience-dependent spine growth.

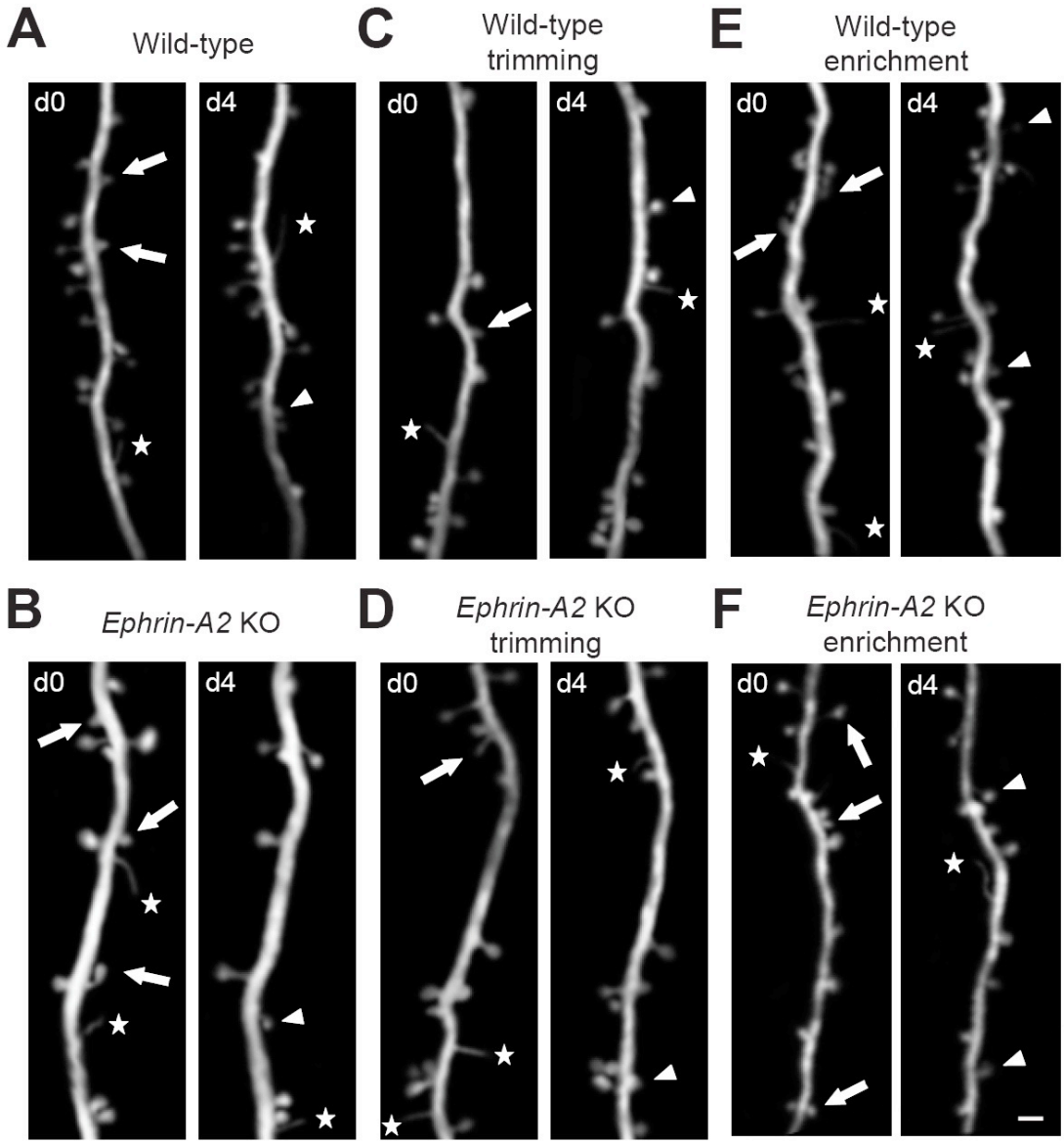

Figure 27. Examples of repeated imaging of the same dendritic branches over 4 days in the barrel cortex.

Spine elimination (arrows) and formation (arrowheads), as well as filopodia (stars), are indicated in wild-type and *ephrin-A2* KO mice under control (A, B), deprived (C, D) and sensory enrichment (E, F) conditions. Scale bar, 2 μm.

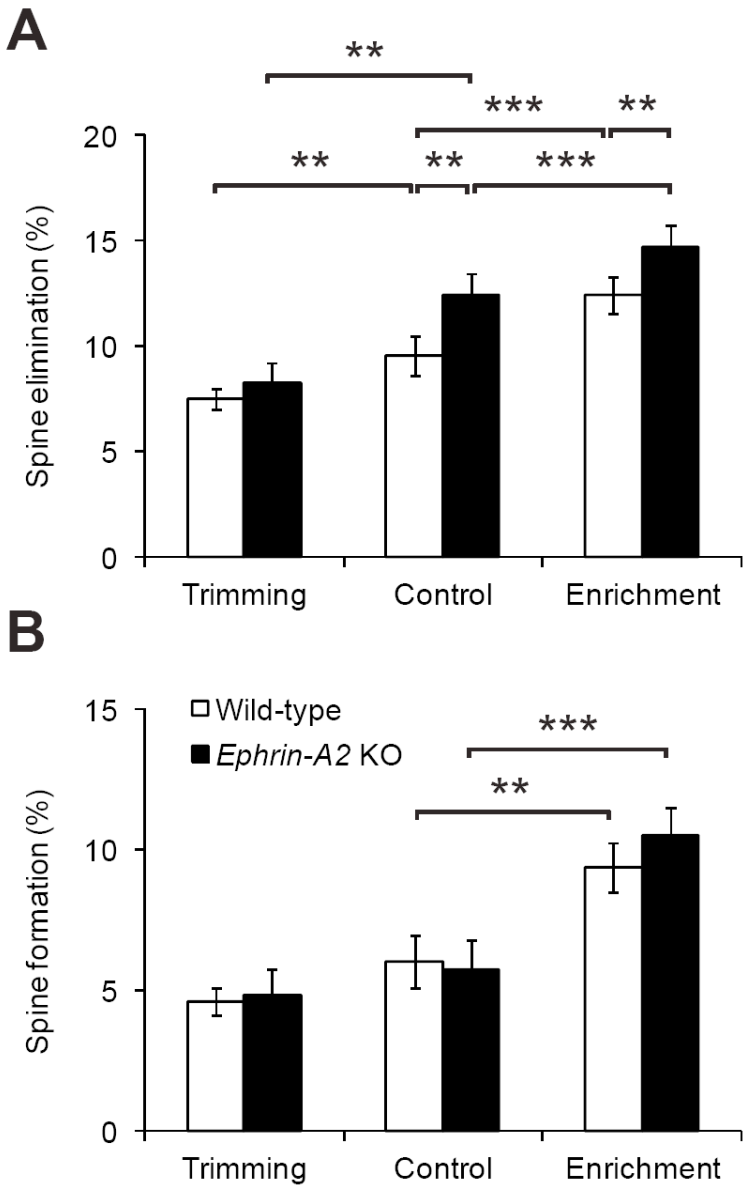

Figure 28. Sensory experience is necessary for elevated spine elimination in *ephrin-A2* KO mice.

Percentages of spines eliminated (A) and formed (B) over 4 days in the barrel cortex of wild-type and *ephrin-A2* KO mice under different experimental conditions. Data are presented as mean ± s.d. (**P<0.01; ***P<0.001).

3.3.3 Ephrin-A2 highly colocalizes with glial glutamate transporters in the mouse cortex

The expression of both ephrin-A2 and ephrin-A3 mRNAs in embryonic and adult mouse cortices is well documented (Cang et al., 2005; Murai et al., 2003; Torii et al., 2009). Recently, a transcriptome database reported cell-type-specific expression profiles of ephrin-A2 and ephrin-A3 in the mouse forebrain: while ephrin-A2 mRNAs are enriched in astrocytes, ephrin-A3 mRNAs are enriched in neurons (Cahoy et al., 2008). However, little is known about the cortical expression of their protein products. To address this question, we took advantage of array tomography (AT), a high-resolution, proteomic imaging method that offers the ability to resolve individual synapses and analyze their protein profiles with high fidelity and throughput (Micheva et al., 2010; Micheva and Smith, 2007). As illustrated in Figures 29A and 29B, individual ephrin-A2 and ephrin-A3 puncta were clearly resolved using AT from cortical sections of adolescent wild-type mice, but not *ephrin-A2/A3* KOs (Figure 30). The densities of ephrin-A2 and ephrin-A3 puncta were relatively consistent throughout all cortical layers (Figure 31). Subsequent quantitative analyses further revealed that the density of ephrin-A2 puncta was approximately 3 times the density of ephrin-A3 puncta in the superficial cortical layers (0.11±0.03 vs. 0.04±0.01 puncta/μm^3, $P<0.05$; Figure 29C).

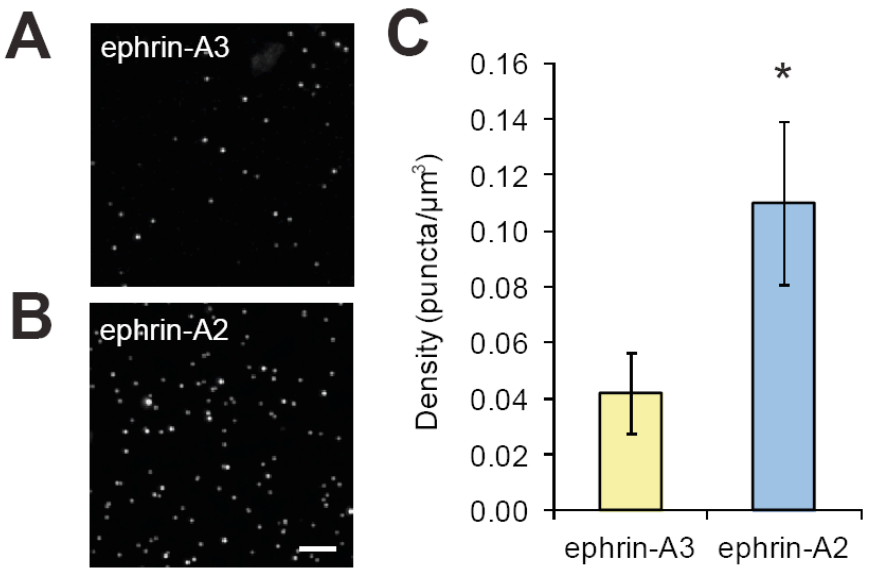

Figure 29. The abundance of ephrin-A2 puncta in the cortex of adolescent mice.

(A, B) Representative image volumes of ephrin-A2 and ephrin-A3 immunofluorescence staining in superficial layer I of one-month-old mouse cortex. Each image is a max projection of 5 serial sections. Scale bar, 10 μm. (C) Quantification of puncta density shows that ephrin-A2 is approximately 3 times enriched, compared to ephrin-A3 in the cortex. Data are presented as mean ± s.e.m. (**P*<0.05).

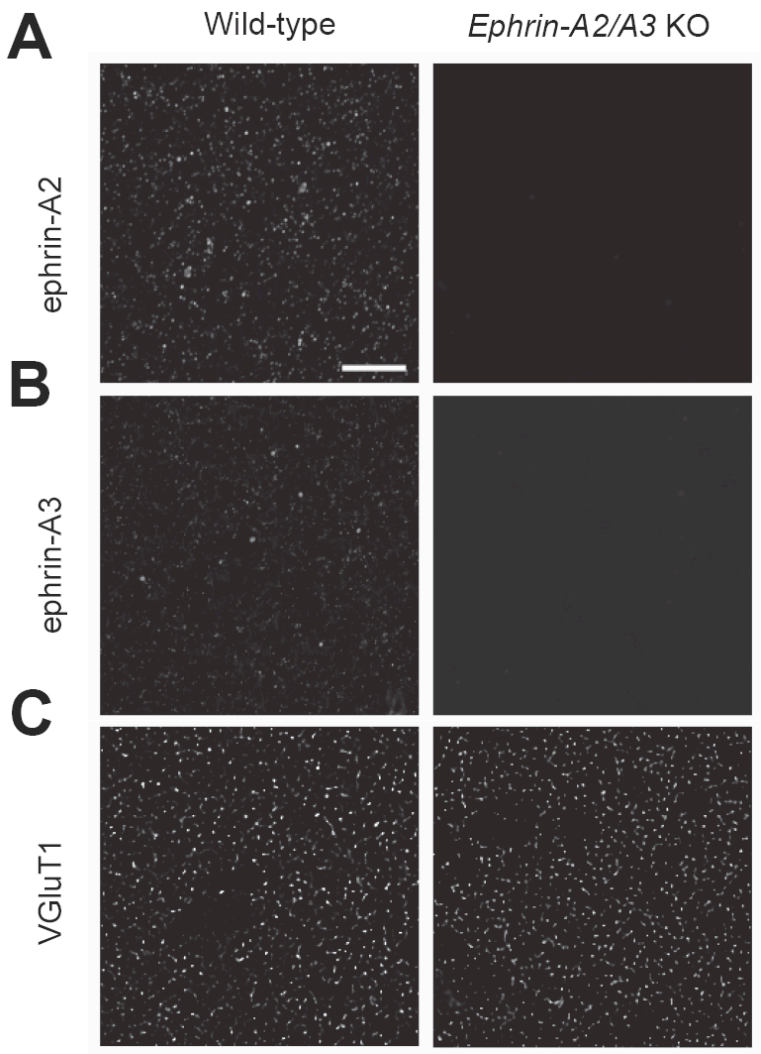

Figure 30. Array tomography reveals specific labeling of ephrin-A2 and ephrin-A3 puncta in the mouse cortex.

(A, B) The labeling of ephrin-A2 and ephrin-A3 puncta is abundant in layer I of the barrel cortex in one-month-old wild-type mice, but is completely absent in age-matched *ephrin-A2/A3* KO mice. (C) The labeling of presynaptic marker VGluT1 is comparable between wild-type and *ephrin-A2/A3* KO mice. Scale bar, 10 μm.

Figure 31. Expression of ephrin-A2 is consistently higher than that of ephrin-A3 in all the cortical layers.

(A) Volume rendering of 5 serial sections (70 nm each) through the entire cortical depth of the barrel cortex reveals that ephrin-A2 (purple) and ephrin-A3 (yellow) are expressed throughout all the cortical layers in wild-type mice. Nuclei are stained with DAPI (cyan). (B) Density plot of the two proteins reveals a consistent higher expression of ephrin-A2 compared to ephrin-A3 throughout all cortical layers. Scale bar, 50 μm. (C-E) Magnified images of the boxed regions in layer II/III (C), layer IV (D) and layer V (E) from panel (A). Scale bar, 15 μm.

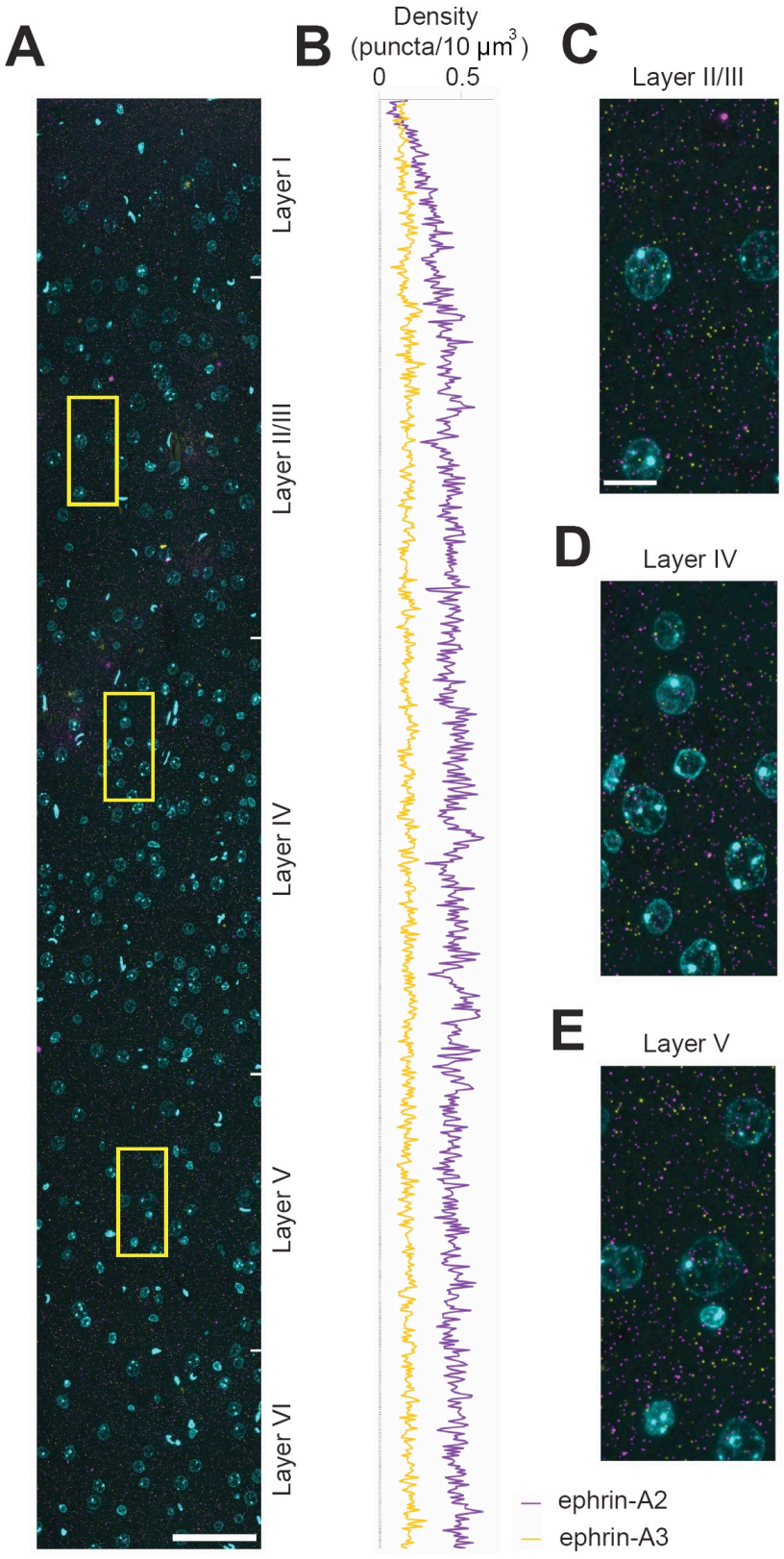
A
B
Density
(puncta/10 µm3)
0
0.5
C
Layer II/III
D
Layer IV
E
Layer V
Layer I
Layer II/III
Layer IV
Layer V
Layer VI
ephrin-A2
ephrin-A3

To further investigate the subcellular localizations of ephrin-A2 protein near cortical synapses, we co-labeled ephrin-A2 protein with different synaptic and astrocytic markers (Figure 32), and compared the relative distance of ephrin-A2 to different protein constituents. We used bassoon, synapsin, VGluT1 and SV2 as presynaptic markers, PSD95 as the postsynaptic marker for excitatory glutamatergic synapses, and GLAST, GLT-1 and GS (glutamine synthetase) as astrocytic markers. Three dimensional distance analysis revealed that ephrin-A2 puncta did not colocalize with any neuronal synaptic marker. They rather lay in close vicinity of all three astrocytic markers (Figure 33), especially membrane-bound GLAST and GLT-1, which are enriched in perisynaptic astrocytic processes and associated tightly with excitatory synapses (Chaudhry et al., 1995).

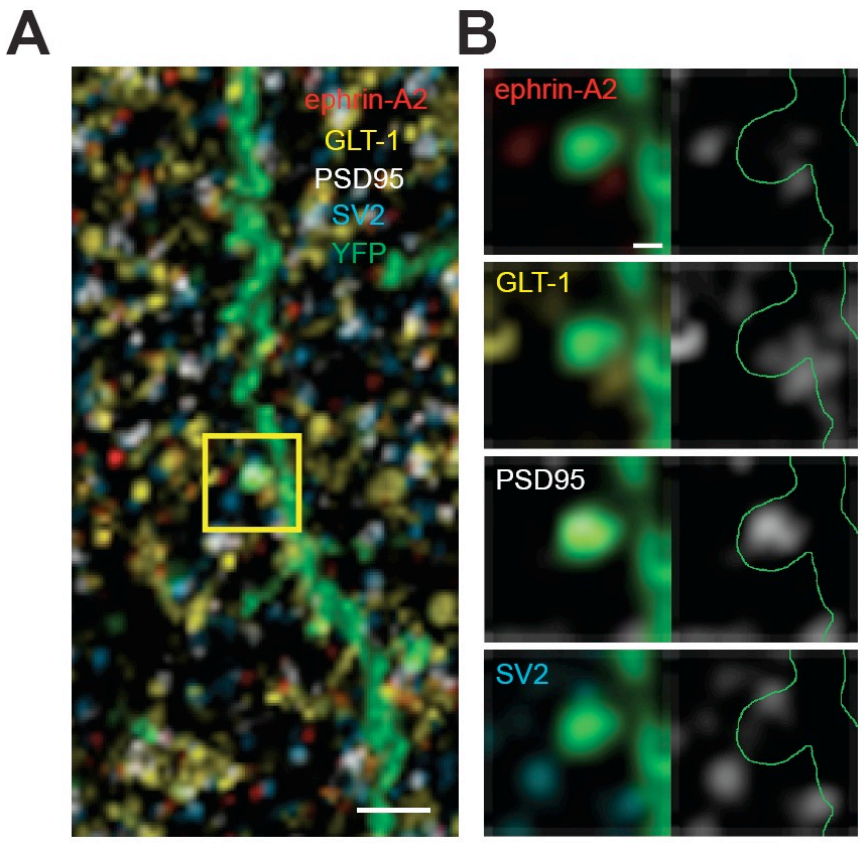

Figure 32. Ephrin-A2 colocalizes with astrocytic glutamate transporters in the mouse cortex.

(A) Max projection of 10 serial sections of ephrin-A2 immunofluorescence (red) with protein markers of presynaptic SV2 (cyan), postsynaptic PSD95 (white), astrocytic GLT-1 (yellow) and dendritic segment labeled with YFP (green). Scale bar, 1 μm. (B) Images of a spine from the boxed region in (A) at higher magnification with various protein markers. Scale bar, 200 nm.

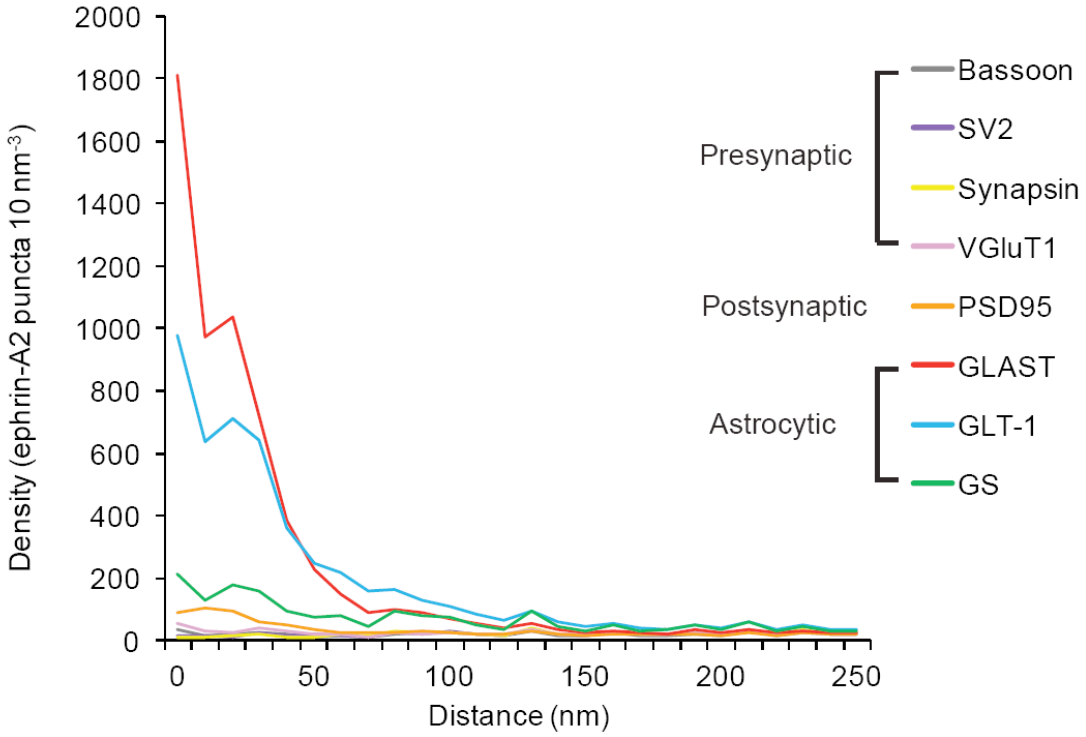

Figure 33. The density of ephrin-A2 puncta is plotted as a function of the distance from markers of presynaptic (bassoon, SV2, synapsin and VGluT1), postsynaptic (PSD95) and astrocytic (GLAST, GLT-1 and GS) constituents.

Furthermore, the average numbers of ephrin-A2 puncta within a 50 nm sphere of any glial markers were much higher than those of neuronal synaptic markers (Figure 34). Moreover, the average numbers of glial glutamate transporters within a 50 nm sphere of ephrin-A2 puncta were greater than those of other markers (Figure 35). Thus, in agreement with the transcriptome data, our results show that ephrin-A2 proteins localize predominantly to the astrocytic processes near synapses.

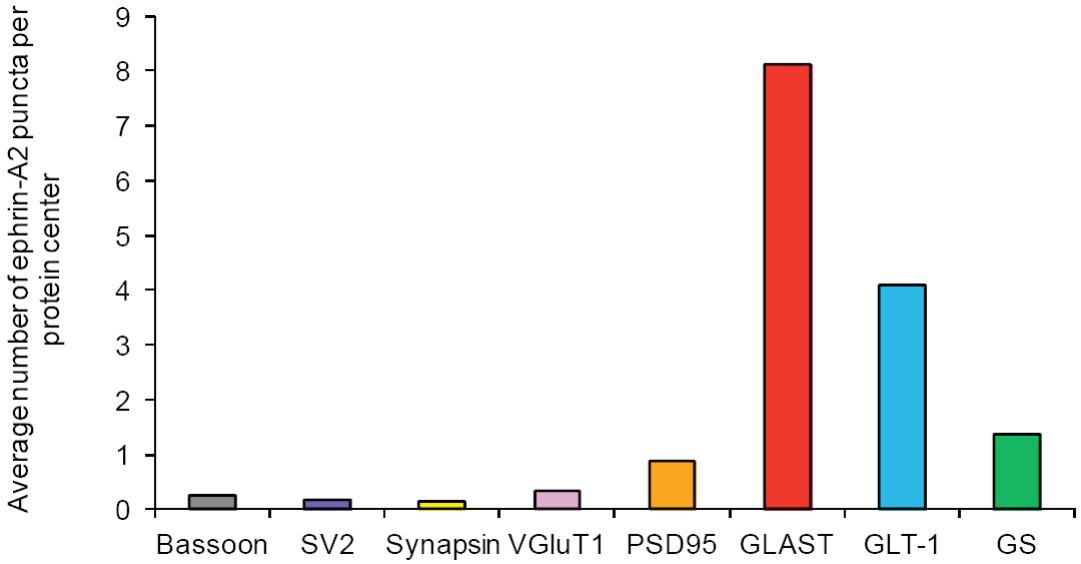

Figure 34. Average numbers of ephrin-A2 puncta within 50 nm spheres of different neuronal and glial markers.

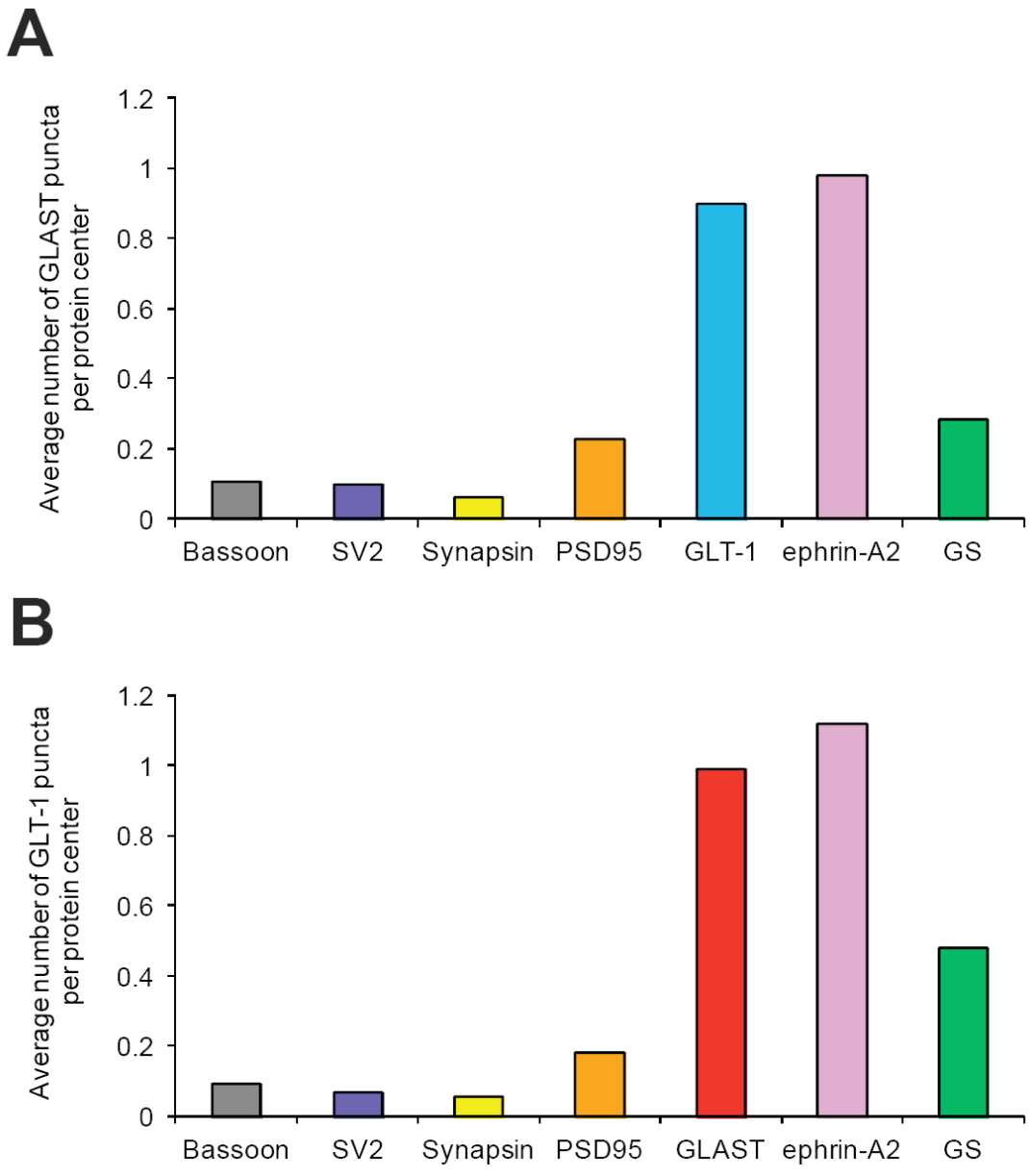

Figure 35. Glial glutamate transporters are closely associated with ephrin-A2 in the mouse cortex.

Average numbers of GLAST (A) and GLT-1 (B) puncta within 50 nm spheres of ephrin-A2, as well as other neuronal and glial markers.

3.3.4 Cortical expression of glial glutamate transporters is down-regulated in *ephrin-A2* KO mice

Membrane-bound glial glutamate transporters, GLAST and GLT-1, uptake glutamate from the synaptic cleft and regulate synaptic transmission (Tzingounis and Wadiche, 2007). Given their colocalization with ephrin-A2, we next asked if cortical expression of GLAST and GLT-1 was altered in *ephrin-A2* KOs. Using western blot, we found that the expression levels of both proteins were significantly decreased in the cortex of *ephrin-A2* KOs compared to wild-type controls. Specifically, there was more than a 50% reduction of GLAST and an approximately 30% reduction of GLT-1 in *ephrin-A2* KOs (Figure 36, $P<0.01$ for GLAST and $P<0.05$ for GLT-1). In contrast, the expression of GS, another astrocytic enzyme involved in glutamate recycling (Hertz and Zielke, 2004), remained unaltered in *ephrin-A2* KOs (Figure 36, $P>0.4$).

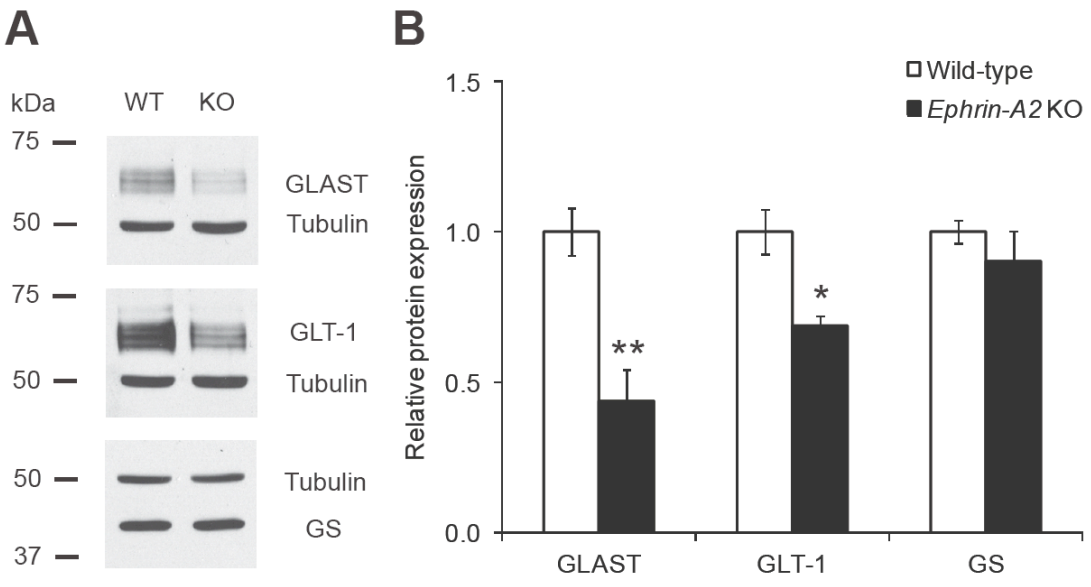

Figure 36. Glia glutamate transporters are down-regulated in the cortex of *ephrin-A2* KO mice.

(A) Western blot examples of GLAST, GLT-1, GS and tubulin from the cortex of wild-type and *ephrin-A2* KO mice. (B) Quantification of western blots indicates a significant decrease in expression levels of glial glutamate transporters (GLAST and GLT-1), but not GS, in *ephrin-A2* KOs, as compared to wild-type controls. Data are presented as mean ± s.e.m. (**P*<0.05; ***P*<0.01).

Furthermore, the density, size and morphology of cortical astrocytes were indistinguishable between wild-type and *ephrin-A2* KO mice, as revealed by labeling with astrocytic marker S100β (Figure 37). This finding rules out the possibility that down-regulation of glial glutamate transporters in *ephrin-A2* KO cortex is simply due to a global reduction of astrocyte number or size.

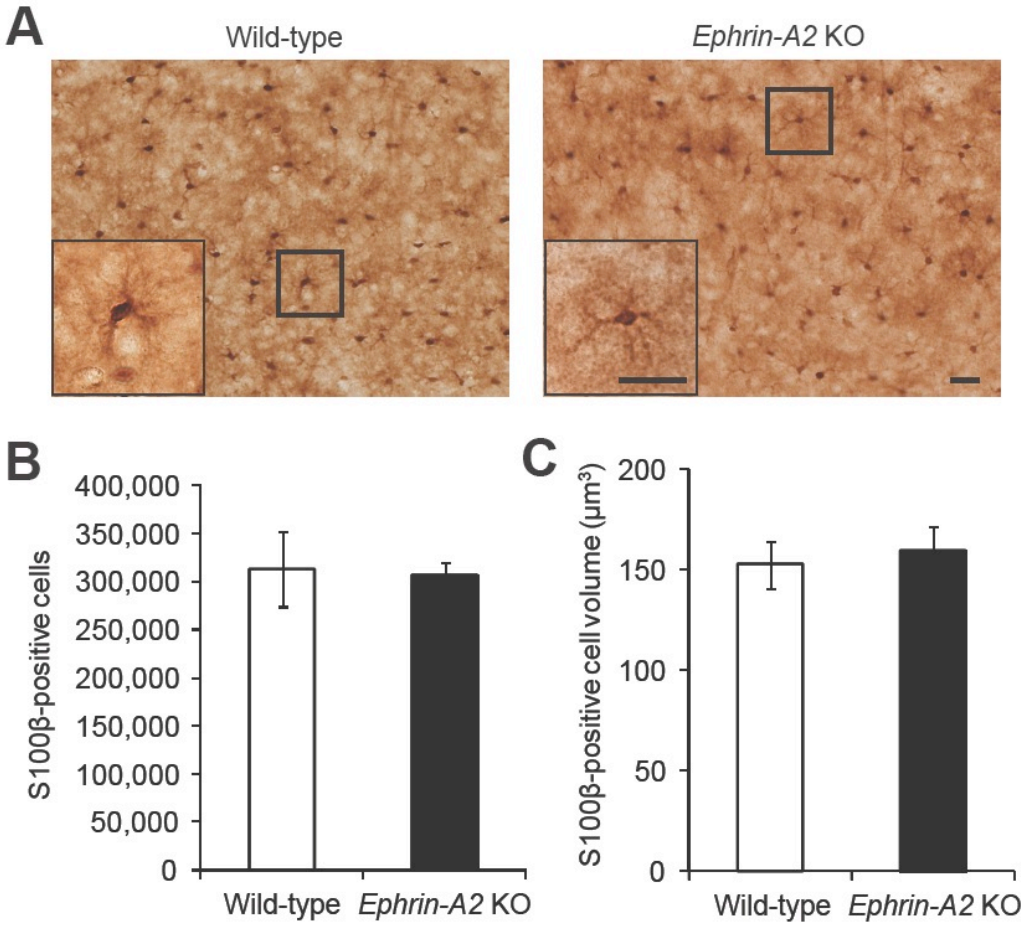

Figure 37. Number and morphology of cortical astrocytes are unaltered in *ephrin-A2* KO mice.

(A) Bright-field immunohistochemistry for S100β in the cortex of both wild-type and *ephrin-A2* KO mice. Inserts show individual astrocytes from boxed regions. Scale bar, 25 μm. (B, C) Quantification of cell number (B) and cell body volume (C) of cortical astrocytes reveals no significant difference between wild-type (n=3) and *ephrin-A2* KO (n=4) mice. Data were presented as mean ± s.e.m.

3.3.5 NMDA receptors mediate elevated spine elimination in *ephrin-A2* KO mice

Reduction in glial glutamate transporters results in accumulation of extracellular glutamate both *in vivo* and *in vitro* (Rothstein et al., 1996). To determine if increased

glutamate signaling through postsynaptic glutamate receptor was responsible for elevated spine elimination in *ephrin-A2* KOs, we treated mice with MK801, a selective antagonist of NMDA receptors, and followed spine dynamics *in vivo*. We found that, in the barrel cortex, blockade of NMDA receptors affected spine elimination in a fashion similar to that of sensory deprivation. Four-day MK801 treatment significantly decreased spine elimination in *ephrin-A2* KOs (Figure 38A; $P<0.005$), but did not alter spine formation (Figure 38B, $P>0.4$). More importantly, under MK801 treatment wild-type and KO mice no longer exhibited any difference in the rate of spine elimination ($P>0.7$), suggesting that elevated spine elimination in *ephrin-A2* KOs is mediated by NMDA receptors.

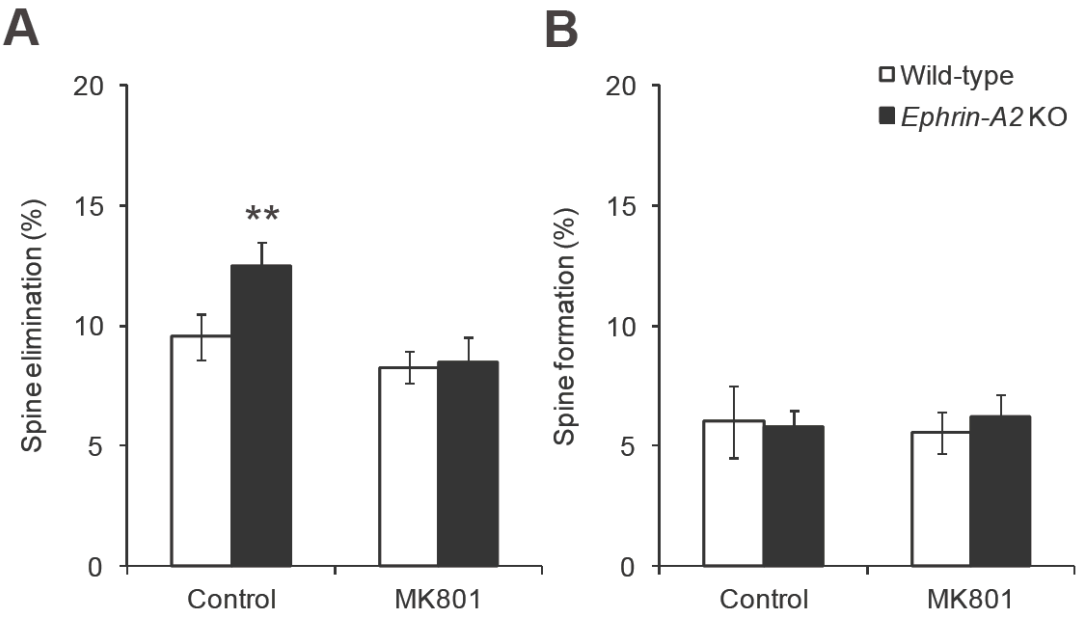

Figure 38. Activation of NMDA receptors is necessary for the elevated spine elimination in *ephrin-A2* KO mice.

Percentages of spines eliminated (A) and formed (B) over 4 days in wild-type and *ephrin-A2* KOs with or without MK801 treatment. Data are presented as mean ± s.d. (*P<0.05; **P<0.01).

3.4 Discussion

During early development, generation of excessive synapses occurs in a constitutive, genetically programmed manner. This initial overproduction of synapses is followed by an experience-dependent pruning process that reduces synaptic connections considerably and leads to maturation of refined neural circuits. While experience is generally believed to be crucial for synaptic elimination at this stage, little is known about its underlying molecular mechanisms. Here, we identify cell adhesion molecule ephrin-A2 as a participant in experience-dependent pruning of cortical synapses. Deficiency of ephrin-A2 specifically promotes experience-induced removal of existing spines, without affecting spine formation or initial stabilization. We further show that ephrin-A2 proteins localize at perisynaptic astrocytic processes in the cortex and regulate expression of glial glutamate transporters, suggesting a potential contribution of astrocytes to synapse pruning during adolescent development.

Glutamate transmission and activation of NMDA receptors are involved in both activity-dependent competition and homeostatic regulations – two fundamental mechanisms underlying synaptic plasticity (Bock and Braun, 1999; Turrigiano and

Nelson, 2004; Yashiro and Philpot, 2008; Zuo et al., 2005b). A critical task of astrocytes in the brain is to remove excess glutamate from the synaptic cleft, thereby ensuring precise synaptic transmission and preventing overactivation of postsynaptic glutamate receptors (Tzingounis and Wadiche, 2007). Thus, reduced astrocytic glutamate uptake in *ephrin-A2* KOs presumably prolongs the effect of synaptic glutamate on postsynaptic NMDA receptors (Figure 39). Increased glutamate signaling at active synapses would subsequently augment the imbalance between activate and inactivate synapses, promoting competition-dependent spine elimination via a Hebbian mechanism. Alternatively, global overactivation of postsynaptic glutamate receptors could trigger homeostatic regulation and lead to a reduction in total synapse number. It is also possible that a combination of these mechanisms contributes to the increased spine loss in *ephrin-A2* KOs. Finally, it is interesting that stability of pre-existing spines is more sensitive to altered glutamate levels than new spines in *ephrin-A2* KOs. This may be partially attributed to their differences in NMDA receptor subunit compositions, which render different sensitivities to glutamate levels and, thus, dissimilar capabilities for postsynaptic signaling transmission (Bellone and Nicoll, 2007; Zito et al., 2009).

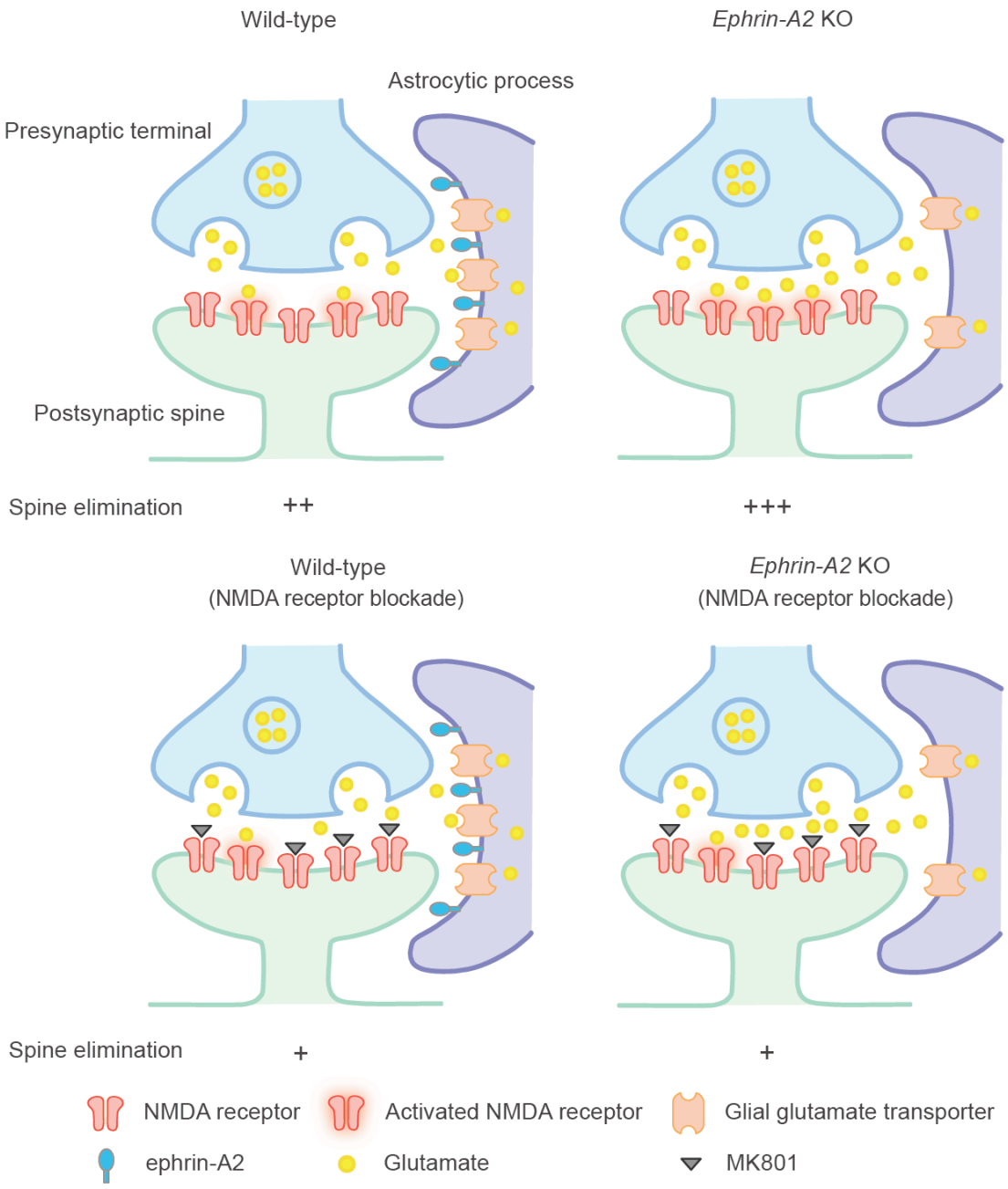

Figure 39. A working model illustrates glutamate transmission in wild-type and *ephrin-A2* KO mice, under control and NMDA receptor blockade conditions.

Inefficient glutamate removal at synapses may not be the only cause of accelerated spine pruning in *ephrin-A2* KOs. Another intriguing possibility is that the contact-dependent interactions between ephrin-As and their EphA receptors may affect the physical contacts between astrocytes and spines, which in turn regulate the motility and stability of dendritic spines (Haber et al., 2006; Nishida and Okabe, 2007). Lack of functional ephrin-A2 may reduce such physical contacts, making spines prone to retract. Alternatively, it is conceivable that abnormal spine dynamics and altered glial protein expression in *ephrin-A2* KOs are independent of one another. In the hippocampus, activation of EphA4 receptor signaling in dendritic spines has been demonstrated to cause spine retraction (Murai et al., 2003). As ultrastructural examination has revealed postsynaptic expression of EphA receptors in the mouse cortex (Bouvier et al., 2008), ephrin-A2 could act through forward signaling of postsynaptic EphA receptors to regulate cortical spine morphogenesis and pruning.

Previous studies have shown that ephrin-A3 is the most abundant ephrin-A ligand in the adult hippocampus and is involved in the morphogenesis of dendritic spines on CA1 pyramidal neurons (Carmona et al., 2009; Murai et al., 2003). Here, we show that ephrin-A2 is more predominant than ephrin-A3 in the cortex and that lack of ephrin-A2, but not ephrin-A3, results in accelerated experience-dependent dendritic spine pruning in the adolescent cortex. Moreover, while GLAST and GLT-1 are up-regulated in the hippocampus of *ephrin-A3* KOs (Carmona et al., 2009; Filosa et al., 2009), they are significantly down-regulated in the cortex of *ephrin-A2* KOs.

Therefore, despite the fact that multiple ephrin-As are functionally redundant in topographic map formation and cortical column integration during early development (Cang et al., 2005; Cutforth et al., 2003; Feldheim et al., 2000; Pfeiffenberger et al., 2005; Torii et al., 2009), our findings reveal that different ephrin-As may regulate synapse morphology and dynamics through distinctive cellular signaling, providing a potential mechanism for achieving the specificity and complexity of mature neuronal networks.

Chapter IV Abnormal Synaptic Pruning In The Living Cortex Of Fragile X Mental Retardation

4.1 Introduction

Fragile X syndrome (FXS) is the most frequent inherited form of human mental retardation with a prevalence of ~1/4000 in males and ~1/8000 in females. Major neurological symptoms of FXS include cognitive impairment in the moderate to severe range, developmental delay, attention deficit and hyperactivity, anxiety with mood lability, poor motor coordination, seizure susceptibility and ~30% FXS patients also have autistic behaviors. Non-neurological symptoms include a long face, large ears, hyperextensible joints and enlarged testes in post-pubescent male patients specifically (Chonchaiya et al., 2009; Penagarikano et al., 2007; Wisniewski et al., 1985).

An important achievement of understanding FXS is the identification of the responsible gene, fragile X mental retardation gene 1 (*FMR1*), which resides on the fragile X site of chromosome X. In most cases, FXS is caused by an expansion of a polymorphic CGG nucleotriplet in the 5' untranslated region of this gene, which leads to a hypermethylation of this locus through a poorly understood mechanism. In

normal individuals, the length of this CGG triplet is usually below 55 repeats, whereas the repeat can be expanded up to over 200 repeats in FXS patients, and is referred as the full mutation. The consequence of this unusual triplet expansion is the transcription silencing of the gene product, fragile X mental retardation protein (FMRP) (O'Donnell and Warren, 2002).

FMRP contains several highly conserved domains: two hnRNP-K-homology (KH) domains and an arginine-glycine-glycine (RGG box), which are typical motifs of RNA-binding proteins; a nuclear localization signal (NLS) and a nuclear export signal (NES), indicating the ability of shuttling between the nucleus and the cytoplasm (Bagni and Greenough, 2005; Bassell and Warren, 2008). The understanding of FMRP functions is still incomplete, but evidence has shown that FMRP plays important roles in regulation of mRNA transportation and translation. Through its NLS FMRP is transported into the neuronal nucleus, where it assembles into a messenger ribonucleopretein complex, thereby interacting with specific mRNA transcripts and proteins (Darnell et al., 2001; Schaeffer et al., 2001). This FMRP-containing complex is transported out of the nucleus into dendrites by the NES of FMRP and delivers mRNA cargoes to the synaptic locations through interactions with specific cytoplasm proteins (Antar et al., 2005; Miyashiro et al., 2003). Interestingly, the mRNA of FMRP itself is one such cargo mRNA, and is translated at synapses in response to the activation of postsynaptic group I metabotropic gluatamate receptors 5 (mGluR5) (Bramham and Wells, 2007; Greenough et al., 2001; Weiler et al., 1997),

thereby further regulates protein synthesis critical for long-term synaptic plasticity (Bechara et al., 2009; Brown et al., 2001; Laggerbauer et al., 2001; Schutt et al., 2009; Todd et al., 2003; Wang et al., 2009; Weiler et al., 2004; Zalfa et al., 2003) and mRNA stability (Zalfa et al., 2007).

It has been shown that mGluR5-induced protein synthesis is required for persistent internalization of the α-amino-3-hydroxy-5-methyl-4-isoxazolepropionic acid receptor (AMPAR) (Lin et al., 2000). The loss of postsynaptic surface AMPAR is proposed to be involved in the long-term depression (LTD) of synaptic transmission (Luscher and Huber, 2010; Waung et al., 2008). In the absence of FMRP, which is the case in FXS, the protein synthesis induced by the exaggerated activation of mGluR5 is proposed to be disturbed (Muddashetty et al., 2007), which increases the loss of surface AMPAR and disrupts the synaptic plasticity (Bear et al., 2004; Dolen and Bear, 2008; Nakamoto et al., 2007).

Several types of mental retardation have been shown to be associated with gross neuroanatomical abnormalities. In contrast, magnetic resonance imaging and postmordem examinations have only revealed non-specific subtle changes in gross brain morphology (Reyniers et al., 1999). However, the autopsy analysis of the neuronal microscopic structures in Golgi-stained human material have shown an abundance of long, thin dendritic spines on apical dendrites of pyramidal neurons in the adult neocortex (Beckel-Mitchener and Greenough, 2004; Hinton et al., 1991;

Irwin et al., 2001; Rudelli et al., 1985; Wisniewski et al., 1991). Electron microscopy also revealed that the mean synaptic contact area is ~35% smaller in FXS patients than controls (Wisniewski et al., 1991). Both altered spine morphology and abnormal density are also observed in a fragile X mouse model (*FMR1* knockout mice) (Comery et al., 1997; McKinney et al., 2005; Nimchinsky et al., 2001). *FMR1* knockout mice also exhibit behavioral defects similar with fragile X patients, such as mild deficits in learning, anxiety and hyperactivity, as well as aberrant long-term synaptic plasticity in various brain regions including the cortex (Li et al., 2002; Wilson and Cox, 2007), the cerebellum (Koekkoek et al., 2005) and the hippocampus (Huber et al., 2002). Therefore, the consistency of dendritic spine phenotype suggests that the abnormally developed synaptic connections might provide a structural basis for altered neurological and functional aspects of FXS.

Being postsynaptic components of most excitatory synapses in the mammalian brain, dendritic spines are locations where synaptic transmission and several important forms of synaptic plasticity occur (Nimchinsky et al., 2002; Shepherd, 1996). Based on the relative sizes of spine head and neck, spines can be grouped into three categories: mushroom, stubby and thin spines (Horner, 1993; Spacek and Hartmann, 1983). While thin spines usually have small head and long neck, stubby and mushroom spines have relatively large head and short neck (Harris et al., 1992). Electron microscopy data have indicated that the size of spine head is proportional to

the number of postsynaptic receptors and presynaptic docking vesicles (Harris and Stevens, 1988, 1989).

During normal brain development, neuron generates more synaptic connections than will ultimately survive. This overproduction of synapses is followed by an experience-dependent pruning process, in which some synapses are eliminated while others are stabilized and strengthened, leading to a formation of refined functional neuronal circuitry (Holtmaat et al., 2005). The strengthening of synapses appears to involve a transition from small immature synapses associated with long, thin, dendritic spines to large mature synapses associated with more "mushroom-shaped" dendritic spines (Bourne and Harris, 2007; Schuz, 1986). Thus, the observation of excessive long, thin, immature-looking spines in adulthood indicates that the pruning process might be disrupted in FXS (Galvez and Greenough, 2005). Consistently, FMRP has been shown to regulate synapse loss in the hippocampal slice culture (Pfeiffer and Huber, 2007). It is hypothesized that altered spine development and plasticity can contribute to FXS (Fiala et al., 2002; Purpura, 1974). However, this hypothesis has never been examined in the living brain, and how the spine abnormalities develops and how spine dynamics change during the progression of this mental disorder also remain unknown.

4.2 Methods

4.2.1 Animals

FMR1 KO mice were obtained from Dr. Steve Warren in Emory University. YFP-H line mice (Feng et al., 2000) were purchased from the Jackson Laboratory. Mice were group-housed and bred in the UCSC animal facility, with all experiments performed in accordance with approved animal protocols.

4.2.2 Motor skill training

The protocol of mouse single-pellet retrieval task was described previously (Section 2.2.1). Briefly, the motor skill training includes a short shaping phase to identify the preferred limb and a subsequent training phase for up to 10 days. Each training day consists of one session of 30 trials, or 20 minutes (whichever occurs first). Successful, failed, or dropped reaches are recorded. Success rates are calculated as the percentage of successful reaches over total reach attempts. Data are presented as mean ± s.e.m.

4.2.3 *In vivo* imaging and data quantification

The procedure of transcranial two-photon imaging and data quantification were described previously (Sections 2.2.2 and 2.2.3). Percentage of spines eliminated or

formed is defined as the number of counted spines eliminated or formed over the total spines counted in the initial images. Spine density was calculated by dividing the number of spines by the length of the segment in micrometers. Spines were classified into three categories based on their lengths, the ratios of spine head/spine neck diameters (Harris et al., 1992). Data are presented as mean ± s.d. *P*-values are calculated using the Student's *t*-test.

4.2.4 *In utero* electroporation

In utero electroporation was performed at embryonic stage E15.5, as previously described (Saito and Nakatsuji, 2001). E15.5 pregnant female mice were anesthetized using an isoflurane-oxygen mixture delivered by an anesthetic system. The uterine horns were then gently extracted from the abdominal cavity until all of the embryos exposed. ~0.5 μl DNA solution (containing 0.5 μg/μl of plasmid vector encoding EGFP) was injected by pressure (Picospritzer) into the lateral ventricle (LV) of embryos through a pulled galss capillary tube. The head of each embryo was placed between tweezer-electrodes, with the positive electrode over the intended electroporation area and the negative electrode directly opposing the positive side. An electrical current was applied using a square electroporater (five 50-ms pulses of 40 V with 950-ms intervals).

4.2.5 Transmission electron microscopy and 3D reconstruction

The detailed procedures of transmission electron microscopy were described previously (Yin et al., 2007). Briefly, anesthetized mice were transcardially perfused with 2% dextran in 0.1M phosphate buffer (PB; pH 7.4), followed by 4% paraformaldehyde and 0.125% glutaraldehyde in PB. After postfixation overnight at 4 °C, desired cortical regions were dissected and embedded. Tissue blocks were then trimmed on an ultramicrotome (Leica EM UC6, Vienna). Serial ultrathin sections (70-80 nm thick) were cut using a diamond knife (Diatome Ultra 45) and collected on formvar-coated gold slot grids (Electron Microscopy Sciences). The postembedding immunogold labeling was applied to label endogenous YFP expression. Ultrastructural images were then acquired on a transmission electron microscope (Philips EM208, Eindhoven, The Netherlands) with a digital camera (AMT HR 1Mb). Structures were identified from serial images and aligned using the software Reconstruct (Fiala, 2005).

4.3 Results

4.3.1 Adult *FMR1* KO mice exhibit defects in spine morphology and motor learning behavior

FMR1 knockout (KO) mice have mild deficits in learning and abnormalities in dendritic morphology, which are also observed in fragile X patients. Therefore,

FMR1 KO mice serve as a good model to understanding the cellular mechanisms underlying fragile X syndrome and provide a system to investigate future possible treatments for this neuronal disorder. To visualize synaptic structures in the intact brain, we crossed *FMR1* KO mice with YFP-H line mice, which express yellow fluorescent protein in a subpopulation of layer V pyramidal neurons. Analyzing apical dendrites of layer V pyramidal neurons in the motor cortex, we found that spine density was comparable in *FMR1* KO and wild-type mice at one month old of age ($P>0.3$). However, in adult (> 2 months old) brain, the spine density of layer V cortical neurons is significantly higher in *FMR1* KO than age-matched wild-type mice (Figure 40A). Further detailed analysis of spine morphological classification showed that adult *FMR1* KO mice showed significantly higher density of thin spines, but normal densities of mushroom spines and thin spines (Figure 40B, $P<0.001$). These results are in agreement with defects in spine pruning in the sensory cortex during postnatal development, as suggested by many previous studies (Comery et al., 1997; Galvez et al., 2003; Grossman et al., 2006; Irwin et al., 2001; McKinney et al., 2005).

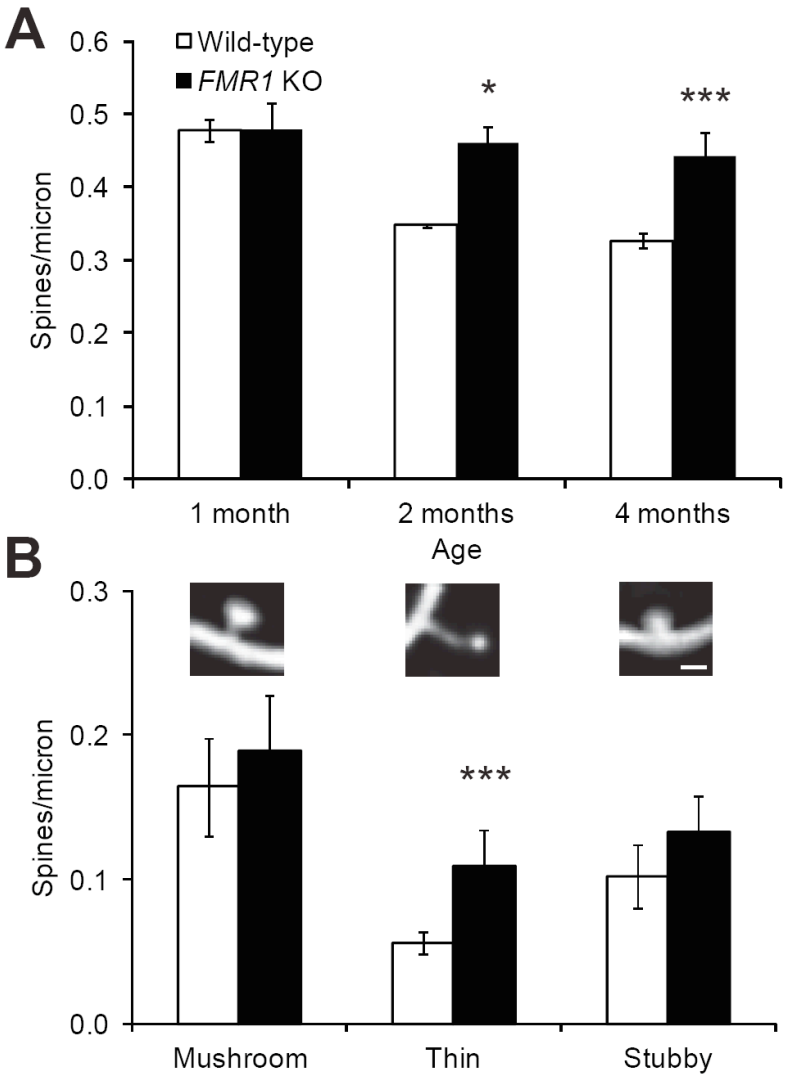

Figure 40. Adult *FMR1* KO mice exhibit elevated spine density with an abundance of immature spines.

(A) Spine density of apical dendrites of layer V neurons in the motor cortex of both wild-type and *FMR1* KO mice at different ages. (B) Spine classification based on morphology. Density of different spine categories of adult wild-type and *FMR1* KO mice. Scale bar, 1 μm. Data are presented as mean ± s.d. (**P*<0.05, ****P*<0.001).

To investigate how functional synaptic connections are altered in the cortex of adult *FMR1* KO mice, we applied transmission electron microcopy (EM) to examine

ultrastructural changes of synapses. Serial sectioning and immunogold labeling were applied to reconstruct several dendritic segments expressing YFP in the motor cortex of adult wild-type and age-matched *FMR1* KO mice. We found that spines of layer V pyramidal neurons tended to have longer spine neck and thinned spine head size, compared to age-matched wild-type controls (Figure 41). Moreover, the sizes of synapses formed either on spine heads or dendritic shafts seemed to be smaller in *FMR1* KO adult mice.

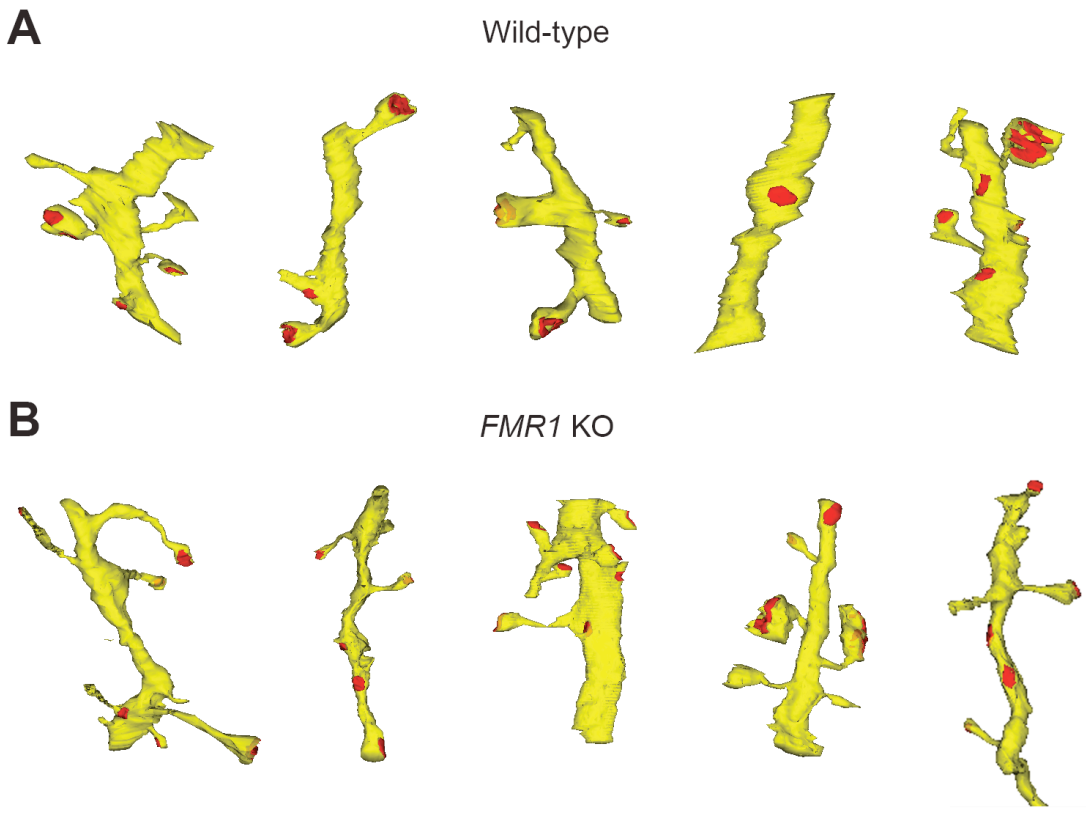

Figure 41. Cortical dendrites of *FMR1* KO mice tend to have smaller synaptic contact areas than those of wild-type mice.

Reconstructed transmission electron microcopy images of 5 dendritic segments from the cortex of adult wild-type (A) and *FMR1* KO (B) mice show YFP-expressing dendritic structures (yellow) in 3D details. Synapses formed either on spine heads or dendritic shafts are shown in red.

Spine plasticity in the superficial layers of the motor cortex has been shown to be associated with the acquisition of motor learning and the formation of long-lasting motor memory, adult *FMR1* KO mice presumably have defects in motor skill learning as they have abundant immature spines in the motor cortex. To test this hypothesis, we trained adult *FMR1* KO and wild-type mice in a reaching task for up to 10 days (Figure 42). We found that while wild-type mice exhibited a progressive improvement in the percentage of successful reaches, *FMR1* KO mice failed to make significant improvements over time. Therefore, significant differences in reaching successful rates were observed between adult wild-type and *FMR1* KO mice at training day 3 and later (Figure 42, $P<0.05$ at day 3-10). These results indicate a defect in motor skill learning ability in adult *FMR1* KO mice.

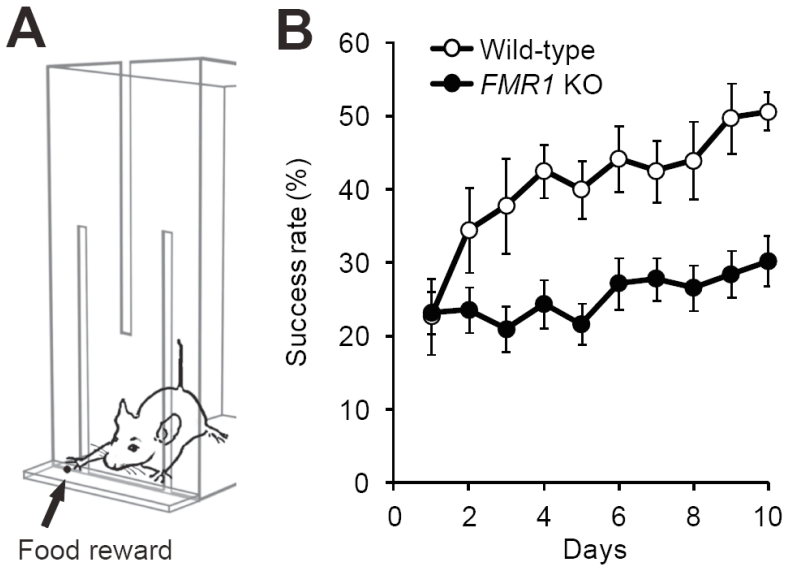

Figure 42. Adult *FMR1* KO mice fail to learn a skilled motor task.

(A) A cartoon of a mouse motor training paradigm. (B) Average success rates during training for adult WT and *FMR1* KO mice. Data are presented as mean ± s.e.m.

4.3.2 Spine formation is specifically elevated in the motor cortex of adolescent *FMR1* KO mice

To determine whether the defect in adult spine density is caused by inadequate removal of spines or excess addition of spines, we followed the same dendritic spines and examined the turnover of spines over time in the living motor cortex at different ages. We found that both spine formation and elimination appeared normal in the motor cortex of adult *FMR1* KO mice over various imaging intervals (Figure 43, $P>0.8$ for all the cases).

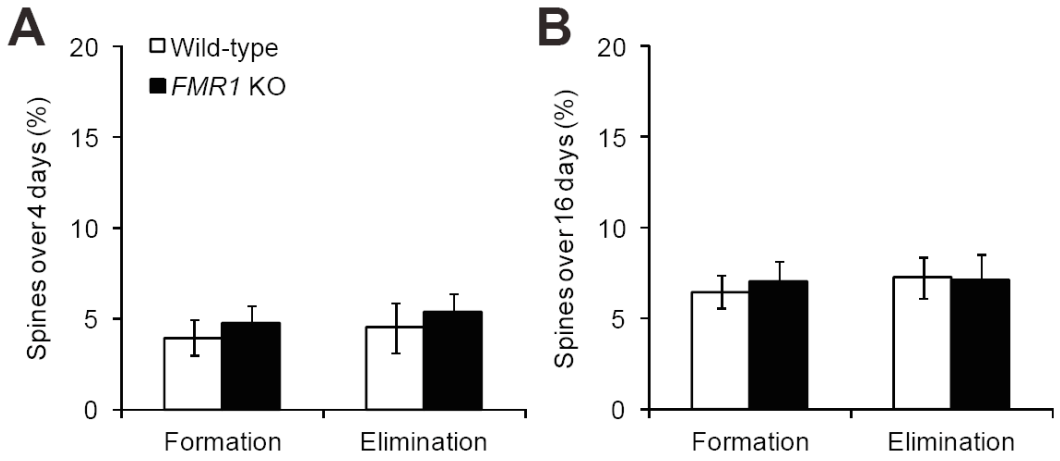

Figure 43. Adult *FMR1* KO mice show normal spine turnover in the motor cortex.

(A, B) Percentages of spines formed and eliminated over 4-day (A) and 16-day (B) intervals in the motor cortex of both *FMR1* KO and wild-type mice at 4-month old of age. Data are presented as mean ± s.d.

In contrast, at one month old of age, while spine elimination in the motor cortex of adolescent *FMR1* KO mice over 4-day interval was comparable to age-matched wild-type mice ($P>0.1$), spine formation was significantly increased (Figure 44, wild-type 6.0±1.1% vs. *FMR1* KO 9.7±1.4%, $P<0.001$). In addition, such enhanced formation in *FMR1* KO mice persisted over longer period of time, accompanied by normal spine elimination (Figure 44). Thus, elevated spine formation during adolescent development leads to excessive synapses in the motor cortex of adult *FMR1* KO mice.

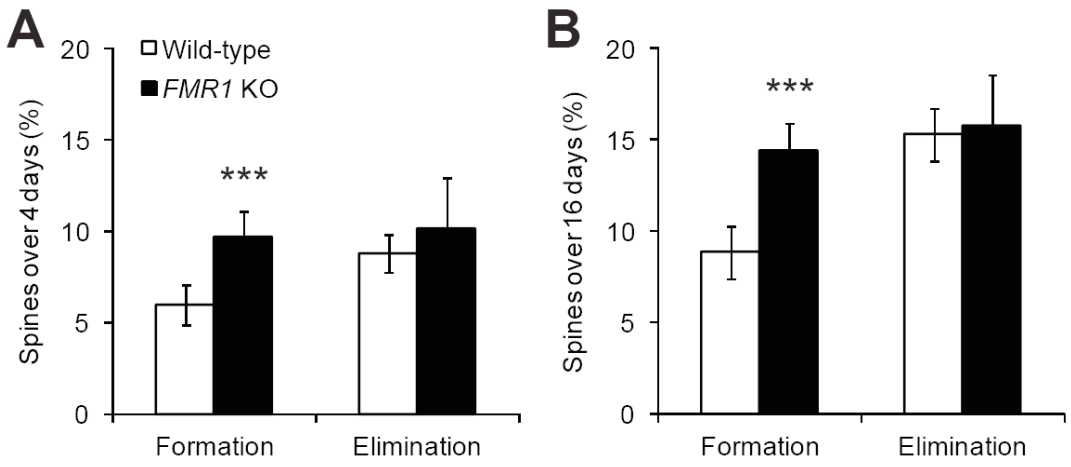

Figure 44. Adolescent *FMR1* KO mice show increased spine formation in the motor cortex.

(A, B) Percentages of spines formed and eliminated over 4-day (A) and 16-day (B) intervals in the motor cortex of both *FMR1* KO and wild-type mice at one-month old of age. Data are presented as mean ± s.d. (***P<0.001).

4.3.3 Newly formed spines are more stable in the cortex of *FMR1* KO mice

The elevated spine formation in the absence of FMRP could be caused by an accumulation of newly formed spines over time. To test this possibility, we imaged the same mice three times (day 0-1-4 and day 0-4-16), classified new and pre-existing spines based on their appearance in the first two imaging sessions and examined their survival rates in the last imaging session. We found that the survival rate of new spines formed over one day was significantly increased in *FMR1* KO mice 4 days later, compared to wild-type controls (Figure 45, wild-type 25.2±4.2% vs. *FMR1* KO 52.3±8.0%, P<0.001). In contrast, the survival rate of pre-existing spines was comparable between *FMR1* KO and wild-type mice (Figure 45, P>0.2). Similarly,

when the survival of spines formed between day 0-4 was examined on day 16, similar findings on spine survival rates were observed (Figure 46). Together, these data indicate an increase in new spine stabilization in *FMR1* KO mice, which leads to the accumulation of synaptic connections over time.

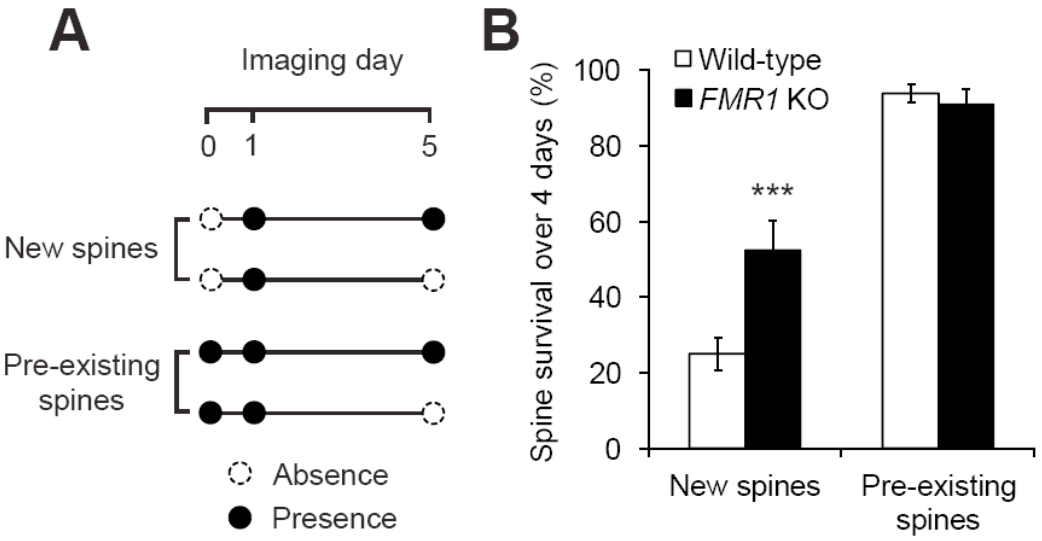

Figure 45. Increased survival rate of newly formed spines in the motor cortex of adolescent *FMR1* KO mice over 4 days.

(A) Timeline of experiments and classifications of new and pre-existing spines. (B) Survival percentages of new and pre-existing spines over 4 days in wild-type and *FMR1* KO mice. Data are presented as mean ± s.d. (***P<0.001).

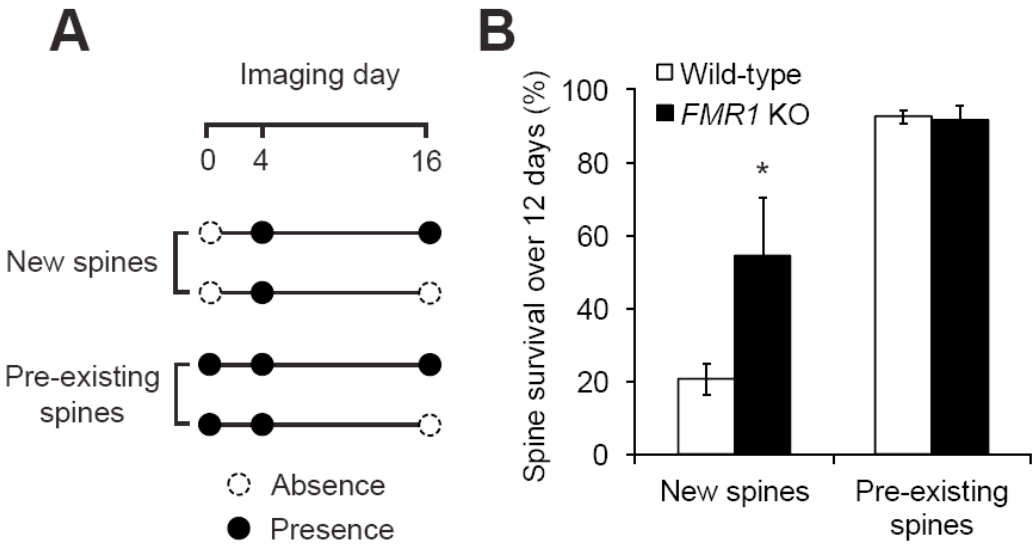

Figure 46. Increased survival rate of newly formed spines in the motor cortex of adolescent *FMR1* KO mice over 12 days.

(A) Timeline of experiments and classifications of new and pre-existing spines. (B) Survival percentages of new and pre-existing spines over 12 days in wild-type and *FMR1* KO mice. Data are presented as mean ± s.d. (**P*<0.05).

4.3.4 Spine abnormalities in *FMR1* KO mice are layer-specific

The mammalian cerebral cortex is a complex, highly-organized, laminar structure. To test if abnormal spine dynamics and morphology in the cortex of *FMR1* KO mice are layer-specific, we utilized *in utero* electroporation (IUE)-mediated gene transfer technique to label layer II/III pyramidal neurons and then investigated apical tufts in the motor cortex of both young and adult mice *in vivo*. To target layer II/III cortical neurons, IUE with EGFP (enhanced green fluorescent protein) plasmids was performed at embryonic stage E15.5 (Figure 47). Postnatal expression of EGFP

persisted into adulthood, which allows long-term imaging and examinations of spine development.

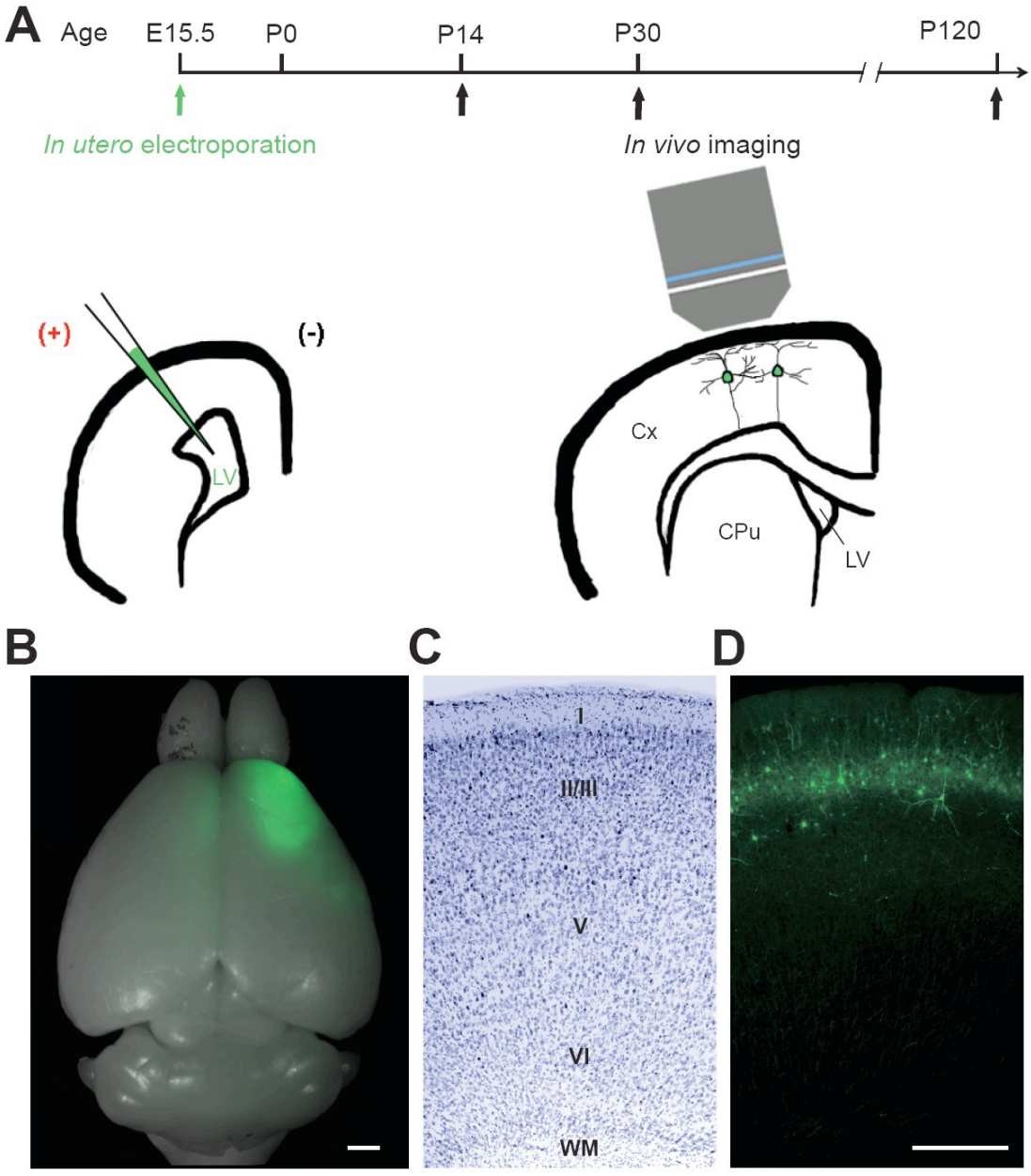

Figure 47. Layer II/III cortical neurons persistently express EGFP in the motor cortex of mice electroporated at E15.5.

(A) The timeline of experimental design and a schematic representation of *in utero* electroporation and in vivo imaging. LV, lateral ventricle; Cx, cortex; CPu, striatum; cc, corpus callosum. (B) GFP expression in the motor cortex of the whole adult mouse brain under fluorescent dissection microscope. (C, D) Successive motor cortex coronal sections by Cresyl violet staining (C) and fluorescence (D), indicating that GFP-positive neurons are located in layer II/III. I-VI, cortical layer I to layer VI; WM, white matter. Scale bars: 1 mm (B) and 250 μm (C, D).

Interestingly, we found that the intrinsic spine properties of apical dendrites of layer II/III cortical neurons were distinct from those of layer V cortical neurons. While spine density of layer V neurons apical dendrites decreased substantially during postnatal development, spine density of layer II/III neurons remained relatively constant (Figure 48A). Moreover, there were more immature dendritic spines in apical dendrites of layer II/III neurons than layer V neurons (Figure 48B). These results suggest an absence of spine pruning in layer II/III pyramidal neurons during postnatal development.

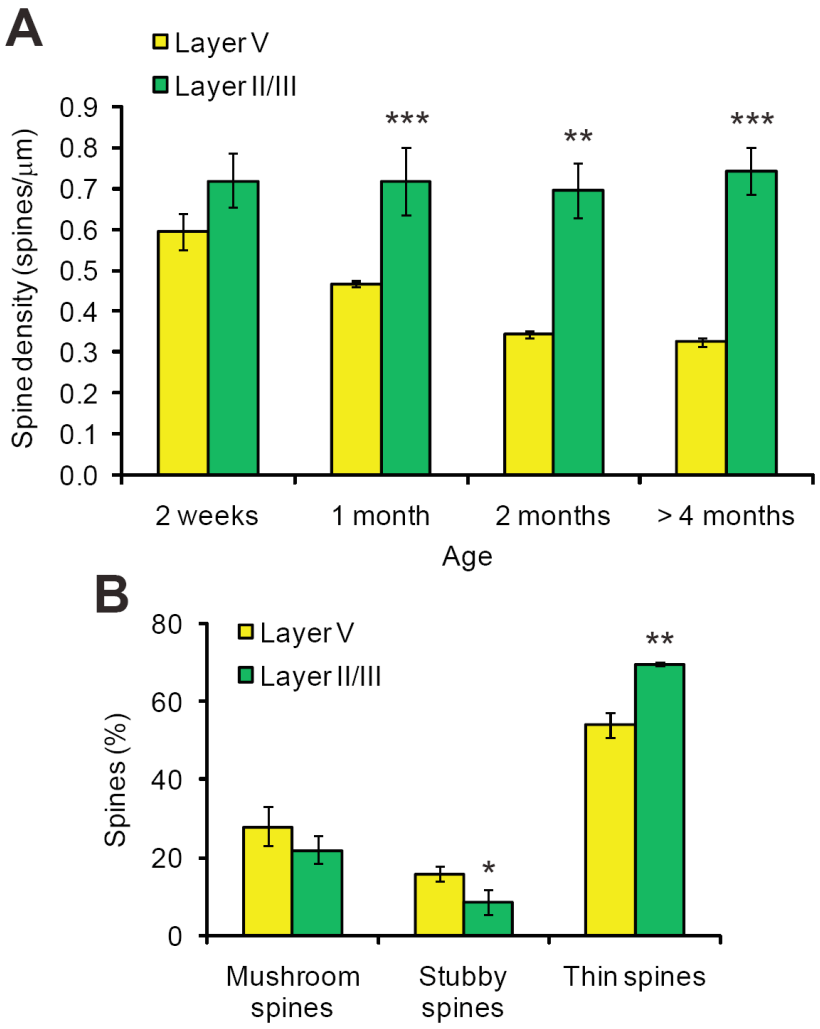

Figure 48. The differences of spine morphology on the apical dendrites between layer V and layer II/III cortical neurons.

(A) Spine density of apical dendrites of layer V and layer II/III neurons at different ages. (B) Distribution of different spine categories of layer V and layer II/III neurons from one-month-old adolescent mice. Data are presented as mean ± s.d. (**P*<0.05, ***P*<0.01, ****P*<0.001).

Next, we examined spine dynamics of layer II/III neurons in both adolescence and adulthood *in vivo* (Figure 49). We found that layer II/III neurons had higher spine turnover than layer V neurons at different developmental stages (Figures 50). In

addition, the rates of spine formation and spine elimination were comparable in layer II/III neurons (Figure 50), therefore, resulting in constant spine density throughout postnatal stages.

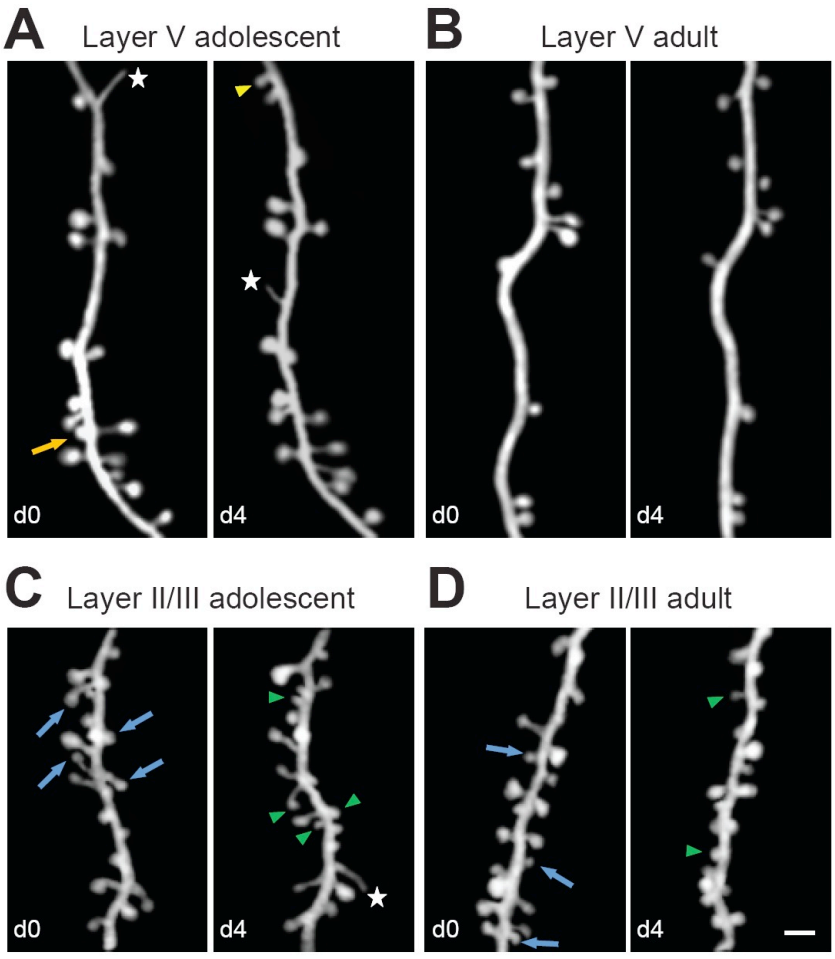

Figure 49. Examples of repeated imaging of the same dendritic branches over 4 days.

Spine elimination (arrows) and formation (arrowheads), as well as filopodia (stars), are indicated in layer V (A, B) and layer II/III (C, D) neurons of adolescent mice (1-month old) (A, C) and adult mice (> 4 months old) (C, D). Scale bar, 2 μm.

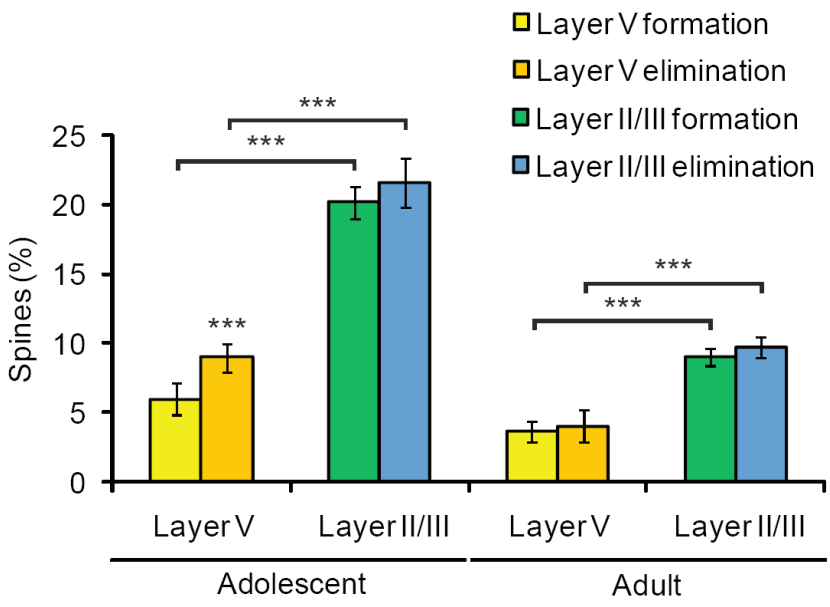

Figure 50. The differences of spine turnover on the apical dendrites between layer V and layer II/III cortical neurons.

Percentage of spines formed and eliminated over 4-day intervals in layer V and layer II/III pyramidal neurons of adolescent and adult mice. Data are presented as mean ± s.d. (***P<0.001).

Furthermore, we found that layer II/III pyramidal neurons had similar spine turnover in the motor cortex of adolescent *FMR1* KO mice compared to wild-type controls over 4-day interval (Figure 51, P>0.3 for both formation and elimination), suggesting diverse functions of FMRP at synapses in neurons residing different cortical layers.

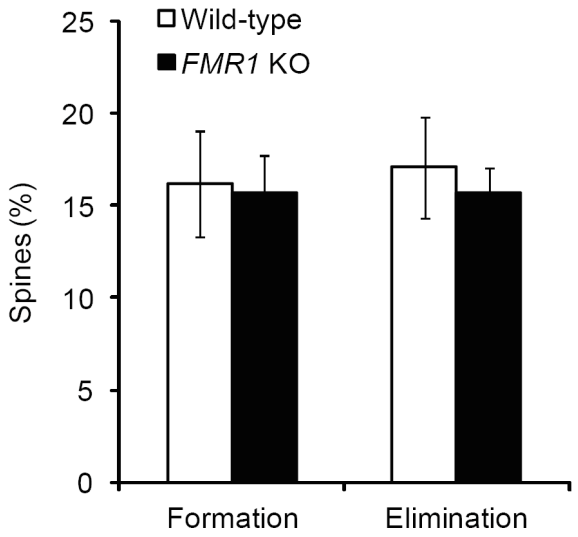

Figure 51. Spine turnover of layer II/III cortical neurons is comparable between *FMR1* KO and wild-type mice.

Percentages of spines formed and eliminated over 4-day interval in layer II/III pyramidal neurons of both wild-type and *FMR1* KO mice at one-month old of age. Data are presented as mean ± s.d.

4.3.5 mGluR5 antagonist rescues spine defects in adolescent *FMR1* KO mice by decreasing spine formation

At synapses, FMRP has been proposed to be a negative regulator protein synthesis stimulated by group 1 mGluR activation (Bear et al., 2004). The observation of enhanced mGluR5-dependent plasticity in the fragile X mouse model motivated the hypothesis that overactive mGluR5 function mediates many of the symptoms of fragile X and that mGluR5 antagonism may be a viable therapeutic strategy for the disease (Dolen et al., 2007). Recent studies have shown that the mGluR antagonist, 2-methyl-6-phenylethynyl-pyridine (MPEP), rescues major behavior defects in FXS

animal models (de Vrij et al., 2008; McBride et al., 2005; Yan et al., 2005). However, whether and how abnormal spine dynamics are affected by MPEP treatment remains known.

To answer this question, we intraperitoneally injected MPEP into one-month-old mice for short-term (4 days) and long-term (16 days) treatments, and then examined spine formation and elimination in the motor cortex during treatments. We found that MPEP treatment had no effect on either spine formation or spine elimination in wild-type group (Figure 52). However, both short-term and long-term MPEP treatments significantly decreased spine formation in *FMR1* KOs to a comparable level to wild-type mice, without affecting spine elimination (Figure 52). Thus, MPEP administration rescued the abnormality in spine pruning by decreasing the elevated spine formation in the *FMR1* KO mice. The absence of an effect of MPEP treatment on wild-type mice suggests that MPEP specifically targets excessive spine formation. Together, these data indicate that mGluR pathway is involved in initial formation of dendritic spines and FMRP is a negative regulator in this process.

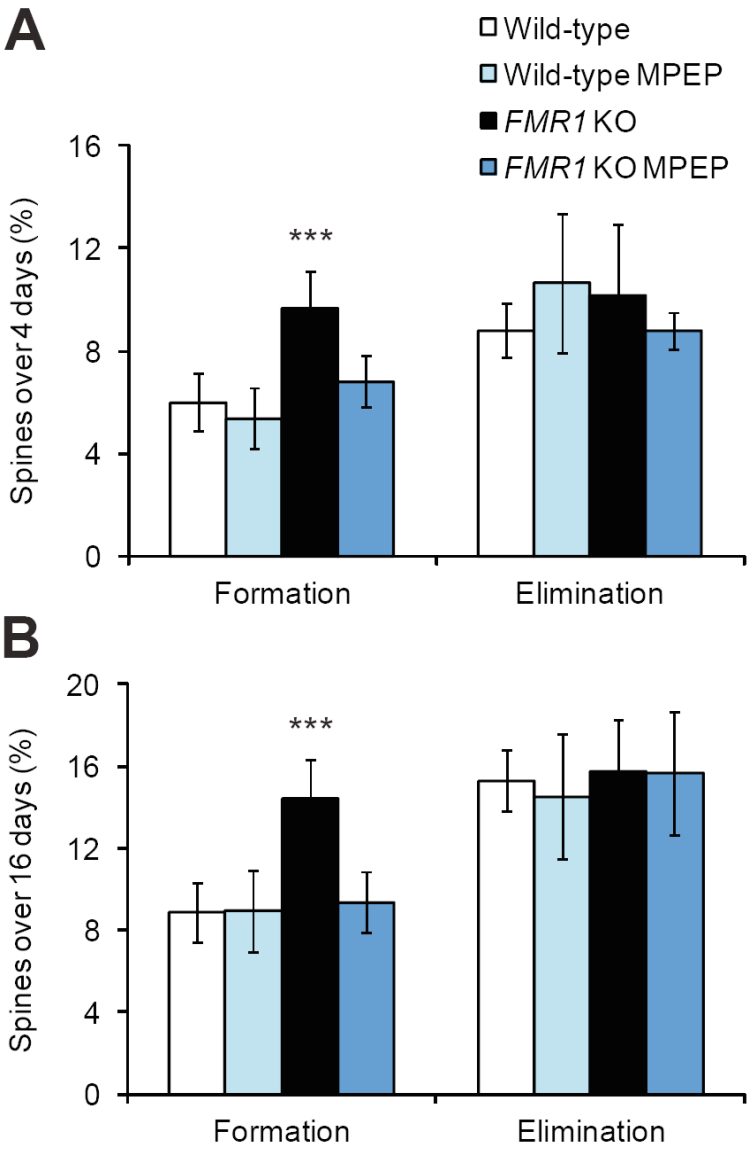

Figure 52. MPEP treatment rescues abnormal spine turnover in adolescent *FMR1* KO mice.

Percentages of spines formed and eliminated over 4-day (A) and 16-day (B) intervals in layer V pyramidal neurons of both wild-type and *FMR1* KO mice at one-month old of age with or without MPEP treatment. Data are presented as mean ± s.d. (***P<0.001).

4.4 Discussion and Future Direction

Fragile X syndrome (FXS) is characterized by an abundance of immature spines in adult brain. Here, we investigate spine dynamics in the living *FMR1* KO mice to explore its cellular mechanisms. We show that normal spine elimination is overwhelmed by the elevated spine formation during adolescent development, resulting in a significantly higher spine density in adulthood. These results contradict the popular belief that the FXS resulted from a defect in spine removal (Comery et al., 1997; Irwin et al., 2001). In addition, the fact that elevated spine formation only occurs during adolescent development but not in adulthood further points out that the spine defect is developmentally regulated. Moreover, we find that newly formed spines are more stable in *FMR1* KO mice, suggesting a role of FMRP in regulating synapse stabilization. To examine if the deficiency of *FMR1* also results in defects in spine maturation, we will next analyze the morphology of these surviving new spines.

The observations of smaller synaptic contact and defects in motor skill learning in adult *FMR1* KO mice point out a potential link between altered functional synaptic connections and behavioral abnormalities. In order to gain further insights into the relationships between structural changes of synapses and learning behaviors, quantitative ultrastructural TEM analysis and motor training will be performed at different ages to reach more solid conclusions.

We have also shown that MPEP treatment rescued the abnormal spine density by reducing spine formation in KO mice back to normal level, suggesting the involvement of mGluR pathway in intrinsic spine formation. However, selectivity of MPEP could present a potential problem. Previous studies have found that MPEP also acts as a weak NMDAR antagonist (Movsesyan et al., 2001; O'Leary et al., 2000), as well as a positive allosteric modulator of mGluR4 (Mathiesen et al., 2003). Despite the low efficacy, it is difficult to rule out the possibility of impacts from other pathways. To address this problem, fenobam, which is a selective and potent mGluR5 antagonist (Jaeschke et al., 2007; Porter et al., 2005), will be tested.

So far, FXS treatments focus on pharmacological interventions. Despite the huge clinical success of behavioral treatments for other mental diseases, it remains unknown if behavioral interventions could successfully contribute to FXS treatment. Many lines of earlier studies have shown that EE has profound effects on neuronal morphology and connectivity, as well as learning behavior (Baroncelli et al., 2010; Bennett et al., 1969; Greenough et al., 1973; Lee et al., 2003; Markham and Greenough, 2004; Moser et al., 1997; Schrijver et al., 2002; Turner and Greenough, 1985). A recent study has also shown that EE alleviates hyperactive and anxiety behaviors, as well as the abnormal neuronal morphology, and increases AMPAR GluR1 levels in *FMR1* KO mice (Restivo et al., 2005). It remains unknown whether EE share similar cellular mechanisms with mGluR antagonist treatment.

To evaluate the potential of EE as a behavioral intervention for FXS treatment, we will raise young (1-month-old) *FMR1* KO and wild-type littermates in either enriched or standard cages for various periods of time (*i.e.*, 4 days, 2 weeks, 1 month and 3 months). We will first examine whether EE for 1 month rescues the spine density defect in *FMR1* KOs. Next we will investigate the dynamics and survival rates of the dendritic spines during EE over various intervals. We will also test motor learning behaviors in mice undergo EE. Our results will provide important information for understanding cellular mechanisms underpinning FXS and potential therapeutic treatments.

References

Adkins, D.L., Boychuk, J., Remple, M.S., and Kleim, J.A. (2006). Motor training induces experience-specific patterns of plasticity across motor cortex and spinal cord. J Appl Physiol 101, 1776-1782.

Allred, R.P., Adkins, D.L., Woodlee, M.T., Husbands, L.C., Maldonado, M.A., Kane, J.R., Schallert, T., and Jones, T.A. (2008). The vermicelli handling test: a simple quantitative measure of dexterous forepaw function in rats. Journal of neuroscience methods 170, 229-244.

Alvarez, V.A., and Sabatini, B.L. (2007). Anatomical and physiological plasticity of dendritic spines. Annu Rev Neurosci 30, 79-97.

Anderson, C.T., Sheets, P.L., Kiritani, T., and Shepherd, G.M. (2010). Sublayer-specific microcircuits of corticospinal and corticostriatal neurons in motor cortex. Nature neuroscience 13, 739-744.

Antar, L.N., Dictenberg, J.B., Plociniak, M., Afroz, R., and Bassell, G.J. (2005). Localization of FMRP-associated mRNA granules and requirement of microtubules for activity-dependent trafficking in hippocampal neurons. Genes Brain Behav 4, 350-359.

Aoto, J., and Chen, L. (2007). Bidirectional ephrin/Eph signaling in synaptic functions. Brain Res 1184, 72-80.

Bagni, C., and Greenough, W.T. (2005). From mRNP trafficking to spine dysmorphogenesis: the roots of fragile X syndrome. Nat Rev Neurosci 6, 376-387.

Baroncelli, L., Braschi, C., Spolidoro, M., Begenisic, T., Sale, A., and Maffei, L. (2010). Nurturing brain plasticity: impact of environmental enrichment. Cell death and differentiation 17, 1092-1103.

Bassell, G.J., and Warren, S.T. (2008). Fragile X syndrome: loss of local mRNA regulation alters synaptic development and function. Neuron 60, 201-214.

Bear, M.F., Huber, K.M., and Warren, S.T. (2004). The mGluR theory of fragile X mental retardation. Trends Neurosci 27, 370-377.

Bechara, E.G., Didiot, M.C., Melko, M., Davidovic, L., Bensaid, M., Martin, P., Castets, M., Pognonec, P., Khandjian, E.W., Moine, H., and Bardoni, B. (2009). A

novel function for fragile X mental retardation protein in translational activation. PLoS Biol 7, e16.

Beckel-Mitchener, A., and Greenough, W.T. (2004). Correlates across the structural, functional, and molecular phenotypes of fragile X syndrome. Ment Retard Dev Disabil Res Rev 10, 53-59.

Bellone, C., and Nicoll, R.A. (2007). Rapid bidirectional switching of synaptic NMDA receptors. Neuron 55, 779-785.

Bennett, E.L., Rosenzweig, M.R., and Diamond, M.C. (1969). Rat brain: effects of environmental enrichment on wet and dry weights. Science (New York, N.Y 163, 825-826.

Bhatt, D.H., Zhang, S., and Gan, W.B. (2009). Dendritic spine dynamics. Annual review of physiology 71, 261-282.

Bock, J., and Braun, K. (1999). Blockade of N-methyl-D-aspartate receptor activation suppresses learning-induced synaptic elimination. Proceedings of the National Academy of Sciences of the United States of America 96, 2485-2490.

Bourne, J., and Harris, K.M. (2007). Do thin spines learn to be mushroom spines that remember? Curr Opin Neurobiol 17, 381-386.

Bouvier, D., Corera, A.T., Tremblay, M.E., Riad, M., Chagnon, M., Murai, K.K., Pasquale, E.B., Fon, E.A., and Doucet, G. (2008). Pre-synaptic and post-synaptic localization of EphA4 and EphB2 in adult mouse forebrain. Journal of neurochemistry 106, 682-695.

Bramham, C.R., and Wells, D.G. (2007). Dendritic mRNA: transport, translation and function. Nat Rev Neurosci 8, 776-789.

Brown, C.E., Aminoltejari, K., Erb, H., Winship, I.R., and Murphy, T.H. (2009). In vivo voltage-sensitive dye imaging in adult mice reveals that somatosensory maps lost to stroke are replaced over weeks by new structural and functional circuits with prolonged modes of activation within both the peri-infarct zone and distant sites. J Neurosci 29, 1719-1734.

Brown, C.E., Boyd, J.D., and Murphy, T.H. (2010). Longitudinal in vivo imaging reveals balanced and branch-specific remodeling of mature cortical pyramidal dendritic arbors after stroke. J Cereb Blood Flow Metab 30, 783-791.

Brown, C.E., Li, P., Boyd, J.D., Delaney, K.R., and Murphy, T.H. (2007). Extensive turnover of dendritic spines and vascular remodeling in cortical tissues recovering from stroke. J Neurosci 27, 4101-4109.

Brown, V., Jin, P., Ceman, S., Darnell, J.C., O'Donnell, W.T., Tenenbaum, S.A., Jin, X., Feng, Y., Wilkinson, K.D., Keene, J.D., et al. (2001). Microarray identification of FMRP-associated brain mRNAs and altered mRNA translational profiles in fragile X syndrome. Cell 107, 477-487.

Cahoy, J.D., Emery, B., Kaushal, A., Foo, L.C., Zamanian, J.L., Christopherson, K.S., Xing, Y., Lubischer, J.L., Krieg, P.A., Krupenko, S.A., et al. (2008). A transcriptome database for astrocytes, neurons, and oligodendrocytes: a new resource for understanding brain development and function. J Neurosci 28, 264-278.

Cang, J., Kaneko, M., Yamada, J., Woods, G., Stryker, M.P., and Feldheim, D.A. (2005). Ephrin-as guide the formation of functional maps in the visual cortex. Neuron 48, 577-589.

Carmona, M.A., Murai, K.K., Wang, L., Roberts, A.J., and Pasquale, E.B. (2009). Glial ephrin-A3 regulates hippocampal dendritic spine morphology and glutamate transport. Proceedings of the National Academy of Sciences of the United States of America 106, 12524-12529.

Changeux, J.P., and Danchin, A. (1976). Selective stabilisation of developing synapses as a mechanism for the specification of neuronal networks. Nature 264, 705-712.

Chaudhry, F.A., Lehre, K.P., van Lookeren Campagne, M., Ottersen, O.P., Danbolt, N.C., and Storm-Mathisen, J. (1995). Glutamate transporters in glial plasma membranes: highly differentiated localizations revealed by quantitative ultrastructural immunocytochemistry. Neuron 15, 711-720.

Chonchaiya, W., Schneider, A., and Hagerman, R.J. (2009). Fragile X: a family of disorders. Adv Pediatr 56, 165-186.

Comery, T.A., Harris, J.B., Willems, P.J., Oostra, B.A., Irwin, S.A., Weiler, I.J., and Greenough, W.T. (1997). Abnormal dendritic spines in fragile X knockout mice: maturation and pruning deficits. Proc Natl Acad Sci U S A 94, 5401-5404.

Contractor, A., Rogers, C., Maron, C., Henkemeyer, M., Swanson, G.T., and Heinemann, S.F. (2002). Trans-synaptic Eph receptor-ephrin signaling in hippocampal mossy fiber LTP. Science 296, 1864-1869.

Cruz-Martin, A., Crespo, M., and Portera-Cailliau, C. (2010). Delayed stabilization of dendritic spines in fragile X mice. J Neurosci 30, 7793-7803.

Cutforth, T., Moring, L., Mendelsohn, M., Nemes, A., Shah, N.M., Kim, M.M., Frisen, J., and Axel, R. (2003). Axonal ephrin-As and odorant receptors: coordinate determination of the olfactory sensory map. Cell 114, 311-322.

Dailey, M.E., and Smith, S.J. (1996). The dynamics of dendritic structure in developing hippocampal slices. J Neurosci 16, 2983-2994.

Darnell, J.C., Jensen, K.B., Jin, P., Brown, V., Warren, S.T., and Darnell, R.B. (2001). Fragile X mental retardation protein targets G quartet mRNAs important for neuronal function. Cell 107, 489-499.

De Paola, V., Holtmaat, A., Knott, G., Song, S., Wilbrecht, L., Caroni, P., and Svoboda, K. (2006). Cell type-specific structural plasticity of axonal branches and boutons in the adult neocortex. Neuron 49, 861-875.

de Vrij, F.M., Levenga, J., van der Linde, H.C., Koekkoek, S.K., De Zeeuw, C.I., Nelson, D.L., Oostra, B.A., and Willemsen, R. (2008). Rescue of behavioral phenotype and neuronal protrusion morphology in Fmr1 KO mice. Neurobiology of disease 31, 127-132.

Dolen, G., and Bear, M.F. (2008). Role for metabotropic glutamate receptor 5 (mGluR5) in the pathogenesis of fragile X syndrome. J Physiol 586, 1503-1508.

Dolen, G., Osterweil, E., Rao, B.S., Smith, G.B., Auerbach, B.D., Chattarji, S., and Bear, M.F. (2007). Correction of fragile X syndrome in mice. Neuron 56, 955-962.

Dombeck, D.A., Graziano, M.S., and Tank, D.W. (2009). Functional clustering of neurons in motor cortex determined by cellular resolution imaging in awake behaving mice. J Neurosci 29, 13751-13760.

Engert, F., and Bonhoeffer, T. (1999). Dendritic spine changes associated with hippocampal long-term synaptic plasticity. Nature 399, 66-70.

Feldheim, D.A., Kim, Y.I., Bergemann, A.D., Frisen, J., Barbacid, M., and Flanagan, J.G. (2000). Genetic analysis of ephrin-A2 and ephrin-A5 shows their requirement in multiple aspects of retinocollicular mapping. Neuron 25, 563-574.

Feng, G., Mellor, R.H., Bernstein, M., Keller-Peck, C., Nguyen, Q.T., Wallace, M., Nerbonne, J.M., Lichtman, J.W., and Sanes, J.R. (2000). Imaging neuronal subsets in transgenic mice expressing multiple spectral variants of GFP. Neuron 28, 41-51.

Fiala, J.C., Spacek, J., and Harris, K.M. (2002). Dendritic spine pathology: cause or consequence of neurological disorders? Brain Res Brain Res Rev 39, 29-54.

Filosa, A., Paixao, S., Honsek, S.D., Carmona, M.A., Becker, L., Feddersen, B., Gaitanos, L., Rudhard, Y., Schoepfer, R., Klopstock, T., et al. (2009). Neuron-glia communication via EphA4/ephrin-A3 modulates LTP through glial glutamate transport. Nature neuroscience 12, 1285-1292.

Fu, M., Yu, X., Lu, J., and Zuo, Y. (2012). Repetitive motor learning induces coordinated formation of clustered dendritic spines in vivo. Nature 483, 92-95.

Galvez, R., and Greenough, W.T. (2005). Sequence of abnormal dendritic spine development in primary somatosensory cortex of a mouse model of the fragile X mental retardation syndrome. Am J Med Genet A 135, 155-160.

Galvez, R., Gopal, A.R., and Greenough, W.T. (2003). Somatosensory cortical barrel dendritic abnormalities in a mouse model of the fragile X mental retardation syndrome. Brain research 971, 83-89.

Ghosh, A., Haiss, F., Sydekum, E., Schneider, R., Gullo, M., Wyss, M.T., Mueggler, T., Baltes, C., Rudin, M., Weber, B., and Schwab, M.E. (2010). Rewiring of hindlimb corticospinal neurons after spinal cord injury. Nature neuroscience 13, 97-104.

Greenough, W.T., Klintsova, A.Y., Irwin, S.A., Galvez, R., Bates, K.E., and Weiler, I.J. (2001). Synaptic regulation of protein synthesis and the fragile X protein. Proc Natl Acad Sci U S A 98, 7101-7106.

Greenough, W.T., Larson, J.R., and Withers, G.S. (1985). Effects of unilateral and bilateral training in a reaching task on dendritic branching of neurons in the rat motor-sensory forelimb cortex. Behavioral and neural biology 44, 301-314.

Greenough, W.T., Volkmar, F.R., and Juraska, J.M. (1973). Effects of rearing complexity on dendritic branching in frontolateral and temporal cortex of the rat. Experimental neurology 41, 371-378.

Grossman, A.W., Elisseou, N.M., McKinney, B.C., and Greenough, W.T. (2006). Hippocampal pyramidal cells in adult Fmr1 knockout mice exhibit an immature-appearing profile of dendritic spines. Brain research 1084, 158-164.

Grutzendler, J., Kasthuri, N., and Gan, W.B. (2002). Long-term dendritic spine stability in the adult cortex. Nature 420, 812-816.

Haber, M., Zhou, L., and Murai, K.K. (2006). Cooperative astrocyte and dendritic spine dynamics at hippocampal excitatory synapses. J Neurosci 26, 8881-8891.

Harms, K.J., and Dunaevsky, A. (2007). Dendritic spine plasticity: looking beyond development. Brain Res 1184, 65-71.

Harms, K.J., Rioult-Pedotti, M.S., Carter, D.R., and Dunaevsky, A. (2008). Transient spine expansion and learning-induced plasticity in layer 1 primary motor cortex. J Neurosci 28, 5686-5690.

Harris, K.M., and Stevens, J.K. (1988). Dendritic spines of rat cerebellar Purkinje cells: serial electron microscopy with reference to their biophysical characteristics. J Neurosci 8, 4455-4469.

Harris, K.M., and Stevens, J.K. (1989). Dendritic spines of CA 1 pyramidal cells in the rat hippocampus: serial electron microscopy with reference to their biophysical characteristics. J Neurosci 9, 2982-2997.

Harris, K.M., Jensen, F.E., and Tsao, B. (1992). Three-dimensional structure of dendritic spines and synapses in rat hippocampus (CA1) at postnatal day 15 and adult ages: implications for the maturation of synaptic physiology and long-term potentiation. J Neurosci 12, 2685-2705.

Hertz, L., and Zielke, H.R. (2004). Astrocytic control of glutamatergic activity: astrocytes as stars of the show. Trends in neurosciences 27, 735-743.

Hinton, V.J., Brown, W.T., Wisniewski, K., and Rudelli, R.D. (1991). Analysis of neocortex in three males with the fragile X syndrome. Am J Med Genet 41, 289-294.

Hodgson, R.A., Ji, Z., Standish, S., Boyd-Hodgson, T.E., Henderson, A.K., and Racine, R.J. (2005). Training-induced and electrically induced potentiation in the neocortex. Neurobiol Learn Mem 83, 22-32.

Hofer, S.B., Mrsic-Flogel, T.D., Bonhoeffer, T., and Hubener, M. (2006). Prior experience enhances plasticity in adult visual cortex. Nature neuroscience 9, 127-132.

Hofer, S.B., Mrsic-Flogel, T.D., Bonhoeffer, T., and Hubener, M. (2009). Experience leaves a lasting structural trace in cortical circuits. Nature 457, 313-317.

Holtmaat, A., and Svoboda, K. (2009). Experience-dependent structural synaptic plasticity in the mammalian brain. Nat Rev Neurosci 10, 647-658.

Holtmaat, A., Wilbrecht, L., Knott, G.W., Welker, E., and Svoboda, K. (2006). Experience-dependent and cell-type-specific spine growth in the neocortex. Nature 441, 979-983.

Holtmaat, A.J., Trachtenberg, J.T., Wilbrecht, L., Shepherd, G.M., Zhang, X., Knott, G.W., and Svoboda, K. (2005). Transient and persistent dendritic spines in the neocortex in vivo. Neuron 45, 279-291.

Horner, C.H. (1993). Plasticity of the dendritic spine. Prog Neurobiol 41, 281-321.

Hubel, D.H., Wiesel, T.N., and LeVay, S. (1977). Plasticity of ocular dominance columns in monkey striate cortex. Philosophical transactions of the Royal Society of London 278, 377-409.

Huber, K.M., Gallagher, S.M., Warren, S.T., and Bear, M.F. (2002). Altered synaptic plasticity in a mouse model of fragile X mental retardation. Proc Natl Acad Sci U S A 99, 7746-7750.

Iezzi, E., Suppa, A., Conte, A., Agostino, R., Nardella, A., and Berardelli, A. (2010). Theta-burst stimulation over primary motor cortex degrades early motor learning. Eur J Neurosci 31, 585-592.

Irwin, S.A., Patel, B., Idupulapati, M., Harris, J.B., Crisostomo, R.A., Larsen, B.P., Kooy, F., Willems, P.J., Cras, P., Kozlowski, P.B., et al. (2001). Abnormal dendritic spine characteristics in the temporal and visual cortices of patients with fragile-X syndrome: a quantitative examination. American journal of medical genetics 98, 161-167.

Jaeschke, G., Porter, R., Buttelmann, B., Ceccarelli, S.M., Guba, W., Kuhn, B., Kolczewski, S., Huwyler, J., Mutel, V., Peters, J.U., et al. (2007). Synthesis and biological evaluation of fenobam analogs as mGlu5 receptor antagonists. Bioorganic & medicinal chemistry letters 17, 1307-1311.

Jung, P., and Ziemann, U. (2009). Homeostatic and nonhomeostatic modulation of learning in human motor cortex. J Neurosci 29, 5597-5604.

Karni, A., Meyer, G., Jezzard, P., Adams, M.M., Turner, R., and Ungerleider, L.G. (1995). Functional MRI evidence for adult motor cortex plasticity during motor skill learning. Nature 377, 155-158.

Katz, L.C., and Shatz, C.J. (1996). Synaptic activity and the construction of cortical circuits. Science 274, 1133-1138.

Keck, T., Mrsic-Flogel, T.D., Vaz Afonso, M., Eysel, U.T., Bonhoeffer, T., and Hubener, M. (2008). Massive restructuring of neuronal circuits during functional reorganization of adult visual cortex. Nature neuroscience 11, 1162-1167.

Kim, B.G., Dai, H.N., McAtee, M., and Bregman, B.S. (2008). Modulation of dendritic spine remodeling in the motor cortex following spinal cord injury: effects of environmental enrichment and combinatorial treatment with transplants and neurotrophin-3. J Comp Neurol 508, 473-486.

Kim, B.G., Dai, H.N., McAtee, M., Vicini, S., and Bregman, B.S. (2006). Remodeling of synaptic structures in the motor cortex following spinal cord injury. Exp Neurol 198, 401-415.

Kleim, J.A., Barbay, S., Cooper, N.R., Hogg, T.M., Reidel, C.N., Remple, M.S., and Nudo, R.J. (2002). Motor learning-dependent synaptogenesis is localized to

functionally reorganized motor cortex. Neurobiology of learning and memory 77, 63-77.

Kleim, J.A., Hogg, T.M., VandenBerg, P.M., Cooper, N.R., Bruneau, R., and Remple, M. (2004). Cortical synaptogenesis and motor map reorganization occur during late, but not early, phase of motor skill learning. J Neurosci 24, 628-633.

Kleim, J.A., Lussnig, E., Schwarz, E.R., Comery, T.A., and Greenough, W.T. (1996). Synaptogenesis and Fos expression in the motor cortex of the adult rat after motor skill learning. J Neurosci 16, 4529-4535.

Kleim, J.A., Vij, K., Ballard, D.H., and Greenough, W.T. (1997). Learning-dependent synaptic modifications in the cerebellar cortex of the adult rat persist for at least four weeks. J Neurosci 17, 717-721.

Klein, R. (2009). Bidirectional modulation of synaptic functions by Eph/ephrin signaling. Nature neuroscience 12, 15-20.

Koekkoek, S.K., Yamaguchi, K., Milojkovic, B.A., Dortland, B.R., Ruigrok, T.J., Maex, R., De Graaf, W., Smit, A.E., VanderWerf, F., Bakker, C.E., et al. (2005). Deletion of FMR1 in Purkinje cells enhances parallel fiber LTD, enlarges spines, and attenuates cerebellar eyelid conditioning in Fragile X syndrome. Neuron 47, 339-352.

Kolb, B., Cioe, J., and Comeau, W. (2008). Contrasting effects of motor and visual spatial learning tasks on dendritic arborization and spine density in rats. Neurobiology of learning and memory 90, 295-300.

Komiyama, T., Sato, T.R., O'Connor, D.H., Zhang, Y.X., Huber, D., Hooks, B.M., Gabitto, M., and Svoboda, K. (2010). Learning-related fine-scale specificity imaged in motor cortex circuits of behaving mice. Nature 464, 1182-1186.

Laggerbauer, B., Ostareck, D., Keidel, E.M., Ostareck-Lederer, A., and Fischer, U. (2001). Evidence that fragile X mental retardation protein is a negative regulator of translation. Hum Mol Genet 10, 329-338.

Lai, K.O., and Ip, N.Y. (2009). Synapse development and plasticity: roles of ephrin/Eph receptor signaling. Curr Opin Neurobiol 19, 275-283.

Lee, E.H., Hsu, W.L., Ma, Y.L., Lee, P.J., and Chao, C.C. (2003). Enrichment enhances the expression of sgk, a glucocorticoid-induced gene, and facilitates spatial learning through glutamate AMPA receptor mediation. The European journal of neuroscience 18, 2842-2852.

Lendvai, B., Stern, E.A., Chen, B., and Svoboda, K. (2000). Experience-dependent plasticity of dendritic spines in the developing rat barrel cortex in vivo. Nature 404, 876-881.

Li, J., Pelletier, M.R., Perez Velazquez, J.L., and Carlen, P.L. (2002). Reduced cortical synaptic plasticity and GluR1 expression associated with fragile X mental retardation protein deficiency. Mol Cell Neurosci 19, 138-151.

Lichtman, J.W., and Colman, H. (2000). Synapse elimination and indelible memory. Neuron 25, 269-278.

Lim, B.K., Matsuda, N., and Poo, M.M. (2008). Ephrin-B reverse signaling promotes structural and functional synaptic maturation in vivo. Nature neuroscience 11, 160-169.

Lin, J.W., Ju, W., Foster, K., Lee, S.H., Ahmadian, G., Wyszynski, M., Wang, Y.T., and Sheng, M. (2000). Distinct molecular mechanisms and divergent endocytotic pathways of AMPA receptor internalization. Nat Neurosci 3, 1282-1290.

Luft, A.R., and Buitrago, M.M. (2005). Stages of motor skill learning. Molecular neurobiology 32, 205-216.

Luscher, C., and Huber, K.M. (2010). Group 1 mGluR-dependent synaptic long-term depression: mechanisms and implications for circuitry and disease. Neuron 65, 445-459.

Majewska, A.K., Newton, J.R., and Sur, M. (2006). Remodeling of synaptic structure in sensory cortical areas in vivo. J Neurosci 26, 3021-3029.

Markham, J.A., and Greenough, W.T. (2004). Experience-driven brain plasticity: beyond the synapse. Neuron glia biology 1, 351-363.

Mathiesen, J.M., Svendsen, N., Brauner-Osborne, H., Thomsen, C., and Ramirez, M.T. (2003). Positive allosteric modulation of the human metabotropic glutamate receptor 4 (hmGluR4) by SIB-1893 and MPEP. British journal of pharmacology 138, 1026-1030.

McBride, S.M., Choi, C.H., Wang, Y., Liebelt, D., Braunstein, E., Ferreiro, D., Sehgal, A., Siwicki, K.K., Dockendorff, T.C., Nguyen, H.T., et al. (2005). Pharmacological rescue of synaptic plasticity, courtship behavior, and mushroom body defects in a Drosophila model of fragile X syndrome. Neuron 45, 753-764.

McClelland, A.C., Hruska, M., Coenen, A.J., Henkemeyer, M., and Dalva, M.B. (2010). Trans-synaptic EphB2-ephrin-B3 interaction regulates excitatory synapse

density by inhibition of postsynaptic MAPK signaling. Proceedings of the National Academy of Sciences of the United States of America 107, 8830-8835.

McKinney, B.C., Grossman, A.W., Elisseou, N.M., and Greenough, W.T. (2005). Dendritic spine abnormalities in the occipital cortex of C57BL/6 Fmr1 knockout mice. Am J Med Genet B Neuropsychiatr Genet 136B, 98-102.

Micheva, K.D., and Smith, S.J. (2007). Array tomography: a new tool for imaging the molecular architecture and ultrastructure of neural circuits. Neuron 55, 25-36.

Micheva, K.D., Busse, B., Weiler, N.C., O'Rourke, N., and Smith, S.J. (2010). Single-synapse analysis of a diverse synapse population: proteomic imaging methods and markers. Neuron 68, 639-653.

Miyashiro, K.Y., Beckel-Mitchener, A., Purk, T.P., Becker, K.G., Barret, T., Liu, L., Carbonetto, S., Weiler, I.J., Greenough, W.T., and Eberwine, J. (2003). RNA cargoes associating with FMRP reveal deficits in cellular functioning in Fmr1 null mice. Neuron 37, 417-431.

Monfils, M.H., and Teskey, G.C. (2004). Induction of long-term depression is associated with decreased dendritic length and spine density in layers III and V of sensorimotor neocortex. Synapse 53, 114-121.

Monfils, M.H., Plautz, E.J., and Kleim, J.A. (2005). In search of the motor engram: motor map plasticity as a mechanism for encoding motor experience. Neuroscientist 11, 471-483.

Monfils, M.H., VandenBerg, P.M., Kleim, J.A., and Teskey, G.C. (2004). Long-term potentiation induces expanded movement representations and dendritic hypertrophy in layer V of rat sensorimotor neocortex. Cereb Cortex 14, 586-593.

Moser, M.B., Trommald, M., Egeland, T., and Andersen, P. (1997). Spatial training in a complex environment and isolation alter the spine distribution differently in rat CA1 pyramidal cells. The Journal of comparative neurology 380, 373-381.

Movsesyan, V.A., O'Leary, D.M., Fan, L., Bao, W., Mullins, P.G., Knoblach, S.M., and Faden, A.I. (2001). mGluR5 antagonists 2-methyl-6-(phenylethynyl)-pyridine and (E)-2-methyl-6-(2-phenylethenyl)-pyridine reduce traumatic neuronal injury in vitro and in vivo by antagonizing N-methyl-D-aspartate receptors. The Journal of pharmacology and experimental therapeutics 296, 41-47.

Muddashetty, R.S., Kelic, S., Gross, C., Xu, M., and Bassell, G.J. (2007). Dysregulated metabotropic glutamate receptor-dependent translation of AMPA receptor and postsynaptic density-95 mRNAs at synapses in a mouse model of fragile X syndrome. J Neurosci 27, 5338-5348.

Murai, K.K., and Pasquale, E.B. (2004). Eph receptors, ephrins, and synaptic function. Neuroscientist 10, 304-314.

Murai, K.K., Nguyen, L.N., Irie, F., Yamaguchi, Y., and Pasquale, E.B. (2003). Control of hippocampal dendritic spine morphology through ephrin-A3/EphA4 signaling. Nature neuroscience 6, 153-160.

Murphy, T.H., and Corbett, D. (2009). Plasticity during stroke recovery: from synapse to behaviour. Nat Rev Neurosci 10, 861-872.

Nakamoto, M., Nalavadi, V., Epstein, M.P., Narayanan, U., Bassell, G.J., and Warren, S.T. (2007). Fragile X mental retardation protein deficiency leads to excessive mGluR5-dependent internalization of AMPA receptors. Proc Natl Acad Sci U S A 104, 15537-15542.

Nimchinsky, E.A., Oberlander, A.M., and Svoboda, K. (2001). Abnormal development of dendritic spines in FMR1 knock-out mice. J Neurosci 21, 5139-5146.

Nimchinsky, E.A., Sabatini, B.L., and Svoboda, K. (2002). Structure and function of dendritic spines. Annual review of physiology 64, 313-353.

Nishida, H., and Okabe, S. (2007). Direct astrocytic contacts regulate local maturation of dendritic spines. J Neurosci 27, 331-340.

Nudo, R.J. (2006). Mechanisms for recovery of motor function following cortical damage. Curr Opin Neurobiol 16, 638-644.

Nudo, R.J., Milliken, G.W., Jenkins, W.M., and Merzenich, M.M. (1996). Use-dependent alterations of movement representations in primary motor cortex of adult squirrel monkeys. J Neurosci 16, 785-807.

O'Donnell, W.T., and Warren, S.T. (2002). A decade of molecular studies of fragile X syndrome. Annu Rev Neurosci 25, 315-338.

O'Leary, D.M., Movsesyan, V., Vicini, S., and Faden, A.I. (2000). Selective mGluR5 antagonists MPEP and SIB-1893 decrease NMDA or glutamate-mediated neuronal toxicity through actions that reflect NMDA receptor antagonism. British journal of pharmacology 131, 1429-1437.

Penagarikano, O., Mulle, J.G., and Warren, S.T. (2007). The pathophysiology of fragile x syndrome. Annu Rev Genomics Hum Genet 8, 109-129.

Penzes, P., Beeser, A., Chernoff, J., Schiller, M.R., Eipper, B.A., Mains, R.E., and Huganir, R.L. (2003). Rapid induction of dendritic spine morphogenesis by trans-

synaptic ephrinB-EphB receptor activation of the Rho-GEF kalirin. Neuron 37, 263-274.

Pfeiffenberger, C., Cutforth, T., Woods, G., Yamada, J., Renteria, R.C., Copenhagen, D.R., Flanagan, J.G., and Feldheim, D.A. (2005). Ephrin-As and neural activity are required for eye-specific patterning during retinogeniculate mapping. Nature neuroscience 8, 1022-1027.

Pfeiffer, B.E., and Huber, K.M. (2007). Fragile X mental retardation protein induces synapse loss through acute postsynaptic translational regulation. J Neurosci 27, 3120-3130.

Porter, R.H., Jaeschke, G., Spooren, W., Ballard, T.M., Buttelmann, B., Kolczewski, S., Peters, J.U., Prinssen, E., Wichmann, J., Vieira, E., et al. (2005). Fenobam: a clinically validated nonbenzodiazepine anxiolytic is a potent, selective, and noncompetitive mGlu5 receptor antagonist with inverse agonist activity. The Journal of pharmacology and experimental therapeutics 315, 711-721.

Purpura, D.P. (1974). Dendritic spine "dysgenesis" and mental retardation. Science 186, 1126-1128.

Restivo, L., Ferrari, F., Passino, E., Sgobio, C., Bock, J., Oostra, B.A., Bagni, C., and Ammassari-Teule, M. (2005). Enriched environment promotes behavioral and morphological recovery in a mouse model for the fragile X syndrome. Proceedings of the National Academy of Sciences of the United States of America 102, 11557-11562.

Reyniers, E., Martin, J.J., Cras, P., Van Marck, E., Handig, I., Jorens, H.Z., Oostra, B.A., Kooy, R.F., and Willems, P.J. (1999). Postmortem examination of two fragile X brothers with an FMR1 full mutation. Am J Med Genet 84, 245-249.

Rioult-Pedotti, M.S., Donoghue, J.P., and Dunaevsky, A. (2007). Plasticity of the synaptic modification range. J Neurophysiol 98, 3688-3695.

Rioult-Pedotti, M.S., Friedman, D., and Donoghue, J.P. (2000). Learning-induced LTP in neocortex. Science 290, 533-536.

Roberts, T.F., Tschida, K.A., Klein, M.E., and Mooney, R. (2010). Rapid spine stabilization and synaptic enhancement at the onset of behavioural learning. Nature 463, 948-952.

Rosenkranz, K., Kacar, A., and Rothwell, J.C. (2007). Differential modulation of motor cortical plasticity and excitability in early and late phases of human motor learning. J Neurosci 27, 12058-12066.

Rothstein, J.D., Dykes-Hoberg, M., Pardo, C.A., Bristol, L.A., Jin, L., Kuncl, R.W., Kanai, Y., Hediger, M.A., Wang, Y., Schielke, J.P., and Welty, D.F. (1996). Knockout of glutamate transporters reveals a major role for astroglial transport in excitotoxicity and clearance of glutamate. Neuron 16, 675-686.

Rudelli, R.D., Brown, W.T., Wisniewski, K., Jenkins, E.C., Laure-Kamionowska, M., Connell, F., and Wisniewski, H.M. (1985). Adult fragile X syndrome. Clinico-neuropathologic findings. Acta Neuropathol 67, 289-295.

Saito, T., and Nakatsuji, N. (2001). Efficient gene transfer into the embryonic mouse brain using in vivo electroporation. Dev Biol 240, 237-246.

Sanes, J.N., and Donoghue, J.P. (2000). Plasticity and primary motor cortex. Annu Rev Neurosci 23, 393-415.

Schaeffer, C., Bardoni, B., Mandel, J.L., Ehresmann, B., Ehresmann, C., and Moine, H. (2001). The fragile X mental retardation protein binds specifically to its mRNA via a purine quartet motif. EMBO J 20, 4803-4813.

Schrijver, N.C., Bahr, N.I., Weiss, I.C., and Wurbel, H. (2002). Dissociable effects of isolation rearing and environmental enrichment on exploration, spatial learning and HPA activity in adult rats. Pharmacology, biochemistry, and behavior 73, 209-224.

Schutt, J., Falley, K., Richter, D., Kreienkamp, H.J., and Kindler, S. (2009). Fragile X mental retardation protein regulates the levels of scaffold proteins and glutamate receptors in postsynaptic densities. J Biol Chem 284, 25479-25487.

Schuz, A. (1986). Comparison between the dimensions of dendritic spines in the cerebral cortex of newborn and adult guinea pigs. J Comp Neurol 244, 277-285.

Segal, M. (2005). Dendritic spines and long-term plasticity. Nat Rev Neurosci 6, 277-284.

Shepherd, G.M. (1996). The dendritic spine: a multifunctional integrative unit. J Neurophysiol 75, 2197-2210.

Spacek, J., and Hartmann, M. (1983). Three-dimensional analysis of dendritic spines. I. Quantitative observations related to dendritic spine and synaptic morphology in cerebral and cerebellar cortices. Anat Embryol (Berl) 167, 289-310.

Spires, T.L., Meyer-Luehmann, M., Stern, E.A., McLean, P.J., Skoch, J., Nguyen, P.T., Bacskai, B.J., and Hyman, B.T. (2005). Dendritic spine abnormalities in amyloid precursor protein transgenic mice demonstrated by gene transfer and intravital multiphoton microscopy. J Neurosci 25, 7278-7287.

Stepanyants, A., and Chklovskii, D.B. (2005). Neurogeometry and potential synaptic connectivity. Trends Neurosci 28, 387-394.

Tada, T., and Sheng, M. (2006). Molecular mechanisms of dendritic spine morphogenesis. Curr Opin Neurobiol 16, 95-101.

Teskey, G.C., Young, N.A., van Rooyen, F., Larson, S.E., Flynn, C., Monfils, M.H., Kleim, J.A., Henry, L.C., and Goertzen, C.D. (2007). Induction of neocortical long-term depression results in smaller movement representations, fewer excitatory perforated synapses, and more inhibitory synapses. Cereb Cortex 17, 434-442.

Todd, P.K., Mack, K.J., and Malter, J.S. (2003). The fragile X mental retardation protein is required for type-I metabotropic glutamate receptor-dependent translation of PSD-95. Proc Natl Acad Sci U S A 100, 14374-14378.

Toni, N., Buchs, P.A., Nikonenko, I., Bron, C.R., and Muller, D. (1999). LTP promotes formation of multiple spine synapses between a single axon terminal and a dendrite. Nature 402, 421-425.

Torii, M., Hashimoto-Torii, K., Levitt, P., and Rakic, P. (2009). Integration of neuronal clones in the radial cortical columns by EphA and ephrin-A signalling. Nature 461, 524-528.

Trachtenberg, J.T., Chen, B.E., Knott, G.W., Feng, G., Sanes, J.R., Welker, E., and Svoboda, K. (2002). Long-term in vivo imaging of experience-dependent synaptic plasticity in adult cortex. Nature 420, 788-794.

Tsai, J., Grutzendler, J., Duff, K., and Gan, W.B. (2004). Fibrillar amyloid deposition leads to local synaptic abnormalities and breakage of neuronal branches. Nat Neurosci 7, 1181-1183.

Turner, A.M., and Greenough, W.T. (1985). Differential rearing effects on rat visual cortex synapses. I. Synaptic and neuronal density and synapses per neuron. Brain research 329, 195-203.

Turrigiano, G.G., and Nelson, S.B. (2004). Homeostatic plasticity in the developing nervous system. Nat Rev Neurosci 5, 97-107.

Tzingounis, A.V., and Wadiche, J.I. (2007). Glutamate transporters: confining runaway excitation by shaping synaptic transmission. Nat Rev Neurosci 8, 935-947.

Wang, D.O., Kim, S.M., Zhao, Y., Hwang, H., Miura, S.K., Sossin, W.S., and Martin, K.C. (2009). Synapse- and stimulus-specific local translation during long-term neuronal plasticity. Science 324, 1536-1540.

Waung, M.W., Pfeiffer, B.E., Nosyreva, E.D., Ronesi, J.A., and Huber, K.M. (2008). Rapid translation of Arc/Arg3.1 selectively mediates mGluR-dependent LTD through persistent increases in AMPAR endocytosis rate. Neuron 59, 84-97.

Weiler, I.J., Irwin, S.A., Klintsova, A.Y., Spencer, C.M., Brazelton, A.D., Miyashiro, K., Comery, T.A., Patel, B., Eberwine, J., and Greenough, W.T. (1997). Fragile X mental retardation protein is translated near synapses in response to neurotransmitter activation. Proc Natl Acad Sci U S A 94, 5395-5400.

Weiler, I.J., Spangler, C.C., Klintsova, A.Y., Grossman, A.W., Kim, S.H., Bertaina-Anglade, V., Khaliq, H., de Vries, F.E., Lambers, F.A., Hatia, F., et al. (2004). Fragile X mental retardation protein is necessary for neurotransmitter-activated protein translation at synapses. Proc Natl Acad Sci U S A 101, 17504-17509.

Wilson, B.M., and Cox, C.L. (2007). Absence of metabotropic glutamate receptor-mediated plasticity in the neocortex of fragile X mice. Proc Natl Acad Sci U S A 104, 2454-2459.

Wisniewski, K.E., French, J.H., Fernando, S., Brown, W.T., Jenkins, E.C., Friedman, E., Hill, A.L., and Miezejeski, C.M. (1985). Fragile X syndrome: associated neurological abnormalities and developmental disabilities. Ann Neurol 18, 665-669.

Wisniewski, K.E., Segan, S.M., Miezejeski, C.M., Sersen, E.A., and Rudelli, R.D. (1991). The Fra(X) syndrome: neurological, electrophysiological, and neuropathological abnormalities. Am J Med Genet 38, 476-480.

Withers, G.S., and Greenough, W.T. (1989). Reach training selectively alters dendritic branching in subpopulations of layer II-III pyramids in rat motor-somatosensory forelimb cortex. Neuropsychologia 27, 61-69.

Xu, N.J., Sun, S., Gibson, J.R., and Henkemeyer, M. (2011). A dual shaping mechanism for postsynaptic ephrin-B3 as a receptor that sculpts dendrites and synapses. Nature neuroscience 14, 1421-1429.

Xu, T., Yu, X., Perlik, A.J., Tobin, W.F., Zweig, J.A., Tennant, K., Jones, T., and Zuo, Y. (2009). Rapid formation and selective stabilization of synapses for enduring motor memories. Nature 462, 915-919.

Yan, Q.J., Rammal, M., Tranfaglia, M., and Bauchwitz, R.P. (2005). Suppression of two major Fragile X Syndrome mouse model phenotypes by the mGluR5 antagonist MPEP. Neuropharmacology 49, 1053-1066.

Yang, G., Pan, F., and Gan, W.B. (2009). Stably maintained dendritic spines are associated with lifelong memories. Nature 462, 920-924.

Yashiro, K., and Philpot, B.D. (2008). Regulation of NMDA receptor subunit expression and its implications for LTD, LTP, and metaplasticity. Neuropharmacology 55, 1081-1094.

Yin, W., Mendenhall, J.M., Bratton, S.B., Oung, T., Janssen, W.G., Morrison, J.H., and Gore, A.C. (2007). Novel localization of NMDA receptors within neuroendocrine gonadotropin-releasing hormone terminals. Exp Biol Med (Maywood) *232*, 662-673.

Yu, J., Anderson, C.T., Kiritani, T., Sheets, P.L., Wokosin, D.L., Wood, L., and Shepherd, G.M. (2008). Local-Circuit Phenotypes of Layer 5 Neurons in Motor-Frontal Cortex of YFP-H Mice. Frontiers in neural circuits 2, 6.

Yuste, R., and Bonhoeffer, T. (2001). Morphological changes in dendritic spines associated with long-term synaptic plasticity. Annual review of neuroscience 24, 1071-1089.

Zalfa, F., Eleuteri, B., Dickson, K.S., Mercaldo, V., De Rubeis, S., di Penta, A., Tabolacci, E., Chiurazzi, P., Neri, G., Grant, S.G., and Bagni, C. (2007). A new function for the fragile X mental retardation protein in regulation of PSD-95 mRNA stability. Nat Neurosci 10, 578-587.

Zalfa, F., Giorgi, M., Primerano, B., Moro, A., Di Penta, A., Reis, S., Oostra, B., and Bagni, C. (2003). The fragile X syndrome protein FMRP associates with BC1 RNA and regulates the translation of specific mRNAs at synapses. Cell 112, 317-327.

Ziemann, U., Ilic, T.V., Pauli, C., Meintzschel, F., and Ruge, D. (2004). Learning modifies subsequent induction of long-term potentiation-like and long-term depression-like plasticity in human motor cortex. J Neurosci 24, 1666-1672.

Zito, K., Scheuss, V., Knott, G., Hill, T., and Svoboda, K. (2009). Rapid functional maturation of nascent dendritic spines. Neuron 61, 247-258.

Ziv, N.E., and Smith, S.J. (1996). Evidence for a role of dendritic filopodia in synaptogenesis and spine formation. Neuron 17, 91-102.

Zuo, Y., Lin, A., Chang, P., and Gan, W.B. (2005a). Development of long-term dendritic spine stability in diverse regions of cerebral cortex. Neuron 46, 181-189.

Zuo, Y., Yang, G., Kwon, E., and Gan, W.B. (2005b). Long-term sensory deprivation prevents dendritic spine loss in primary somatosensory cortex. Nature 436, 261-265.